la pluviometría, etc. En la Tabla I del anexo III se muestra la composición de varias muestras de aguas de mina tomadas en diferentes épocas del año.

La Figura 2 del anexo II muestra la influencia de la composición en la capacidad de la resina TP-207. En la Tabla I del anexo II se observa que las principales diferencias de composición entre las muestras 1 y 2 son el cobre, aluminio, sodio, zinc y hierro. En la Figura 2a se aprecia que la resina TP-207 es muy sensible a la concentración de hierro y se confirma la necesidad de reducir la concentración de este metal a nivel de inferior a 1 ppm. Para el resto de los iones metálicos no se observan grandes diferencias, aunque puede apreciarse que al aumentar la concentración de metal en disolución aumenta su adsorción en la resina. En la Figura 2b se observa que una disminución del 20% de la concentración de aluminio disminuye la adsorción de este metal del 15 al 8%. Este resultado es interesante ya que la disminución de la concentración de aluminio permite aumentar la adsorción de metales más valiosos como por ejemplo el cobre.

Por otro lado, se ha estudiado el efecto de la temperatura sobre la capacidad de ambas resinas. En la Figura 3a del anexo II se observa que la influencia de la temperatura sobre la capacidad de la resina TP-207 para la mayoría de los iones metálicos del agua de Riotinto es poco importante. Las diferencias más significativas los encontramos en el caso del cobre y aluminio. En la Figura 3b de dicho anexo se observa un apreciable aumento de la adsorción de aluminio y disminución de la adsorción de cobre al aumentar la temperatura.

Del mismo modo, se ha estudiado el efecto de la temperatura sobre la capacidad de la resina R 250-K hacia los iones del agua de Riotinto. En la Figura 4a del anexo II puede apreciarse, para la mayoría de los iones metálicos, una ligera disminución de la capacidad de la resina por estos iones al aumentar la temperatura. El comportamiento del aluminio es opuesto al resto de los iones metálicos, es decir, la adsorción de este metal aumenta de manera importante al aumentar la temperatura como se aprecia en la Figura 4b. Dado que el aumento de la adsorción de aluminio es considerablemente mayor que la disminución de la

adsorción del resto de iones metálicos, el resultado final es un aumento importante de la capacidad total de la resina al aumentar la temperatura.

El grado de concentración de cualquier especie metálica mediante procesos de intercambio iónico a temperatura dual es directamente proporcional a la variación de la capacidad de la resina entre ambas temperaturas, e inversamente proporcional a la concentración del ion metálico en la disolución inicial. Por lo tanto, es posible predecir el grado de concentración de un ion metálico en una mezcla de multicomponentes a partir del parámetro **b**, que se calcula mediante la siguiente expresión:

$$b = \frac{\Delta q}{C_o \, V_o} \qquad (12)$$

donde Δq representa la variación de capacidad de la resina, C_o la concentración del ion en la disolución inicial y V_o el volumen de disolución pasado a T_2.

En la Tabla II.2 que se presenta a continuación se muestran los valores de **b** determinados para ambas resinas TP-207 y R 250-K.

Tabla II.2. Valores del parámetro **b**x10^3 determinados para las resinas Lewatit TP-207 y R 250-K en aguas de mina. T_1=20°C y T_2=80°C.

Resina	Cu^{2+}	Zn^{2+}	Mn^{2+}	Mg^{2+}	Ca^{2+}	Na^{+}	Al^{3+}
TP-207	6,63	0,47	0,31	0,23	-0,36	0	-8,31
R 250-K	74,36	15,17	4,94	0,96	1,93	0,42	-59,05

A partir de los resultados de la tabla anterior se puede predecir para la resina TP-207 que el cobre será la única especie cuya concentración aumentará significativamente mediante la técnica de intercambio iónico con temperatura dual. El comportamiento inverso puede predecirse para el aluminio, en este caso, se espera una disminución importante de su concentración durante el proceso.

En el caso de la resina R 250-K es posible predecir, a partir de los valores de **b**, que el grado de concentración de los iones metálicos del agua de Riotinto seguirá el siguiente orden:

$$Cu^{2+} >> Zn^{2+} > Mn^{2+} > Ca^{2+} > Mg^{2+} > Na^{+} \qquad (13)$$

Hemos de puntualizar que la diferencia en valor absoluto de los valores de **b** entre las dos resinas se debe a la diferencia de altura del lecho de resina utilizada en ambos casos, en el caso de la resina R 250-K era diez veces mayor. De cualquier modo, a partir de los resultados de la tabla anterior se puede preveer un comportamiento similar de ambas resinas en los procesos de intercambio iónico con temperatura dual.

2. Selectividad de las Resinas.

Se han determinado los valores de α_{M2}^{M1} para las diferentes parejas de iones presentes en el agua de Riotinto en ambas resinas Lewatit TP-207 y R 250-K utilizando el método directo (ver ecuación 1).

El estudio de la dependencia de α_{M2}^{M1} con la temperatura para la resina TP-207 se ha realizado utilizando la muestra 1 (ver Tabla 1 del anexo II). En la Figura 5a del anexo II se observa que los valores de α_{M2}^{Fe} son mucho más elevados que para el resto de los iones metálicos, lo cual demuestra la elevada selectividad de la resina TP-207 para el hierro y de nuevo confirma la necesidad de eliminar este metal.

Los elevados valores de α_{M2}^{Cu} que aparecen en la Figura 5b demuestran que esta resina es también muy selectiva a cobre. En el caso de α_{Mg}^{Cu}, se aprecia un considerable aumento de la selectividad con la temperatura, mientras que el resto de los iones metálicos (excepto el aluminio) muestran una dependencia más débil.

El caso más interesante es para α_{Al}^{Cu} ya que disminuye de manera importante al aumentar la temperatura.

La Figura 5c muestra que la influencia de la temperatura sobre los valores de α_{M2}^{Al} es bastante considerable, ya que los valores de α aumentan de modo importante al aumentar la temperatura. En las Figuras 5d y 5e se observa que el

efecto de la temperatura sobre α para el resto de las parejas de iones metálicos es mucho menos importante. La fuerte dependencia de los valores de α_{M2}^{Al} con la temperatura puede explicarse a partir de los valores de ΔH° de la reacción de complejación entre los metales y compuestos que contienen grupos iminodiacético. Los valores de entalpía son muy positivos para el aluminio y negativos para el cobre y otros iones metálicos presentes en las aguas ácidas.[13]

En el caso de la resina R 250-K, la dependencia con la temperatura de los valores de α_{M2}^{M1} se ha estudiado utilizando la muestra 2 de agua de Riotinto.

En la Figura 1a del anexo III se aprecia que la influencia positiva de la temperatura sobre los valores de α_{M2}^{Al} es incluso más fuerte que la observada en la resina TP-207. Para el resto de parejas de iones metálicos se observa una tendencia opuesta, este es el caso de α_{Mg}^{Cu}, α_{Na}^{Cu} y α_{M2}^{Zn}, o bien una influencia mucho más débil (ver Figuras 1b, 1c y 1d del anexo III).

La influencia de la temperatura sobre los valores de α puede apreciarse más claramente mediante el parámetro **a** que representa el cociente entre dos valores de α a diferente temperatura y que se expresa del siguiente modo:

$$a = \frac{\alpha_{M_2}^{M_1}(T_1)}{\alpha_{M_2}^{M_1}(T_2)} = \frac{Y_{M_1}(T_1)}{Y_{M_1}(T_1) + \Delta Y_{M_1}} \cdot \frac{Y_{M_2}(T_1) + \Delta Y_{M_2}}{Y_{M_2}(T_1)} \qquad (14)$$

donde T_1 y T_2 se escogen de modo que **a**>1 , y $\Delta Y_M = Y_M(T_1) - Y_M(T_2)$. El valor máximo de **a** se obtiene cuando $\Delta Y_{M1} < 0$ y $\Delta Y_{M2} > 0$, es decir, cuando la adsorción de los iones considerados muestra una dependencia opuesta con la temperatura, como sucede con el aluminio y el resto de los metales de las aguas ácidas. La siguiente tabla muestra los valores del parámetro **a** calculados para el aluminio y el resto de las parejas de iones presentes en el agua de Riotinto.

El parámetro **a** también puede utilizarse como criterio para medir la eficacia de cualquier proceso de separación con temperatura dual,[14,15] y predecir la separación entre los diferentes iones del sistema estudiado. En el caso de la resina R 250-K

los máximos valores de separación se observan para el aluminio y los iones cobre, zinc y manganeso, por lo tanto, se espera que la mayor separación tenga lugar entre estas parejas de iones.

Tabla II.3. Valores del parámetro **a** calculado para las diferentes parejas de iones Al^{3+}-M^{n+} a T_1=80°C y T_2 variable en las resinas Lewatit TP-207 y R 250-K.

			Lewatit R 250-K			
T_2 (°C)	Cu^{2+}	Zn^{2+}	Mn^{2+}	Mg^{2+}	Ca^{2+}	Na^{+}
20	3,43	4,26	4,02	1,85	1,95	2,23
40	2,13	1,25	1,45	1,37	0,91	1,35
60	1,62	1,09	1,19	1,18	0,73	1,14
			Lewatit TP-207			
T_2 (°C)	Cu^{2+}	Zn^{2+}	Mn^{2+}	Mg^{2+}	Ca^{2+}	Na^{+}
20	2,68	3,20	3,55	3,57	2,36	2,79
40	1,86	1,99	2,31	2,40	1,48	2,14
60	1,36	1,41	1,55	1,63	1,05	1,55

- ***Procesos de Termoadsorción y Termodesorción de Metales en Aguas Ácidas de Mina***

Los estudios de termo-adsorción-desorción se han llevado a cabo en ambas resinas (Lewatit TP-207 y R 250-K) utilizando agua ácida de mina natural. Los experimentos de termodesorción se han realizado a 80°C con la resina previamente equilibrada a 20°C.

En las Figuras 6a y 6b del anexo II se observa que el proceso de termodesorción de ambas resinas conduce a un incremento selectivo de la concentración de cobre, mientras que la concentración del resto de metales (excepto aluminio) permanece prácticamente inalterada. La considerable disminución de la concentración de aluminio durante el proceso indica que es el aumento de adsorción de este metal lo que provoca la desorción del cobre y otros

metales. En el caso de la resina R 250-K los datos presentados (ver Figura 6b) corresponden al segundo ciclo de termodesorción. El primer ciclo se realizó a 80°C después de equilibrar la resina, en forma sódica, con agua de Riotinto a 20°C. En este caso, se produce un aumento muy importante de la concentración de cobre y de otros iones metálicos como muestra la Figura 2 del anexo III.

El comportamiento observado para ambas resinas durante los experimentos de termodesorción muestra una buena correlación con las predicciones realizadas mediante los valores de **b** calculados a partir de los datos de equilibrio. La única excepción se observa en el caso de la resina R 250-K para el manganeso y zinc, y puede explicarse por la menor difusión en disolución de este último, lo que da lugar a un pico de elución más ancho y más bajo que el del manganeso.[16]

Por otro lado, es posible calcular los valores de **b** a partir de los datos obtenidos en los experimentos de termodesorción utilizando la siguiente ecuación:

$$b_{strip} = \frac{\sum_{i}^{j} (C_i - C_o)\, V_i}{C_o \sum_{i}^{j} V_i} \qquad (15)$$

En el caso de la resina R 250-K se ha llevado a cabo una comparación entre los valores de **b** determinados a partir de los datos de equilibrio ($\mathbf{b}_{equil}$) y los determinados en los experimentos de termodesorción ($\mathbf{b}_{strip}$). Como se observa en la Figura 3 del anexo III la representación de log($\mathbf{b}_{equil}$) versus log ($\mathbf{b}_{strip}$) se ajusta aceptablemente a una linea recta lo que demuestra la validez del modelo propuesto y de las predicciones realizadas.

Una vez finalizado el proceso de termodesorción, las resinas están descargadas de cobre y otros metales de las aguas ácidas (excepto aluminio) y son capaces de adsorberlos de nuevo sin necesidad de ningún tratamiento adicional, simplemente pasando el agua de mina a 20°C. En el caso de la resina acrílica, este proceso es mucho menos eficiente que el observado en el primer ciclo de carga, ya

que tiene lugar en contra de la selectividad de la resina como demuestran los valores de α_{M2}^{Al}.

Por otro lado, conviene tener en cuenta diversos factores que pueden influir en la efectividad del proceso de termodesorción, por ejemplo la altura del lecho de resina y la temperatura a la que se lleva a cabo el proceso.

En la Figura 7 del anexo II se observa que un aumento de la altura del lecho de resina TP-207 de 0,5 a 2,5 cm conduce a un aumento de la concentración de cobre y de la zona de separación entre cobre y aluminio. El mismo efecto se ha observado para la resina R 250-K al aumentar la altura de 5 a 18,5 cm, como se muestra en la Figura 5 del anexo IV.

La disminución de la temperatura a la que tiene lugar el proceso de termodesorción produce el efecto contrario. Así, en la Figura 8a del anexo II se observa para la resina TP-207 como una disminución de la temperatura provoca una importante disminución de la eficacia del proceso de termodesorción. Del mismo modo, en la Figura 8b se observa una disminución de la eficacia del proceso de termoadsorción al disminuir la temperatura a la que tiene lugar la etapa previa de termodesorción. Estos resultados son consecuencia de los cambios de adsorción de cobre y aluminio en la resina a diferentes temperaturas, y pueden ser deducidos a partir de los valores de **a** presentados en la Tabla II.3 antes descrita.

- ***Tratamiento de Aguas Ácidas de Mina Mediante Procesos de Intercambio Iónico a Temperatura Dual***

Los resultados obtenidos anteriormente permiten diseñar procesos de intercambio iónico a temperatura dual para el tratamiento de aguas ácidas de mina. A continuación presentamos algunos posibles tratamientos de aguas de mina basados en este tipo de procesos.

1. Concentración Selectiva de Cobre sin Reactivos.

Una aplicación de la técnica de intercambio iónico a temperatura dual para el tratamiento de las aguas ácidas de mina consiste en la concentración selectiva de cobre aplicando procesos sin reactivos y que por tanto no generan residuos.

El proceso se lleva a cabo mediante una serie consecutiva de ciclos de termo-adsorción-desorción, de modo que en cada ciclo se consigue una disolución cada vez más concentrada en cobre y empobrecida en aluminio mucho más adecuada que la disolución inicial para la recuperación de cobre.

Los experimentos se llevaron a cabo utilizando la resina Lewatit R 250-K y agua ácida preparada en el laboratorio (artificial) cuya composición se recoge en la Tabla 1 del anexo IV. Los resultados obtenidos en una serie de cuatro ciclos se muestran en la Figura 9 del anexo II. La disolución obtenida después del cuarto ciclos contiene 324 ppm de cobre y 51 ppm de aluminio, mientras que la concentración de zinc y sodio prácticamente no varía a lo largo del proceso.

La recuperación final del cobre a partir de esta última disolución se lleva a cabo con la resina TP-207. La elución del cobre con ácido sulfúrico 1 M permite obtener una disolución de sulfato de cobre con una pureza media del 86% (93,5% si se evita la mezcla con la primera fracción del eluato que contiene el mayor nivel de impurezas). En la Figura 10 del anexo II se muestra más exahustivamente estos datos de pureza del cobre de las diferentes fracciones recogidas en el proceso de elución.

La Figura 11 del anexo II muestra un esquema del proceso de intercambio iónico a temperatura dual para la concentración de cobre de las aguas ácidas de mina. El sistema consta de una serie de columnas en contracorriente operando a diferente temperatura. El agua ácida alimenta la primera columna donde se produce el primer concentrado que se dirige a la siguiente columna y así sucesivamente. Es importante señalar que el proceso de concentración de cobre se lleva a cabo sin reactivos por lo que no se generan residuos que deban ser tratados.

2. Agua de Mar como Reactivo Auxiliar.

Otra posibilidad para el tratamiento de aguas ácidas de mina mediante procesos de intercambio iónico a temperatura dual, consiste en la utilización de agua de mar como regenerante de la resina para mejorar la efectividad del proceso de concentración de cobre explicado anteriormente. El agua de mar presenta las

ventajas de ser un reactivo barato (el único coste es el transporte) y no es nocivo para el medio ambiente.

En la Figura I del anexo IV se muestra una comparación del primer y segundo ciclo de termodesorción, en el primer caso la resina está en forma sódica o equilibrada con agua de mar mientras que en el segundo está equilibrada con agua ácida. En dicha figura se observa que la efectividad en el segundo caso es mucho menor que en el primero. Por lo tanto, el proceso anterior puede mejorarse significativamente regenerando la resina con agua de mar de modo que la concentración de cobre de las aguas de mina tenga lugar con mayor efectividad.

La Figura 3 del anexo IV muestra el proceso de regeneración de la resina R 250-K con agua de mar a 80°C. En la Figura 3a se observa que la elución de zinc y manganeso requiere unos 5 volúmenes de resina (BV) mientras que la de cobre requiere unos 15 BV y la de aluminio 30 BV. En la Figura 3b puede apreciarse que es la adsorción de magnesio y sodio del agua de mar lo que provoca la elución de los metales del agua ácida. Una vez enfriada, la resina está lista para el siguiente ciclo de termo-adsorción-desorción.

Una comparación de los resultados de la Figura 2 y 4 del anexo IV muestra que la efectividad del proceso de concentración de cobre de las aguas ácidas de mina con la resina en forma sódica o de los iones del agua de mar es mucho mayor en cada uno de los ciclos. Este hecho puede explicarse por la hidrólisis parcial de la resina acrílica en forma de iones del agua de mar según la reacción:

$$R\text{-}COONa + H_2O \leftrightarrows R\text{-}COOH + NaOH \qquad (16)$$

hecho que no ocurre si la resina está en forma de los iones del agua ácida del mina.

Así, al cargar la resina con agua ácida se produce la precipitación de los hidróxidos metálicos según su solubilidad:[17]

$$Al(OH)_3(pK_{SP}=32.9) << Cu(OH)_2(19.7) < Zn(OH)_2(16.7) < Mn(OH)_2(12.7) < Mg(OH)_2(10.7) < Ca(OH)_2(5.3) \qquad (17)$$

El análisis del precipitado recogido en las primeras fracciones del proceso de carga de la resina R 250-K con agua ácida demuestra que la especie precipitada es hidróxido de aluminio. De este modo, la reducción parcial de la concentración de aluminio en el agua ácida permite una mayor acumulación de cobre durante el proceso de carga de la resina, y por tanto una mejora en el proceso de concentración de este metal.

Un esquema de este proceso se muestra en la Figura 6 del anexo IV. El sistema consta de tres columnas en contracorriente operando a diferente temperatura. En la primera columna tiene lugar la carga de la resina, en forma de iones de agua de mar, con agua ácida a 20°C. Una vez cargada la resina se dirige a la segunda columna donde se trata con agua ácida a 80°C y se produce la disolución concentrada en cobre y empobrecida en aluminio. En la tercera columna tiene lugar la regeneración de la resina con agua de mar a 80°C. Una vez regenerada la resina se dirige de nuevo a la primera columna y el proceso vuelve a comenzar.

Finalmente hemos de señalar que la combinación de ambos procesos (puede llevarse a cabo según el esquema que se presenta en la Figura 7 del anexo IV) conduce a una mejora sustancial de los resultados, ya que permite concentrar el cobre en un factor de aproximadamente tres en cada etapa.

II.2.3. PARTICIÓN POR INTERCAMBIO IÓNICO EN TÁNDEM (TIEF): SEPARACIÓN DE ALUMINIO, COBRE, ZINC Y MAGNESIO MEDIANTE RESINAS CARBOXÍLICAS Y RESINAS CON GRUPOS IMINODIACETICO (ver anexo V)

Los estudios presentados en la memoria incluyen el desarrollo de nuevos procesos de intercambio iónico para el tratamiento de mezclas metálicas multicomponentes.

Los procesos de intercambio iónico que se utilizan normalmente para la separación de mezclas son la separación frontal, la separación frontal inversa y la cromatografía por desplazamiento. La separación frontal permite la separación de la especie más débilmente adsorbida del resto de especies que se adsorben más

fuertemente. Por el contrario, la separación frontal inversa permite la separación de la especie que se adsorbe más fuertemente del resto de especies. La cromatografía por desplazamiento es una combinación en paralelo de los dos procesos anteriores, ya que tienen lugar simultáneamente. En este caso es posible separar varias especies con diferente grado de adsorción. La cromatografía por desplazamiento presenta los inconvenientes ya mencionados que pueden evitarse utilizando una combinación diferente de los procesos de separación frontal y separación frontal inversa. A esta técnica la hemos denominado partición por intercambio iónico en tándem (TIEF).

- ***Explicación Conceptual de la Técnica TIEF (Tandem Ion-Exchange Fractionation)***

La partición por intercambio iónico en tándem consiste en una combinación secuencial de los procesos de separación frontal y separación frontal inversa. En la Figura 2 del anexo V se muestra un esquema de la separación de una mezcla de cuatro componentes **A**, **B**, **C** y **D** mediante dicha técnica utilizando, un sistema de tres columnas conectadas en serie.

Cada columna contiene un intercambiador iónico que adsorbe preferentemente uno de los componentes de la mezcla, y que muestra la afinidad más débil por el componente **A**. El proceso de separación frontal se lleva a cabo cargando la primera columna hasta la aparición del componente **D** (más fuertemente retenido) a la salida de la primera columna. De este modo, se disminuye el número de componentes de cuatro a tres (**A**, **B** y **C**). El proceso de separación frontal continua en la segunda columna. El componente **A** se acumula en la primera parte de la disolución que sale de la columna, mientras que el componente **C** es retenido por la resina. La separación final de la mezcla de **A** y **B** se realiza en la tercera columna.

El esquema del sistema de tres columnas utilizado en el proceso de separación y la distribución de los componentes en la disolución que sale de cada columna se muestran en las Figuras 2a y 2b del anexo V, respectivamente. En

dichas figuras, se observa que el componente **A** es el único que puede obtenerse puro mediante el proceso de separación frontal. El resto de los componentes **D**, **C** y **B** se acumulan en la fase resina de las columnas 1, 2 y 3 respectivamente (linea discontinua de la Figura 2a). Estos componentes pueden obtenerse puros mediante separación frontal inversa en la etapa de elución. La distribución de los componentes en la disolución de elución que sale de cada columna se muestra en la Figura 2c. En la Tabla 1 del anexo V se muestran las condiciones necesarias para llevar a cabo el proceso de separación, así como los productos que pueden obtenerse puros en cada columna.

Es importante señalar que al reducir el número de componentes de la mezcla se mejora la separación del resto de los componentes. Esto se aprecia más claramente a partir de los valores de α_A^B en un sistema de cuatro, tres y dos componentes, donde los cuatro componentes se encuentran inicialmente en la misma concentración:

$$Columna\ 1: \quad \alpha_A^B\ (4) = \frac{1 - Y_A}{Y_A} - (\alpha_A^C + \alpha_A^D) \tag{18}$$

$$Columna\ 2: \quad \alpha_A^B\ (3) = \frac{1 - Y_A}{Y_A} - \alpha_A^C \tag{19}$$

$$Columna\ 3: \quad \alpha_A^B\ (2) = \frac{1 - Y_A}{Y_A} \tag{20}$$

suponiendo que el cociente$(1-Y_A)/Y_A$ tiene aproximadamente el mismo valor en las ecuaciones 18-20 y que $(\alpha_A^D + \alpha_A^C)$ en la primera columna es mayor que α_A^C en la segunda columna se deduce fácilmente que $\alpha_A^B(2) > \alpha_A^B(3) > \alpha_A^B(4)$.

- Equilibrio de Intercambio Iónico

En primer lugar se llevó a cabo el estudio de la separación de un sistema de cuatro componentes (cobre, aluminio, zinc y magnesio) con la resina Lewatit TP-207. En la Figura 3a del anexo V se observa que es posible la separación frontal de magnesio del resto de los metales en la etapa de carga de la resina. La elución de los metales de la resina con ácido sulfúrico 0,05 M permite la separación frontal inversa de cobre, ya que se obtiene una zona de este metal puro en las últimas fracciones recogidas (ver Figura 3b).

Posteriormente se estudió la separación de un sistema de tres componentes (aluminio, zinc y magnesio) con la resina Lewatit R 250-K. Al igual que en el caso anterior se obtiene una zona de magnesio puro durante la carga de la resina (ver Figura 4a del anexo V). La elución con ácido sulfúrico permite obtener aluminio de elevada pureza tal y como se muestra en la Figura 4b.

La separación final de zinc y magnesio se llevó a cabo con la resina Lewatit TP-207, obteniendose una zona de magnesio puro durante la carga de la resina (Figura 5a del anexo V) y una zona de zinc puro mediante la elución con ácido (ver Figura 5b).

En la Tabla 2 del anexo V se recogen los valores de α determinados por el método directo para el sistema de cuatro, tres y dos componentes. En dicha tabla se observa como al disminuir el número de componentes mejora la separación del resto (ver valores de α_{Mg}^{Zn}), lo que demuestra la validez del modelo propuesto y de las aproximaciones realizadas.

- Separación de Mezclas Metálicas Multicomponentes

El experimento final de separación de la mezcla de cobre, aluminio, zinc y magnesio mediante la técnica TIEF se ha llevado a cabo utilizando un sistema de tres columnas conectadas en serie como se muestra en la Figura 1 del anexo V.

La Figura 6a del anexo V muestra las curvas de adsorción de los diferentes metales durante el proceso de carga de la resina. Se observa que tiene lugar la separación frontal de magnesio, ya que se obtiene una zona de este metal puro con

una concentración igual a la concentración total inicial de la mezcla. La amplitud de la zona de magnesio puro es mucho mayor que la obtenida en los experimentos de separación frontal individuales (ver Figura 7a del anexo V). Posteriormente comienza a aparecer el zinc, después el aluminio y finalmente el cobre.

La elución de los metales de las resinas se llevó acabo separadamente con ácido sulfúrico 0,05 M como se muestra en las Figuras 6b, 6c y 6d del anexo V.

Por otro lado, en las Figuras 7b, 7c y 7d se observa que la pureza del cobre, aluminio y zinc obtenido en el proceso de separación frontal inversa es suficientemente elevada. La Tabla 3 del anexo V muestra la pureza inicial, máxima y media de cada uno de los metales separados por al técnica TIEF. Puede observarse que a pesar de que la pureza de todos los componentes de la mezcla inicialmente es baja, es posible recuperar todos los metales con una pureza relativamente elevada lo que demuestra la eficacia de la técnica desarrollada.

II.2.4. TRATAMIENTO INTEGRAL DE LAS AGUAS ÁCIDAS

Los trabajos que se presentan en la parte final de la memoria consisten en el diseño y desarrollo de tecnologías limpias para el tratamiento integral de las aguas ácidas. El proceso permite en la síntesis de sulfato potásico aprovechando el elevado contenido de sulfatos de las aguas ácidas y la recuperación selectiva de los diferentes metales contenidos en estas aguas. Este proceso es una nueva aplicación de la técnica TIEF.

- Conversión de Contaminantes en Fertilizantes: Síntesis de Sulfato Potásico a Partir de Aguas Ácidas Mediante Procesos de Intercambio Iónico

La mayor parte de la producción de sulfato potásico se utiliza para la fabricación de fertilizantes. Dado que el cultivo de algunos vegetales se ve afectado por la presencia de cloruros,[18,19] es interesante el desarrollo de tecnologías que permitan la producción de sulfato potásico libre de cloruros.

El proceso Mannheim es el que se utiliza más frecuentemente para la producción de sulfato potásico debido a su simplicidad y a su elevado rendimiento.[19]

El sulfato potásico se obtiene haciendo reaccionar cloruro potásico con un pequeño exceso de ácido sulfúrico a temperatura elevada (600-700°C). La reacción que tiene lugar es la siguiente:

$$2\ KCl + H_2SO_4 \rightarrow K_2SO_4 + HCl \qquad (21)$$

El proceso Mannheim presenta algunas desventajas como un elevado gasto de energía, problemas de corrosión, etc. Teniendo presente esta situación, el desarrollo de procesos alternativos que incluso permitan la transformación de contaminantes en fertilizantes es de gran interés.

Anteriormente habíamos visto que las aguas ácidas de mina se caracterizan por un pH bajo y un contenido elevado de iones metálicos. Otra característica interesante de estas aguas es su elevada concentración en iones sulfato y bajo contenido en cloruros, lo cual hace que sean muy adecuadas para la síntesis de fertilizantes.

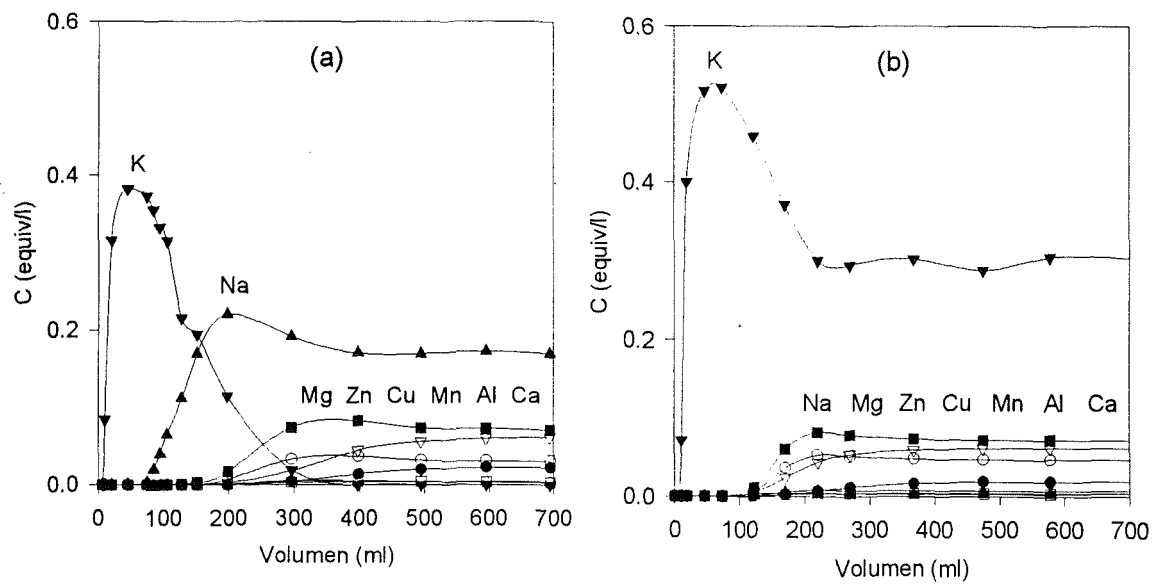

Figura II.6. Síntesis de sulfato potásico en la resina Lewatit S 100 LF WS en forma potásica. (a) Muestra tratada con hidróxido sódico y (b) tratada con hidróxido potásico; (○) Zn, (□) Mn, (△) Cu, (▽) Al, (●) Ca, (■) Mg, (▲) Na, (▼) K.

En las Figuras II.6a y II.6b se observa como el paso de la disolución a través del lecho de resina sulfónica en forma potásica produce la adsorción de los iones metálicos contenidos en el agua de mina y la desorción de potasio según la siguiente reacción:

$$2n\ R\text{-}SO_3K + M_2(SO_4)_n \leftrightharpoons 2\ (R\text{-}SO_3)_nM + n\ K_2SO_4 \qquad (22)$$

La disolución de sulfato potásico pura que se obtiene puede ser concentrada por ósmosis inversa, electrodiálisis u otra técnica, lo que permite producir sulfato potásico que puede ser utilizado como fertilizante y además agua de riego.

La comparación de las Figuras II.6a y II.6b demuestran que el tratamiento con hidróxido potásico es más efectivo que con hidróxido sódico, ya que se evitan las interferencias causadas por el sodio que es el elemento que aparece primero a la salida de la columna disminuyendo la amplitud de la zona de sulfato potásico puro.

Una vez que la resina está agotada el paso de cloruro o sulfato potásico (3 ó 0,67 M respectivamente) produce la elución de los metales adsorbidos en la resina según:

$$(R\text{-}SO_3)_nM + n\ KCl \leftrightharpoons n\ R\text{-}SO_3K + MCl_n \qquad (23)$$

obteniéndose una disolución de los diferentes iones metálicos de las aguas ácidas más concentrada que la disolución original.

En la Figura II.7 se observa como la elución de cobre, manganeso, magnesio y zinc requiere unos 7 volúmenes (BV) de regenerante, mientras que el aluminio y el calcio más fuertemente adsorbidos requieren unos 12 BV de cloruro potásico.

La elución de los metales permite la regeneración de la resina y la recuperación de la forma potásica inicial quedando lista para la siguiente etapa después de lavar con agua desionizada. El agua de lavado se recircula y se utiliza para preparar más disolución regenerante.

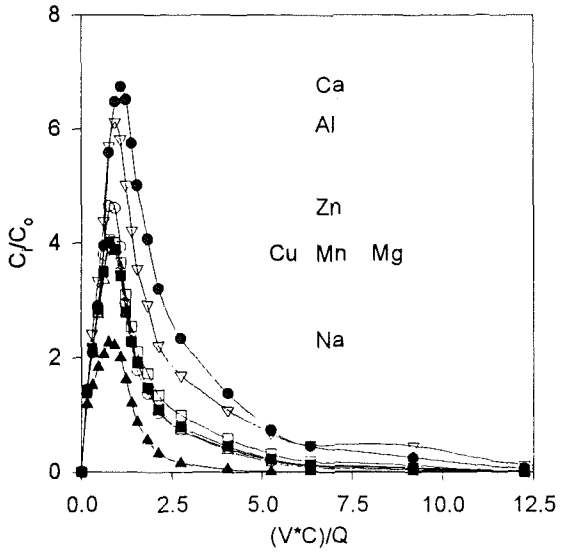

Figura II.7. Regeneración de la resina Lewatit S 100 LF WS con cloruro potásico 3 M; (○) Zn, (□) Mn, (△) Cu, (▽) Al, (●) Ca, (■) Mg, (▲) Na, (▼) K.

- **Recuperación selectiva de los Metales Contenidos en las Aguas Ácidas de mina**

La separación y recuperación selectiva de los metales del concentrado obtenido en la etapa anterior se lleva a cabo secuencialmente utilizando la técnica de partición por intercambio iónico en tándem (TIEF) descrita anteriormente.

El proceso se lleva a cabo pasando el concentrado metálico obtenido en la etapa anterior a través de un sistema de tres columnas conectadas en serie. En la Figura II.8 (a) se observa como el paso de la disolución a través de las columnas permite la separación frontal de magnesio del resto de los iones metálicos, ya que es la especie que se adsorbe más débilmente.

Posteriormente la elución por separado con ácido sulfúrico de los metales retenidos en cada una de las columnas permite la separación frontal inversa de cobre, aluminio y zinc (ver Figuras II.8 (b), (c) y (d)) respectivamente. De este modo es posible recuperar dichos metales con un grado aceptable de pureza. La pureza de los metales puede aumentarse fácilmente mediante electrólisis de los sulfatos

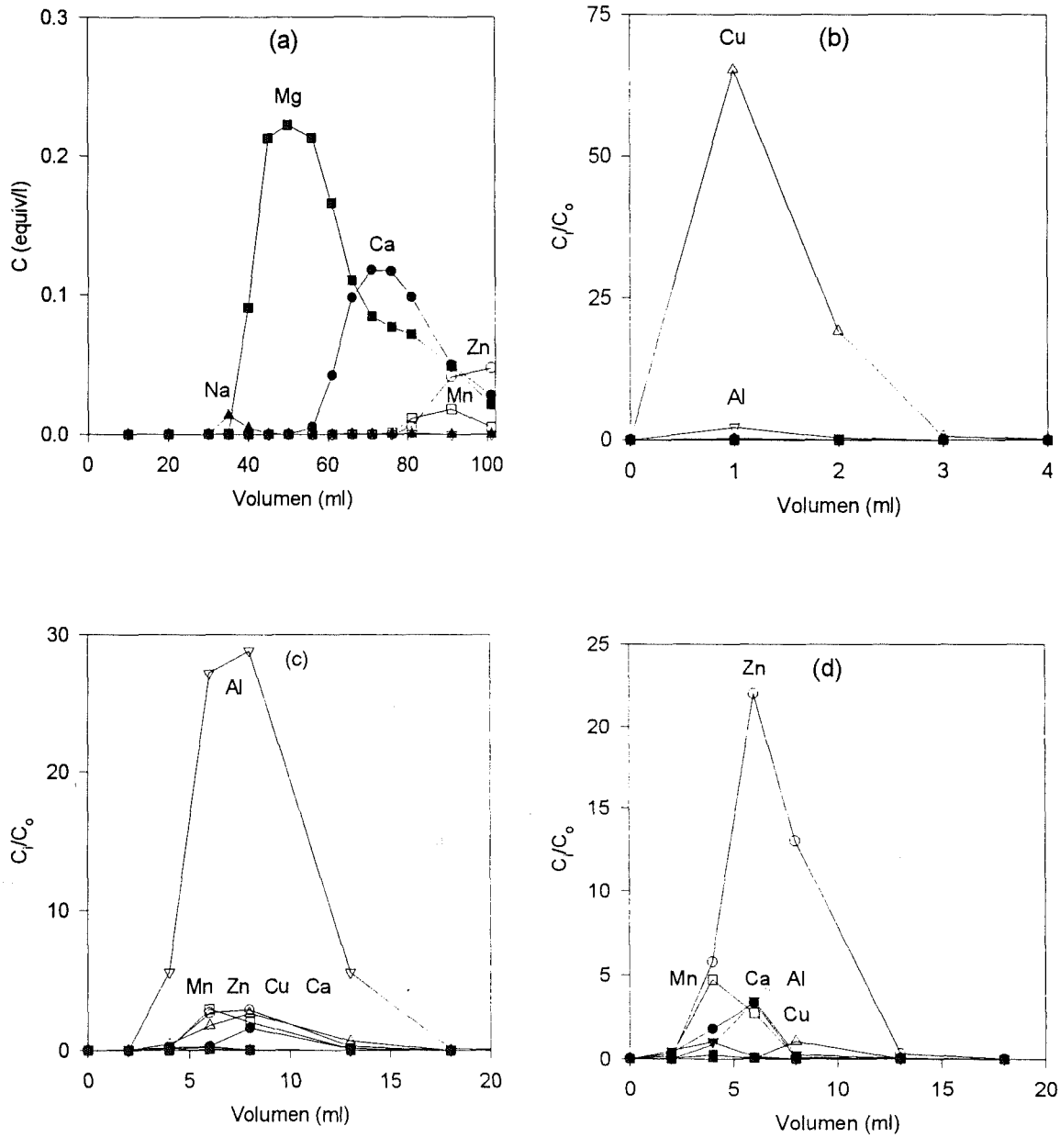

Figura II.8. Recuperación de los valores metálicos del agua de Riotinto. (a) Separación frontal de magnesio a la salida del sistema de tres columnas, y separación frontal inversa de cobre (b), aluminio (c) y zinc (d) obtenida mediante la elución con H_2SO_4 en las columnas 1, 2 y 3 respectivamente; (○) Zn, (□) Mn, (△) Cu, (▽) Al, (●) Ca, (■) Mg, (▲) Na, (▼) K.

metálicos obtenidos en la etapa anterior obteniéndose cobre, aluminio y zinc de calidad electrolítica.

Por otro lado, la disolución obtenida a la salida del sistema de columnas contiene una elevada concentración de potasio y magnesio y una menor cantidad de iones metálicos tales como calcio, manganeso, etc que no han sido adsorbidos por las resinas. El magnesio presente en la primera fracción recogida se recupera mediante precipitación con disolución concentrada de hidróxido potásico a pH 12. Los metales residuales contenidos en la segunda fracción pueden ser precipitados a pH 10 con hidróxido potásico. Una vez que la disolución ha sido filtrada y el pH ajustado a 5-6 con ácido clorhídrico, sólo contiene pequeñas impurezas de calcio que podrían ser eliminadas con una resina carboxílica en forma potásica, lo que permite la reutilización de la disolución de regeneración. En la Tabla II.4 se muestra la composición de ambas fracciones una vez que los iones metálicos han sido precipitados.

Tabla II.4. Composición de la disolución de KCl después de la regeneración y precipitación de los iones metálicos residuales con KOH.

Muestra	Fe^{3+}	Cu^{2+}	Zn^{2+}	Al^{3+}	Mn^{2+}	Mg^{2+}	Ca^{2+}	K^{+}	pH
1	0	0	0	0	0	0	362	25.642	12
2	0	0	0	8	0	0	670	65.602	10

- Planta Piloto para el Tratamiento de las Aguas Ácidas de Mina

Los resultados obtenidos en la planta piloto demuestran que el escalado del sistema no afecta a la eficacia del proceso. En la Figura II.9 se observa como el paso de la disolución a través del lecho de resina sulfónica en forma potásica produce la adsorción de los iones metálicos contenidos en el agua de mina y la desorción de potasio lo que permite obtener una zona de sulfato potásico puro de concentración igual a la concentración total de la disolución inicial (Figura II.9 (b)). Posteriormente comienzan a aparecer los diferentes iones metálicos y finalmente calcio que es la especie que se adsorbe más fuertemente (Figura II.9 (a)).

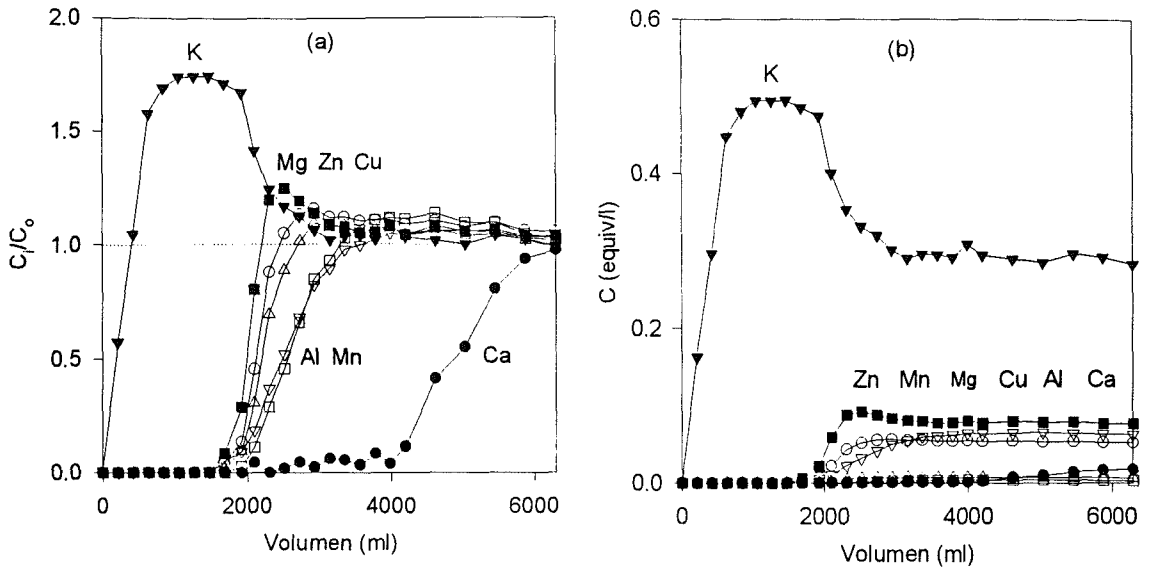

Figura II.9. Síntesis de sulfato potásico en la resina Lewatit SP 112 en forma potásica a partir del agua de mina. (a) Concentración relativa y (b) concentración absoluta en equiv/l; (○) Zn, (□) Mn, (△) Cu, (▽) Al, (●) Ca, (■) Mg, (▲) Na, (▼) K.

La regeneración de la resina se lleva a cabo con disolución concentrada de cloruro o sulfato potásico (3 ó 0,67 M respectivamente) que produce la elución de los metales adsorbidos en la resina, obteniéndose una disolución concentrada de los diferentes iones metálicos. En la Figura II.10 se aprecia que la regeneración de la resina con sulfato potásico es mucho más efectiva debido a que la precipitación de sulfato de calcio desplaza el equilibrio de la reacción de intercambio iónico a la derecha según:

$$(R\text{-}SO_3)_nM + \frac{n}{2}\,K_2SO_4 \leftrightharpoons n\,R\text{-}SO_3K + \frac{1}{2}\,M_2(SO_4)_n \qquad (24)$$

$$Ca^{2+} + SO_4^{2-} \leftrightharpoons CaSO_4\downarrow \qquad (25)$$

La precipitación del sulfato de calcio tiene lugar a la salida de la columna y no en el lecho de la resina debido al fenómeno de supersaturación isotérmica.[20]

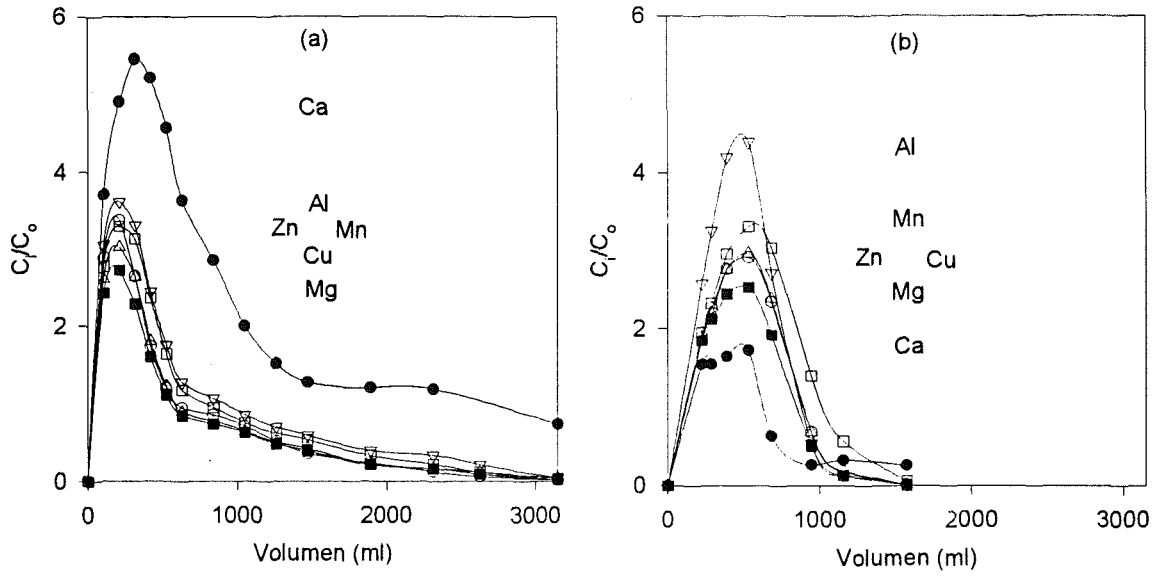

Figura II.10. Regeneración de la resina Lewatit SP 112 con (a) cloruro potásico 3 M y (b) sulfato potásico 0,67 M; (○) Zn, (□) Mn, (△) Cu, (▽) Al, (●) Ca, (■) Mg, (▲) Na, (▼) K.

La precipitación del calcio en forma de sulfato evita que la concentración de este metal en la disolución sea muy elevada e interfiera en la etapa de recuperación de los metales.

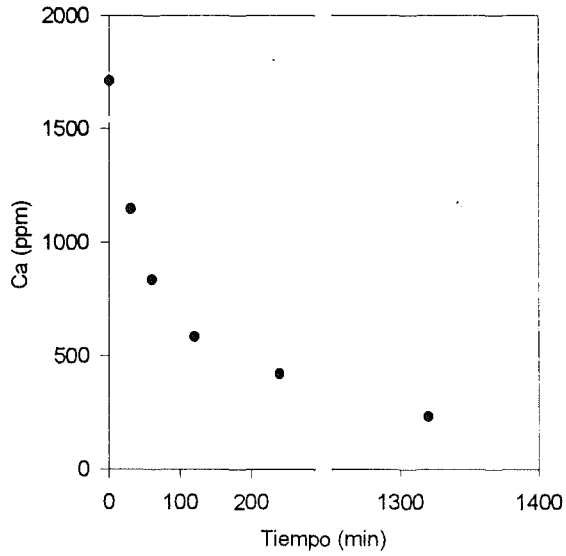

Figura II.11. Cinética de precipitación del sulfato cálcico en la disolución de regeneración de la resina Lewatit SP 112.

También se ha estudiado la cinética de precipitación del calcio en la disolución de regeneración de la resina Lewatit SP 112 con sulfato potásico. En la Figura II.11 se observa que al principio la precipitación es muy rápida y luego tiene lugar más lentamente.

El paso del concentrado metálico obtenido en la etapa anterior a través de una columna que contiene resina Lewatit TP-207 permite la separación del cobre del resto de los metales tal y como se observa en la Figura II.12 (a). El comportamiento anómalo del calcio se debe a que continua precipitando a la salida de la columna. La elución de los metáles adsorbidos en la resina con ácido sulfúrico permite concentrar selectivamente el cobre casi 200 veces como se muestra en la Figura II.12 (b). La pureza de la disolución de sulfato de cobre que se obtiene es bastante elevada lo que demuestra la selectividad y eficacia de la resina empleada para la recuperación de este metal (ver Figura II.12 (c)).

En la Figura II.13 (a) se observa como el paso de la disolución libre de cobre obtenida en la etapa anterior a través de una columna que contiene resina Lewatit CNP 80 no permite una buena separación entre el aluminio y el zinc . La razón de que la separación no sea muy efectiva puede estar motivada por cuestiones cinéticas ya que el aluminio se adsorbe muy lentamente.

La elución de los metáles adsorbidos en la resina con ácido sulfúrico permite concentrar el aluminio más de 30 veces. La pureza de la disolución de sulfato de aluminio que se obtiene no es demasiado elevada debido a que se encuentra impurificado por la presencia de otros metales, especialmente zinc (ver Figuras II.13 (b) y (c)). Una posible solución para mejorar el proceso sería trabajar con columnas termostatizadas de manera que aumente la capacidad y el coeficiente de difusión del aluminio. Otra posibilidad es realizar una purga con disolución concentrada de sulfato de aluminio antes de llevar a cabo la elución con sulfúrico.

A continuación se pasa la disolución obtenida en la etapa anterior, libre de cobre y que contiene una pequeña impureza de aluminio, a través de la resina Lewatit TP-207. En la Figura II.14 (a) se observa que tiene lugar la separación frontal de magnesio del resto de los iones metálicos polivalentes. En este caso la

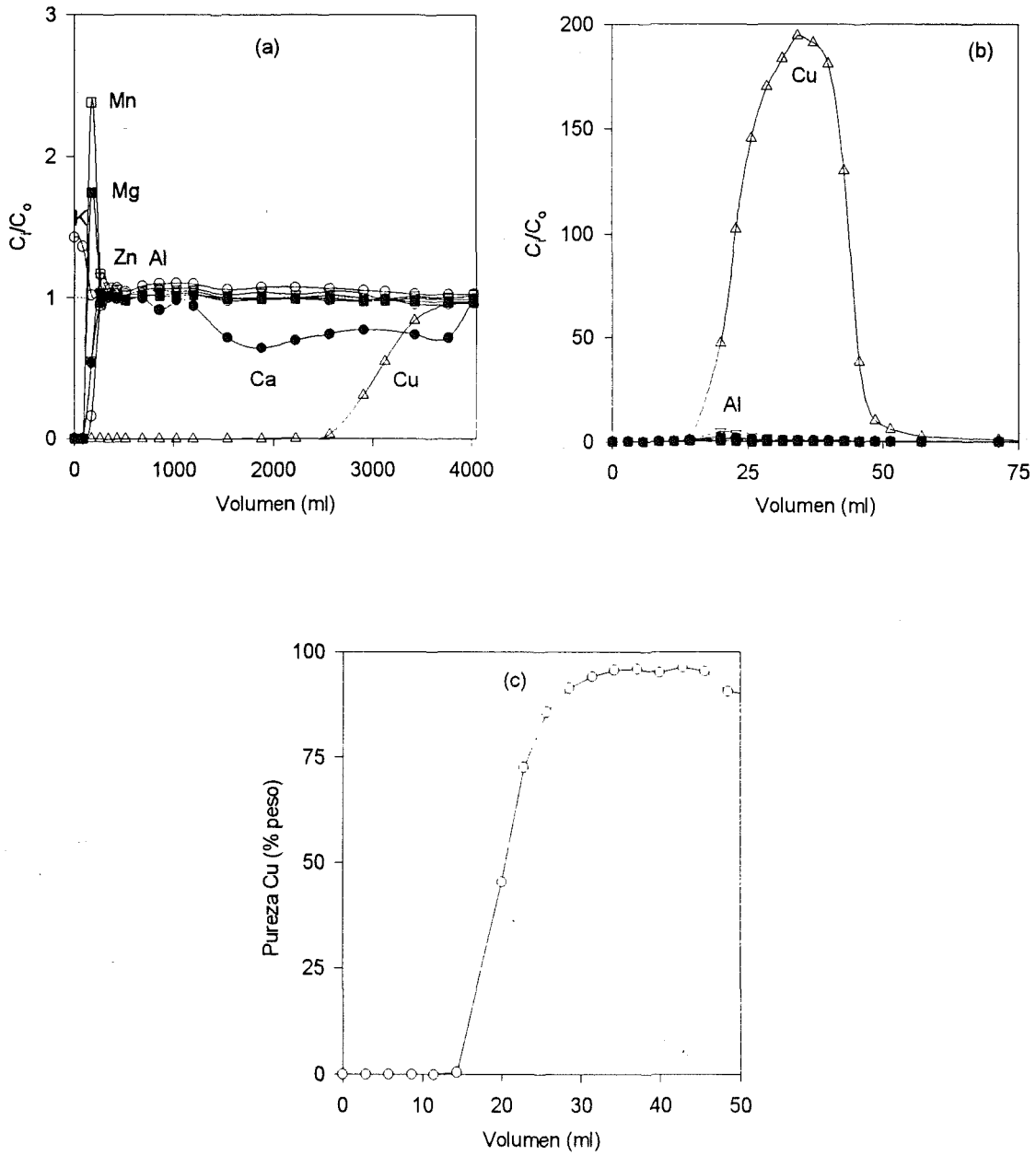

Figura II.12. (a) curvas de carga de la resina Lewatit TP-207 con la disolución de regeneración de la resina sulfónica; (b) curvas de elución de los metales adsorbidos en la resina con ácido sulfúrico y (c) pureza de la disolución de sulfato de cobre recogida en la etapa de elución; (○) Zn, (□) Mn, (△) Cu, (▽) Al, (●) Ca, (■) Mg, (▲) Na, (▼) K.

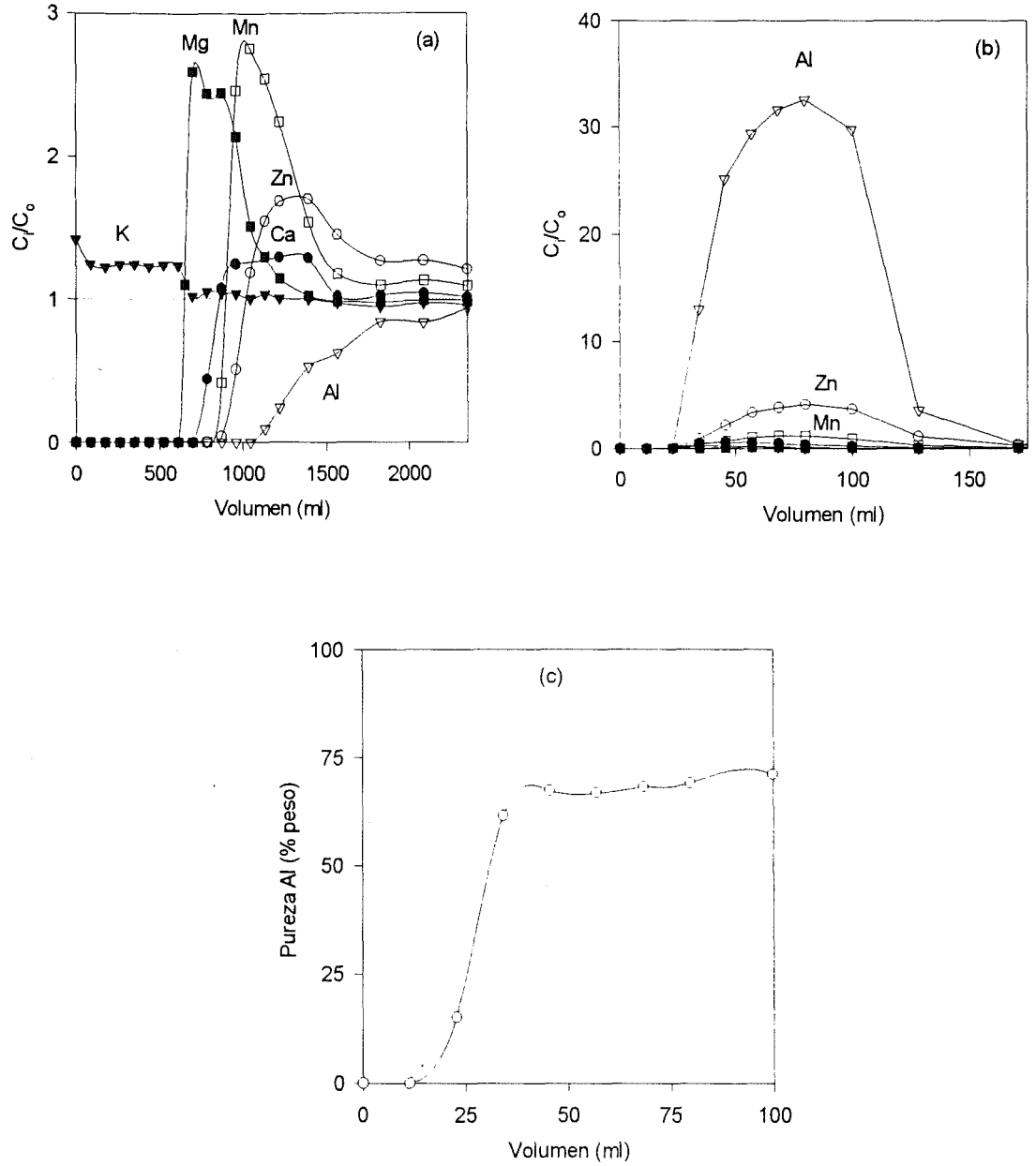

Figura II.13. (a) curvas de carga de la resina Lewatit CNP 80 con la disolución obtenida en la etapa anterior; (b) curvas de elución de los metales adsorbidos en la resina con ácido sulfúrico y (c) pureza de la disolución de sulfato de aluminio obtenido en la etapa de elución;(○) Zn, (□) Mn, (△) Cu, (▽) Al, (●) Ca, (■) Mg, (▲) Na, (▼) K.

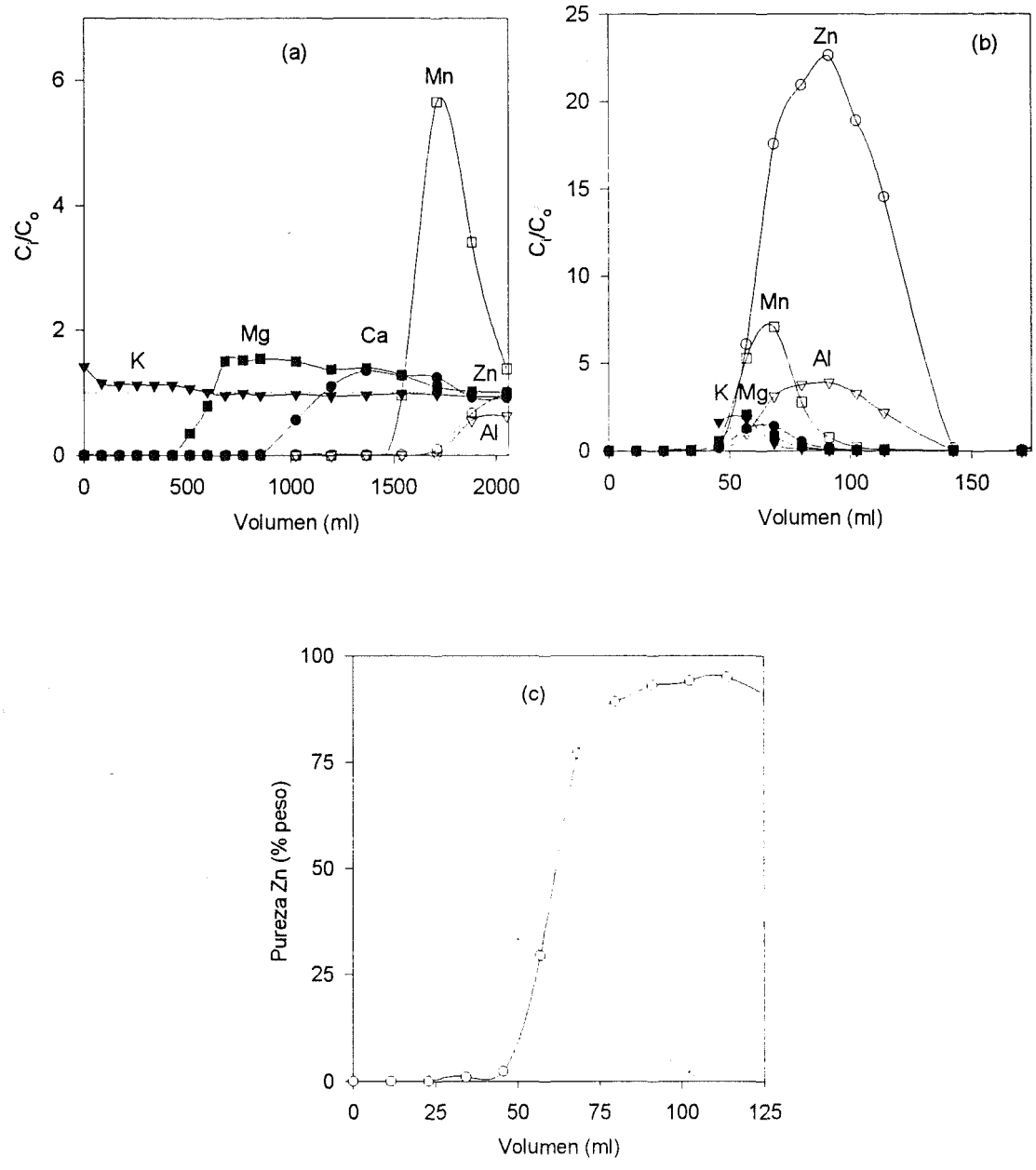

Figura II.14. (a) curvas de carga de la resina Lewatit TP-207 con la disolución obtenida en la etapa anterior; (b) curvas de elución de los metales adsorbidos en la resina con ácido sulfúrico y (c) pureza de la disolución de sulfato de zinc obtenido en la etapa de elución;(○) Zn, (□) Mn, (△) Cu, (▽) Al, (●) Ca, (■) Mg, (▲) Na, (▼) K.

de los metáles con ácido sulfúrico concentra el zinc casi 25 veces. La pureza de la disolución de sulfato de zinc que se obtiene es bastante aceptable aunque presenta algunas impurezas de aluminio y manganeso (ver Figuras II.14 (b) y (c)).

El experimento final de separación y recuperación de metales utilizando la técnica TIEF permite la concentración y la separación frontal de magnesio del resto de los iones metálicos a la salida del sistema de seis columnas conectadas en serie tal y como se muestra en la Figura II.15. En dicha figura se observa que es posible obtener una disolución 0,3 equiv/l de magnesio libre del resto de iones metálicos polivalentes.

La elución de los metales retenidos en las resinas con ácido sulfúrico permite la separación frontal inversa y recuperación selectiva de cobre en las dos primeras columnas, aluminio en las dos siguientes y zinc en las dos últimas.

La Figura II.16 (a) muestra que el resultado obtenido en la primera columna del sistema TIEF es similar al obtenido en el experimento individual ya que es posible concentrar selectivamente el cobre unas 150 veces respecto a la concentración inicial. La pureza de la disolución obtenida en este caso también es bastante aceptable tal y como se observa en la Figura II.16 (b).

También el resultado de la tercera columna es similar al obtenido anteriormente ya que el aluminio se concentra de nuevo casi 30 veces (ver Figura II.17 (a)). La pureza que se consigue en este caso es ligeramente superior a la obtenida en el experimento individual, como se muestra en la Figura II.17 (b).

Igualmente el comportamiento del zinc en la quinta columna es prácticamente idéntico al anterior, concentrándose unas 30 veces y con una pureza bastante aceptable, tal y como se muestra en las Figuras II.18 (a) y (b) respectivamente.

La siguiente etapa consistiría en el diseño y desarrollo de una planta piloto capaz de tratar entre 0,3 y 1 m^3/h de agua de mina. En la Figura II.19 se muestra esquemáticamente el aspecto de una hipotética planta piloto. En las columnas 1 y 2 tiene lugar la síntesis de sulfato potásico. La disolución recogida se dirige a un módulo de ósmosis inversa donde se produce sulfato potásico y agua de riego. En

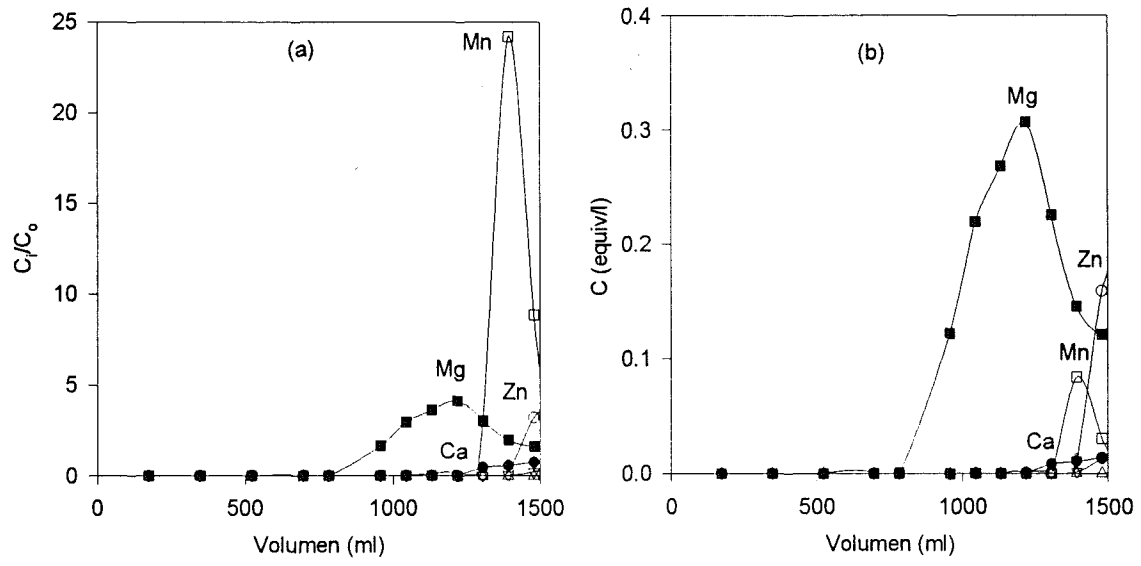

Figura II.15. Separación frontal de magnesio a la salida del sistema de columnas conectadas en serie. (a) Concentración relativa y (b) concentración absoluta en equiv/l. (○) Zn, (□) Mn, (△) Cu, (▽) Al, (●) Ca, (■) Mg, (▲) Na, (▼) K.

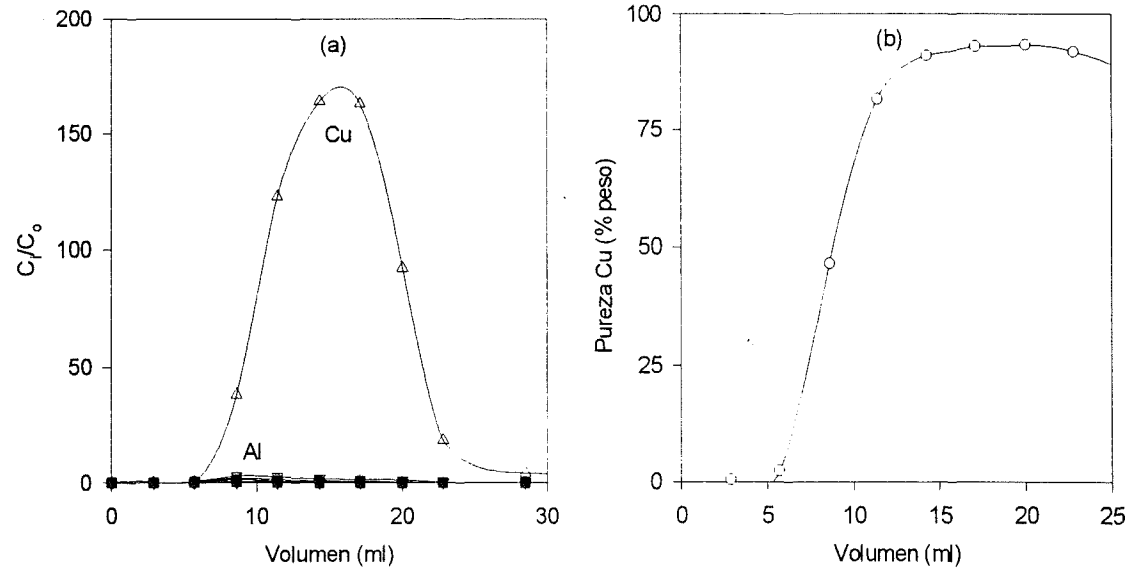

Figura II.16. (a) Curvas de elución con ácido sulfúrico de los metales adsorbidos en la resina Lewatit TP-207 de la columna 1 y (b) pureza de la disolución de sulfato de cobre. (○) Zn, (□) Mn, (△) Cu, (▽) Al, (●) Ca, (■) Mg, (▲) Na, (▼) K.

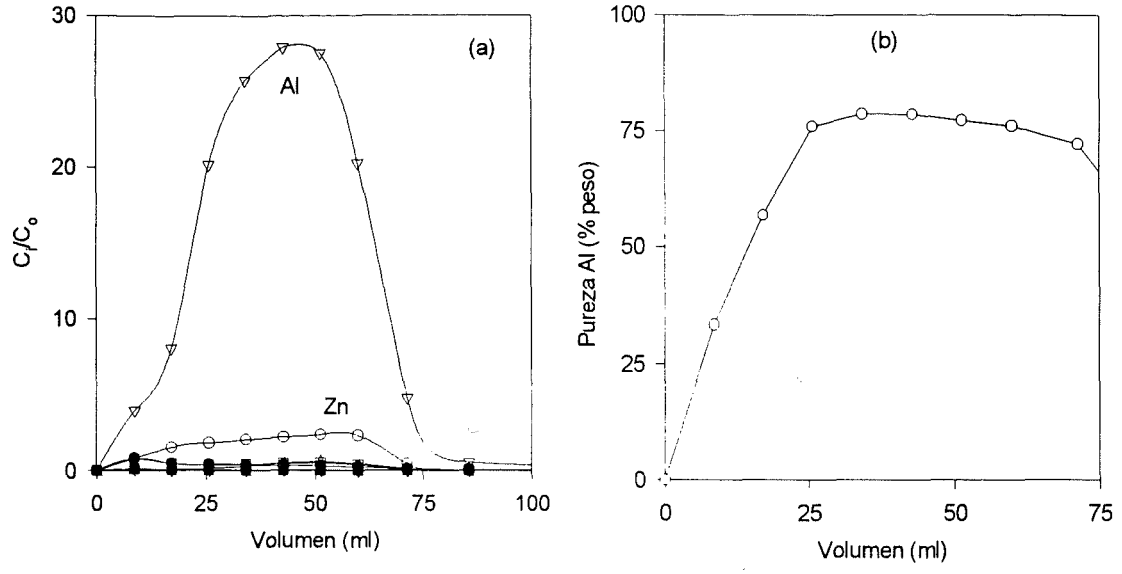

Figura II.17. (a) Curvas de elución con ácido sulfúrico de los metales adsorbidos en la resina Lewatit CNP 80 de la columna 3 y (b) pureza de la disolución de sulfato de aluminio. (○) Zn, (□) Mn, (△) Cu, (▽) Al, (●) Ca, (■) Mg, (▲) Na, (▼) K.

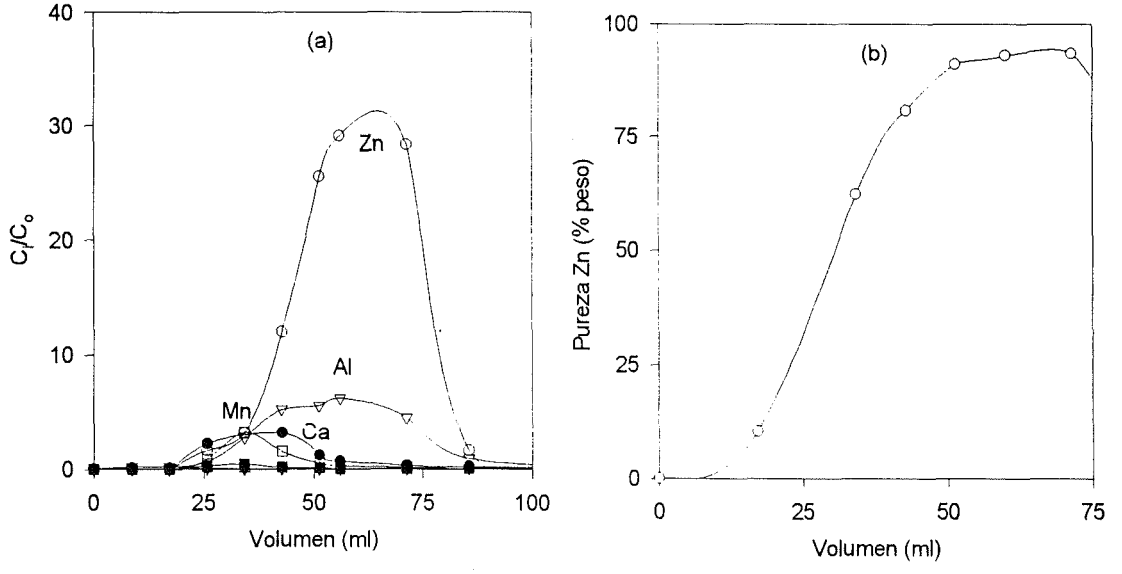

Figura II.18. (a) Curvas de elución con ácido sulfúrico de los metales adsorbidos en la resina Lewatit TP-207 de la columna 5 y (b) pureza de la disolución de sulfato de zinc. (○) Zn, (□) Mn, (△) Cu, (▽) Al, (●) Ca, (■) Mg, (▲) Na, (▼) K.

las columnas 3-8 se lleva a cabo la recuperación selectiva de los metales contenidos en el agua de mina. Las disoluciones obtenidas en las diferentes columnas mediante la elución con ácido sulfúrico se dirigen a una planta electrolítica donde pueden recuperarse los diferentes metales con una pureza elevada.

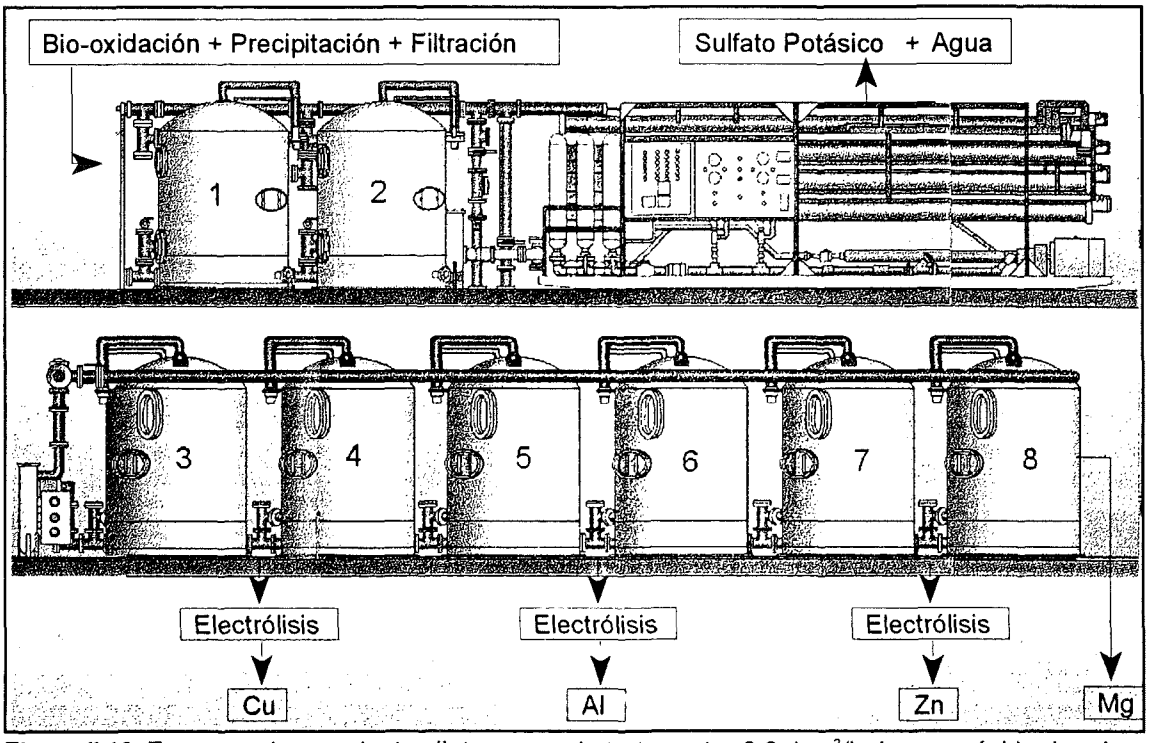

Figura II.19. Esquema de una planta piloto capaz de tratar entre 0,3-1 m^3/h de agua ácida de mina.

Finalmente indicar que el proceso de intercambio iónico puede incluirse dentro de un tratamiento integral de las aguas ácidas de mina que permite la producción de varios compuestos interesantes desde un punto de vista económico a la vez que reducir el impacto ecológico que las aguas ácidas tienen para el medio ambiente.

En la siguiente figura se muestra una estimación de la productividad de una hipotética planta capaz de tratar 1.000 m^3/h con un 50% de efectividad en la recuperación de los diversos compuestos.

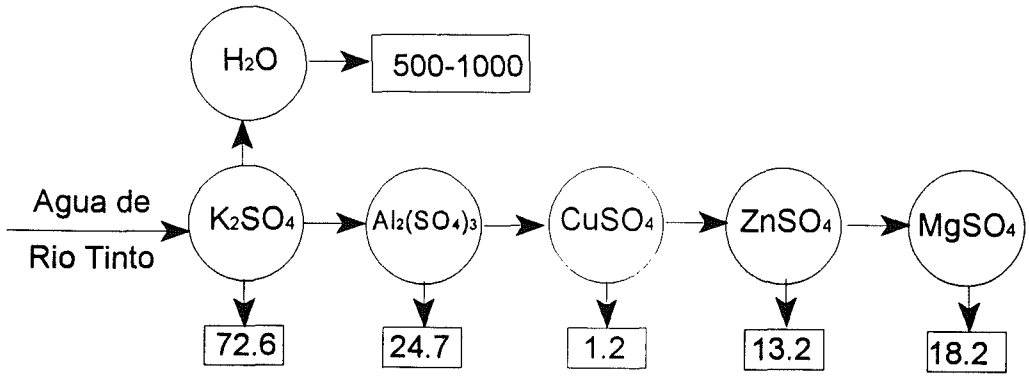

Figura II.20. Estimación de la productividad de una hipotética planta para la síntesis de sulfato potásico y recuperación de metales del agua de Riotinto. Los valores de cada compuesto se expresan en miles de Tn/año.

II.3. BIBLIOGRAFÍA

1. Dorfner, K., in: *"Ion Exchangers"*, K. Dorfner, Ed., Walter de Gruyter, Berlin-New York, **1991**, p. 94.
2. Dorfner, K., *ibid.*, p.339.
3. Muraviev, D., *Chemica Scripta*, 29, **1989**, 9.
4. Timofeevskaya, V. D., Ivanov, V. A. and Gorshkov, V. I., *Russ. J. Phys. Chem.*, 62(2), **1988**, 1314.
5. Samchenko, Z.A., Nekrjach, E.F. and Kurilenko, O.D., *Zhur. Fiz. Khim.*, 41(10), **1975**, 1042.
6. Soldatov, V.S. and Bychkova, V.A., *Nauka i Tekhnika*, Minsk, **1988**, p. 86.
7. Fletcher, P. and Townsend, R.P., *J. Chem. Soc. Farad. Trans. 2*, 77(6), **1981**, 955.
8. Fletcher, P. and Townsend, R.P., *ibid.*, 77(11), **1981**, 2077.
9. Spedding, F. H., Powell, J. E. and Svec, H. J., *J. Am. Chem. Soc.*, 77, **1955**, 6125.
10. Gorshkov, V. I., in: *"Thermodynamics of Ion Exchange"*, B. Nykolsky, Ed., Nauka, Minsk, **1968**, p.122. (Russ).
11. Helfferich, F., *Ion Exchange*, McGraw-Hill, New York, **1962**.
12. Helfferich, F.G. and Yng-Long Hwang., in: *"Ion Exchangers"*, K. Dorfner, Ed., Walter de Gruyter, Berlin-New York, **1991**, p. 1288.
13. Christensen, J. J. and Izatt, R. M., in: *"Handbook of Metal Ligands Heats"*, Dekker, M., New York, **1983**.
14. Tondeur, D.; Grevillot, G., in: *"Ion-Exchange: Science and Technology"*. NATO ASI series, Rodrigues, A.E. Ed.; Martinus Nijhoff: Dordrecht, Vol. 107, **1986**, p. 369.
15. Gorshkov, V. I., in: "Ion Exchange and Solvent Extraction", Marinsky, J.A.; Marcus, Y., Eds.; Marcel Dekker: New York, Vol. 12, **1995**, Chapter 2.
16. Dorfner, K., in: *"Ion Exchangers"*; K. Dorfner, Ed.; Walter de Gruyter: Berlin, **1991**, p. 90.

17. *"Lange's Handbook of Chemistry"*, 11th edn.; Dean, J.A., Ed.; McGraw-Hill: New York, **1973**, p. 5-7.
18. Slack, A.V., *Fertilizer Development and Trends.* Noyes Development Corp.: Park Ridge, NJ, **1968**.
19. Ullman, F., in: *"Ullmann´s Encyclopedia of Industrial Chemistry"*, B. Elvers, S. Hawkins, W. Russey and G. Schulz, eds.,**1993**, v. A22, p. 84-91.
20. Khamizov, R. KH., Mironova, L. I., Tikhonov, N. A. Bychkov, A. V. and Poezd, A. D., *Separation Science and Technology*, **1996**, 31(1), 1.

II.4. CONCLUSIONES

De los resultados recogidos en la presente memoria podemos extraer como más relevantes las siguientes conclusiones:

1. El factor de separación α del intercambio Ca^{2+}-Na^{+} y Mg^{2+}-Na^{+} en el agua de mar para las resinas carboxílicas Lewatit R 249-K y R 250-K muestra una elevada dependencia con la temperatura. Esta dependencia es mucho menor para el intercambio Ca^{2+}-Mg^{2+} tal y como se puede predecir a partir de los valores de entalpía asociados a las correspondientes reacciones de intercambio iónico.

2. Es posible la termodesorción selectiva de calcio y magnesio de la resinas carboxílicas previamente equilibradas con agua de mar a 80°C pasando la misma disolución a 10°C. La sucesiva repetición de cuatro ciclos de termo-desorción-adsorción permiten una concentración adicional de calcio y magnesio de casi cuatro veces respecto a su concentración en el agua de mar.

3. Los estudios cinéticos realizados demuestran que la termodesorción de calcio y magnesio de la resina Lewatit R 250-K está controlada por la difusión intragranular. El resultado obtenido confirma que el proceso de termodesorción puede llevarse a cabo sin problemas cinéticos.

4. Las resinas carboxílicas en forma sódica permiten la separación frontal de calcio y magnesio del agua de mar.

5. La capacidad de las resinas Lewatit TP-207 y R 250-K es similar para la mayoría de los metales presentes en el agua ácida de mina excepto para el cobre y aluminio cuya capacidad es muy superior, es decir, la resina TP-207 es selectiva a cobre mientras que la resina R 250-K es muy selectiva a aluminio.

6. En el caso de la resina TP-207 la dependencia de α con la temperatura no es demasiado importante para la mayoría de las parejas de iones exceptuando Cu^{2+}-Mg^{2+} y Al^{3+}-M^{n+} que aumentan apreciablemente y Cu^{2+}-Al^{3+}

que, al contrario, disminuye de modo importante al aumentar la temperatura. En el caso de la resina R 250-K el efecto de la temperatura sobre α para las parejas de iones Al^{3+}-M^{n+} es el mayor de los observados, mientras que el resto de las parejas de iones muestran una tendencia opuesta y, en cualquier caso, más débil.

7. Es posible predecir la eficacia de la separación y concentración de los iones metálicos en un proceso de intercambio iónico a temperatura dual mediante los parámetros **a** y **b** respectivamente, calculados a partir de los datos de equilibrio. La mayor eficacia en el proceso de separación y concentración se ha determinado para las parejas aluminio-cobre, aluminio-zinc y aluminio-manganeso.

8. El paso de agua de mina a 80°C a través de la resinas TP-207 y R 250-K previamente equilibradas con agua de mina a 20°C conduce a la selectiva desorción de cobre y adsorción de aluminio. La sucesiva repetición de cuatro ciclos de termo-desorción-adsorción permite una concentración adicional de cobre de casi tres veces y una disminución de la concentración de aluminio del 90%. Esta disolución es mucho más adecuada que la inicial para la recuperación de cobre.

9. Se ha demostrado la eficacia de reactivos baratos y no dañinos para el medio ambiente como el agua de mar para regenerar la resina carboxílica R 250-K y de este modo mejorar la efectividad del proceso de concentración de cobre sin reactivos agresivos para el medio ambiente (caso del ácido sulfúrico).

10. Se ha puesto de manifiesto que la disminución del número de componentes de una mezcla mejora la separación del resto, como puede deducirse de los valores de α en mezclas de cuatro, tres y dos componentes.

11. Se ha desarrollado la nueva técnica de partición por intercambio iónico en tándem (TIEF) que permite la separación y recuperación de **n** componentes de una mezcla utilizando **n-1** columnas de manera sencilla y eficaz.

12. Se ha mostrado efectivo el proceso de conversión del contenido en sales metálicas de aguas ácidas de mina en sulfato potásico (aditivo de fertilizantes) utilizando una resina sulfónica Lewatit S 100 LF WS o SP-112 en forma potásica.

13. La aplicación de la técnica TIEF permite la recuperación selectiva de los metales contenidos en las aguas de mina: cobre, aluminio, zinc y magnesio con un grado aceptable de pureza utilizando las resinas comerciales TP-207 y CNP 80.

CAPÍTULO III

ANEXOS

ANEXO I

Reprinted from

REACTIVE
&
FUNCTIONAL
POLYMERS

Reactive & Functional Polymers 28 (1996) 111–126

Separation and concentration of calcium and magnesium from sea water by carboxylic resins with temperature-induced selectivity

Dmitri Muraviev *, Joan Noguerol, Manuel Valiente *

Departament de Química, Química Analítica, Universitat Autònoma de Barcelona, E-08193 Bellaterra, Barcelona, Spain

ELSEVIER

ELSEVIER

Reactive & Functional Polymers 28 (1996) 111–126

REACTIVE & FUNCTIONAL POLYMERS

Separation and concentration of calcium and magnesium from sea water by carboxylic resins with temperature-induced selectivity

Dmitri Muraviev *, Joan Noguerol, Manuel Valiente *

Departament de Química, Química Analítica, Universitat Autònoma de Barcelona, E-08193 Bellaterra, Barcelona, Spain

Received 20 June 1994; revised version accepted 16 February 1995

Abstract

Processes of concentration and separation of calcium and magnesium from artificial and natural sea water by carboxylic ion-exchange resins of acrylic and methacrylic types at different temperatures have been investigated. The values of equilibrium separation factor α for Ca^{2+}–Na^{+}, Mg^{2+}–Na^{+} and Ca^{2+}–Mg^{2+} exchanges in ternary systems have been determined in the temperature range of 10°C to 80°C. A significant increase of α values at elevated temperatures has been observed in the first two cases while for Ca^{2+}–Mg^{2+} exchange less remarkable temperature dependence of α can be distinguished. This effect has been shown to allow a selective thermostripping of Ca^{2+} and Mg^{2+} from the resins equilibrated at 80°C with sea water in applying cool sea water at 10°C. The thermostripping leads to a selective desorption of both Ca^{2+} and Mg^{2+} while Na^{+} ions remain sorbed, resulting in the increase of Ca^{2+} and Mg^{2+} concentration in the eluate up to 50% (in comparison with the initial sea water) and a decrease of 10% for Na^{+} concentration. These results may be considered as unique in polythermal concentration in comparison with, e.g. conventional evaporation technique. The results of consecutive sorption–thermostripping cycles have shown the possibility to concentrate calcium and magnesium from natural sea water more than three times by applying reagentless (and wasteless as a result) ion-exchange technique. The results of frontal separation of Ca^{2+} and Mg^{2+} on acrylic resin in Na^{+}-form from natural sea water and thermostripping solutions obtained are also presented. The novel approach for forecasting temperature dependences of the resin selectivity has been proposed. The approach is based on a thermodynamic interpretation of the results obtained that allows to predict the temperature dependences of both α (for binary Mg^{2+}–Na^{+} exchange) and the apparent equilibrium constant of ternary Na^{+}–Ca^{2+}–Mg^{2+} exchange.

Keywords: Ion exchange; Calcium; Magnesium; Separation; Dual-temperature concentration; Carboxylic resins, thermodynamics; Carboxylic resins, sea water treatment

1. Introduction

At present, around 25% of overall world production of magnesium is yielded from hydromineral resources (sea water, underground brines and bitterns of some salty lakes) [1]. Traditional methods for producing magnesium by processing hydromineral sources, despite their profitability, do not satisfy growing ecological standards [2]. Consequently, new alternative ecologically clean technologies, based on e.g. ion-exchange separation methods, have to be developed. Several ion-exchange methods for separation of magnesium and calcium have been discussed in the

* Corresponding authors.

SSDI 1381-5148(95)00046-1

literature. Some of them are based on applying complexing agents for enhancing the separation (see, e.g. [3,4]). Barba et al. [5] have applied supersulfonated resins (containing more than 1 sulfogroup per benzene ring of PS–DVB matrix) for the same purpose. The methods mentioned may be called *conventional ion-exchange separation techniques* which are based as a rule on the multistage procedures, involving sorption, desorption (elution) and regeneration steps. To carry out the last two stages one needs the expenditure of auxiliary chemicals that results in production of wastes.

Another group of separation methods is based on the exploitation of the variation of resin affinity towards target ions with temperature for governing the separation process. Parametric pumping technique (see, e.g. [6–11]), dual-temperature ion-exchange processes [12–14] and thermal ion-exchange fractionation [15,16] can be refered to the ion-exchange separation methods of this type. One feature alone makes these separation techniques most attractive. Actually, all of these separation methods allow to exclude the resin regeneration step (completely or partially), which is known to be the main source of wastes in ion-exchange technology. In this sense, ion-exchange processes based on the above mentioned techniques are ecologically clean and practically wasteless. Nevertheless, the practical interest towards these separation methods is still very limited due to the lack of information about ion-exchange systems with properties for designing reagentless and wasteless (as a result) technologies based on the dual-temperature ion-exchange fractionations. One type of conventional ion exchangers has been used in the majority of studies carried out: sulfonic resins (see, e.g. [15,16]). On the other hand, Klein et al. [17] and later Ivanov et al. [18–21] have reported strong temperature dependence of ion-exchange equilibrium in systems including carboxylic resins and the binary model alkali/alkali-earth metal-ions mixtures. Carboxylic ion exchangers have been applied for the recovery of magnesium from sea water after preliminary decalcination on zeolites (see [1, and refs. 35–37 therein]), but no data on dual-temperature ion-exchange concentration and separation of Ca^{2+} and Mg^{2+} from sea water using this type of ion exchangers can be found in the literature. The same concerns with the equilibrium data in ternary ionic systems involving carboxylic resins and sea water metal ions. For that reasons the following problems are studied in this paper:

(1) ion-exchange equilibrium on commercially available carboxylic resins of acrylic and methacrylic types in ternary ionic systems, including the macrocomponents of sea water Mg^{2+}, Ca^{2+} and Na^{+}, at different temperatures;

(2) a novel approach for predicting temperature dependences of resin selectivities from the enthalpies of binary exchange on the same resins.

(3) kinetics of thermodesorption of the studied metal-ions with natural sea water at low temperature from the resin pre-equilibrated with sea water at high temperature.

(4) prediction and experimental determination of concentration factors for Ca^{2+}, Mg^{2+} and Na^{+} in consecutive thermo-sorption–stripping cycles.

(5) frontal separation of the studied metal-ions by the carboxylic resin, and

(6) conditions for the wasteless conversion (regeneration) of the resin.

2. Experimental

2.1. Materials and analytical methods

Samples of the natural Mediterranean sea water used in the present study were obtained from the area near Tarragona (Spain). Natural sea water was boiled and then filtered for removal of organic matter before the use in ion-exchange equilibrium studies. Artificial sea water samples were prepared from NaCl, $MgCl_2$, $CaCl_2$ and Na_2SO_4 (Probus, Spain) of p.a. quality used as received. The composition of artificial sea water used was as follows; ionic species/C (g-equiv/l); Cl^{-}/0.48; Na^{+}/0.40; Mg^{2+}/0.11; Ca^{2+}/0.02; SO_4^{2-}/0.05.

Table 1
Properties of Lewatit carboxilyc ion exchange resins

Property	R 249-K	R 250-K
Funcional group	methacrylic acid	acrylic acid
Capacity	1.3 mol/l	2.9 mol/l
Average pore diameter	270 Å	260 Å
Surface area (BET)	200 m^2/g	100 m^2/g

Macroporous carboxylic ion exchangers Lewatit R 249-K and Lewatit R 250-K were received from Bayer Hispania Industrial, S.A. The main properties of the resins are shown in Table 1 [22].

The concentrations of metal ions were determined by atomic emission spectroscopy using ICP-AES technique with ARL Model 3410 spectrometer (Fisons, U.S.A.) provided with minitorch. Determination of H^+ and OH^- ions were carried out by potentiometric titration using a Crison pH-meter provided with a combined glass electrode.

2.2. Methods

2.2.1. Ion-exchange equilibrium

The ion-exchange equilibrium was studied under dynamic conditions in thermostatic glass columns (inn. diam. = 1.4 cm). The columns were loaded with a certain amount of the ion exchanger which remained constant during the given series of experiments. The total capacity of each resin bed was determined after converting the ion exchangers into Na^+-form with 0.5 M NaOH solution [1] followed by rinsing with 0.5 M NaCl solution and passing a known volume of 0.5 M HCl through the bed. Hydrochloric acid solution was collected into a volumetric flask and its concentration was then determined. The ion-exchange capacity of the resin bed (Q) was calculated as the amount of acid retained by the resin as follows: $Q = V(C_o - C_i)$, where V is the volume of HCl solution passed through the bed, dm^3 and C_o and C_i are the initial and the final concentration of the acid, mol/dm^3, respectively. Then, the resins were converted back into Na^+-form by rinsing with NaCl solution and equilibrated at certain temperature. Initial solution (artificial or natural sea water) was passed through the columns at constant flow rate (3 cm^3/min) up to achieving the equilibrium. The eluate was collected in portions of known volume where concentrations of Na^+, Ca^{2+} and Mg^{2+} were determined. Achieving to ion-exchange equilibrium in the systems under study was controlled by the periodical comparison of metals concentration in the solution leaving the column with that of the feed solution. When the solution from the column outlet had the concentration of Na^+, Mg^{2+} and Ca^{2+} close to the feed solution the flow was stopped and then resumed after certain period of time. The equality of the feed concentration with that of the solution collected after the break was considered as a criterion of achieving the equilibrium in the system. After equilibration, the solution phase was separated from the resin by evacuating with a water pump followed by the stripping with 0.5 M HCl solution. The analysis of Na^+, Mg^{2+} and Ca^{2+} in the corresponding eluate was carried out. Then the resin was converted back into Na^+-form and prepared for the next run. The results of the stripping solution analysis were used to determine the separation factors α^{Ca}_{Na}, α^{Mg}_{Na} and α^{Ca}_{Mg} by the use of the following expression:

$$\alpha^{Me_2}_{Me_1} = \frac{Y_{Me_2}}{Y_{Me_1}} \times \frac{X_{Me_1}}{X_{Me_2}} \quad (1)$$

where Y and X are the equivalent fractions of ions under separation in the resin and solution phases, respectively; indices 1 and 2 are chosen so that $\alpha > 1$.

The values of Na^+, Ca^{2+} and Mg^{2+} concentration in solution samples collected during the equilibration of the resin were used to obtain the respective breakthrough curves (see Fig. 3) and to calculate α^{Ca}_{Mg} values using the technique based on that proposed by Spedding et al. [23] for determination of separation factors for nitrogen isotopes. The technique allows to calculate α values with-

[1] Rinsing with sodium chloride solution was used to suppress the hydrolysis of the resin in Na^+-form which takes place when the rinsing is made just with water.

out the direct analysis of the resin phase composition [24,25] in applying the following equation:

$$\frac{\varepsilon}{1+\varepsilon X_o} = \sum_{i=1}^{j} \frac{V_i C_i (X_o - X_i)}{Q X_o (1 - X_o)} \quad (2)$$

where $\varepsilon = \alpha - 1$; X_o and X_i are the equivalent fractions of the better sorbed ion in the initial mixture and in the "i" eluate fraction, respectively (Ca^{2+} in our case); V_i is the volume of eluate portion "i" (cm^3); C_i is the total concentration of separated ions mixture (meq/cm^3); Q is the full ion-exchange capacity of the resin bed (meq); "j" is the number of eluate fractions where $X_i \neq X_o$.

Values of α_{Mg}^{Ca} determined by the two independent methods (see Eqs. 1 and 2) were characterized by the uncertainties less than ±5% for the first and around ±7% for the second.

2.2.2. Thermostripping and thermosorption

Experiments on thermostripping and thermosorption of Ca^{2+} and Mg^{2+} were carried out using the following technique: after equilibration of the resin with sea water at certain temperature the excess of the equilibrium solution was removed from the column so that its level coincided with that of the resin bed. Then the cooling (in case of thermostripping) or heating (for thermosorption) of the column was started. After reaching the appropriate temperature the sea water was passed through the column and collected in portions followed by the analysis of Ca^{2+}, Mg^{2+} and Na^{+} content. In the series of experiments of consecutive sorption-thermostripping cycles, the composition of the initial solution used in each cycle corresponded to that of the sample of thermostripping solution obtained during the previous cycle which contained the highest concentration of Ca^{2+} and Mg^{2+}.

2.2.3. Kinetics of thermosorption

Kinetic experiments on thermodesorption of Ca^{2+} and Mg^{2+} were carried out in thermostatic columns applying the shallow bed technique [26]. The narrow granulometric fraction of Lewatit R 250-K was obtained by dry sieving of air-dry samples of the resin using 0.42 mm mesh, so, only those resin beads stuck in the holes of the sieve were collected. The average diameter of the beads was determined by microscopic technique and appeared to be 0.053 ± 0.002 cm. The height of the resin bed used was always constant and ~0.5 cm. The resin was pre-equilibrated with the natural sea water at 80°C and at flow rate of 3 cm^3/min, then, the solution was removed from the column and the column was cooled at 10°C. Cold sea water (at 10°C) was passed through the resin bed at high flow rate (43 cm^3/min)[2] and collected in portions where Ca^{2+} and Mg^{2+} concentrations were determined. The degree of the resin bed conversion, F, was calculated from the results of the analysis as follows:

$$F = \frac{\sum_{i}^{j} V_i (C_i - C_o)}{Q_{Me}} \quad (3)$$

where V_i is the volume of eluate sample number "i"; C_i and C_o are the concentrations of Ca^{2+} or Mg^{2+} in the "i" eluate sample and in the initial sea water, respectively, expressed in mequiv/cm^3; Q_{Me} is the capacity of the resin bed towards the ionic species under consideration, and j is the number of eluate sample where $C_i - C_o \leq \Delta C$, ΔC being the absolute uncertainty on the determination of the concentration.

3. Results and discussion

3.1. Ion-exchange equilibrium

3.1.1. Artificial sea water

Temperature dependences of α_{Na}^{Ca} and α_{Na}^{Mg} determined in the experiments with artificial sea water on Lewatit R 249-K and Lewatit R 250-K resins by direct method[3] (using Eq. 1) are

[2] This value of the solution flow rate has been shown to fit the conditions of the "shallow bed" technique.

[3] Since this method of α determination is based on the results of the direct analysis of the phases composition here and further in the text it is called "direct method". The second method used (see Eq. 2) will be mentioned as "indirect method" for α determination.

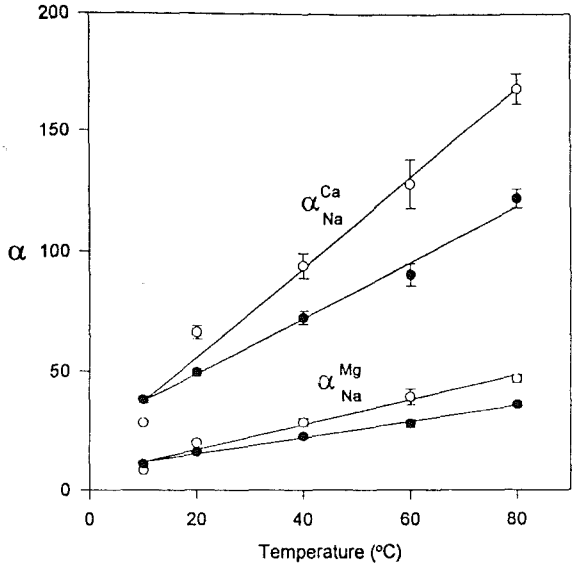

Fig. 1. Temperature dependencies of equilibrium separation factors for Ca^{2+}–Na^+ and Mg^{2+}–Na^+ exchanges from artificial sea water on Lewatit R 249-K (white circles) and Lewatit R 250-K (black circles).

shown in Fig. 1. As seen in Fig. 1, for both acrylic and methacrylic resins, strong positive influence of temperature on their selectivity is observed, i.e. separation factors for Ca^{2+}–Na^+ and Mg^{2+}–Na^+ exchanges increase significantly at elevated temperature. The absolute α values are lower for the acrylic ion exchanger than those determined for the methacrylic one. This results can be attributed to the significant difference in their capacity (see Table 1). The selectivity of ion exchangers are known to decrease with the increase of their capacity [27,28].

The temperature dependences of α^{Ca}_{Na} and α^{Mg}_{Na} are also different (in the first case it is much stronger than in the second). In this case, the difference has to be connected with the respective enthalpies (ΔH) of Ca^{2+}–Na^+ and Mg^{2+}–Na^+ exchange reactions. Despite the separation factor is not a thermodynamically meaningful parameter, it can be associated in certain cases with the thermodynamic equilibrium constant, K, of ion-exchange reaction which can be written as follows [29–31]:

$$\log K = \int_0^1 \log \kappa(Y)\, dY \tag{4}$$

where Y has the same meaning as in Eq. 1 and κ is the dimensionless equilibrium "constant" [31] defined for, e.g. Na^+–Ca^{2+} binary exchange by:

$$\kappa_{Ca,Na} = \frac{Y_{Ca}^{1/2} N_{Na} \gamma_{Na}}{Y_{Na} N_{Ca}^{1/2} \gamma_{Ca}} \tag{5}$$

where N_{Na} and N_{Ca} are the normalities of Na^+ and Ca^{2+} in the equilibrium solution (sea water) and γ_{Na} and γ_{Ca} are the activity coefficients of Na^+ and Ca^{2+} in sea water, respectively. The activity coefficient ratio for sea water is constant and can be included in κ. Equation (5) can be rewritten for the equivalent fraction concentration scale as follows:

$$\kappa_{Ca,Na} = \frac{Y_{Ca}^{1/2} X_{Na}}{Y_{Na} X_{Ca}^{1/2} N_{tot}^{1/2}} \tag{6}$$

where Y and X have the same meaning as above and N_{tot} is the total normality of metal ions in sea water.

Comparison of Eqs. 6 and 1 shows that α^{Ca}_{Na} and $\kappa_{Ca,Na}$ are connected with each other by the following expression:

$$\alpha_{Na}^{Ca} = \kappa_{Ca,Na} \left(\frac{Y_{Ca}^{1/2}}{X_{Ca}^{1/2} N_{tot}^{1/2}} \right) \tag{7}$$

The term in brackets is practically constant, i.e. X_{Ca} = const; N_{tot} = const and $Y_{Ca}^{1/2}$ has practically a constant value at least in the temperature range from 20 to 80°C (see Table 3 below). Since $Y_{Mg}^{1/2}$ remains also practically constant in the same temperature interval, Eq. 7 is applicable for connecting α^{Mg}_{Na} and $\kappa_{Mg,Na}$ and can be rewritten as follows:

$$\alpha_{Na}^{Me} = \kappa_{Me,Na} \times a \tag{8}$$

where Me is Ca^{2+} or Mg^{2+} and $a = Y_{Me}^{1/2} / X_{Mg}^{1/2} N_{tot}^{1/2}$ = const. This allows for attributing the temperature dependences of α^{Ca}_{Na} and α^{Mg}_{Na} to the respective ΔH values determined for the exchange of the same ion couples on carboxylic ion exchanger KB-4 in binary systems [18,32].

Thus, Timofeevskaya et al. determined differential enthalpies in applying ion-exchange technique which appeared to be 8 and 5 kJ/equiv for Ca^{2+}–Na^{+} and Mg^{2+}–Na^{+} exchange, respectively, for concentrated solutions [18]. These values are close to those determined calorimetrically for the exchange in diluted solutions i.e. 8.4 and 7.1 kJ/equiv for the respective ion couples [32]. Smaller ΔH value for Mg^{2+}–Na^{+} exchange in comparison with that of Ca^{2+}–Na^{+} ion-exchange reaction will result in a weaker temperature dependence of α_{Na}^{Mg} than in the case of α_{Na}^{Ca}.

The above qualitative interpretations of α vs T dependences can be confirmed by the quantitative predictions of these dependences for different temperature intervals, which are based on the following approach: the standard enthalpy of ion-exchange reaction corresponding to a complete exchange of one ion by another can be determined as follows:

$$\Delta H^{o} = \int_{0}^{1} \Delta H_{ap}\, dY \tag{9}$$

where Y is the same as in equation (1), and ΔH_{ap} is the apparent enthalpy, depending on Y.

ΔH_{ap} can be determined from the temperature dependences of α through the use of the van't Hoff type equation [33–35]:

$$\Delta H_{ap} = -R\left[\frac{\delta \ln \kappa}{\delta(1/T)}\right] Y_1 \tag{10}$$

where Y_1 corresponds to the equivalent fraction of the higher sorbed component in the resin phase, equilibrated with solution of the given composition (sea water in our case). Equation 10 can be also applied for the quantitative prediction of α vs T dependences. For this purpose Eq. 10 must be integrated (assuming ΔH_{ap} independent of T) and rewritten as follows:

$$Y_1 \ln \frac{\kappa_2}{\kappa_1} = \frac{\Delta H_{ap}}{R}\left(\frac{T_2 - T_1}{T_2 T_1}\right) \tag{11}$$

substituting κ by α from equation (8) gives:

$$Y_1 \ln \frac{\alpha_2}{\alpha_1} = \frac{\Delta H_{ap}}{R}\left(\frac{T_2 - T_1}{T_2 T_1}\right) \tag{12}$$

Since differentiation in Eq. 10 is based on the assumption $Y_1 = \text{const}$, the same condition must be fulfilled for the validity of Eqs. 11 and 12. As seen from Table 3 (see below), Y_{Ca} and Y_{Mg} have practically constant values for both resins studied in the temperature range between 20°C and 80°C. An estimation of ΔH_{ap} for the ternary system under study, assuming the independence of the respective binary exchanges, can be done by applying Eq. 10 and assuming the usual Arrhenius dependences of α vs $1/T$. Such estimation results on the following values: for Na–Mg^{2+} exchange on Lewatit R 250-K, $\Delta H_{ap} = 6.7$ kJ/equiv and 7.4 kJ/equiv for Lewatit R 249-K. For Na–Ca^{2+} exchange $\Delta H_{ap} = 4.1$ kJ/equiv for the first and 4.6 kJ/equiv for the second resin.

As follows from the above values of ΔH_{ap} for Na^{+}–Mg^{2+} exchange, it correlates very well with $\Delta H_{ap} = 7.1$ kJ/equiv reported by Samchemko [32] for the same binary exchange. This testifies to the practical independence of ΔH_{ap} of the resin composition (see Eq. 10) and allows for substituting ΔH_{ap} by ΔH^{o} in this case.

Hence, quantitative predictions of $\ln(\alpha_2/\alpha_1)$ for Na–Mg^{2+} exchange in different $T_2 - T_1$ intervals, can be accomplished using Eq. 12 with $\Delta H_{ap} \approx \Delta H^{o} = 7.1$ kJ/equiv determined independently (calorimetrically). The results of these calculations are presented in Table 2.

As seen from the results given in Table 2, the calculated $\ln(\alpha_2/\alpha_1)$ values demonstrate a satisfactory fit with those determined experimentally in the ternary system.

However, for Na^{+}–Ca^{2+} binary exchange in the ternary system, the results of the quantitative predictions of $\ln(\alpha_2/\alpha_1)$ vs $(T_2 - T_1)$ intervals give remarkable deviations of the experimental values from the computed ones. This disagreement can be attributed by a strong dependence of ΔH_{ap} vs Y that follows from the remarkable difference between estimated ΔH_{ap} values 4.1 and 4.6 kJ/equiv mentioned before, and $\Delta H^{o} = 8$ and 8.4 kJ/equiv reported in the literature [18,32].

Consider now the overall ion-exchange process in the system under study, which can be

Table 2
Temperature dependences of α_{Na}^{Mg} for carboxylic resins, calculated and experimentally determined from artificial sea water

T_2-T_1	Lewatit R 250-K			Lewatit R 249-K			$\ln(\alpha_2/\alpha_1)$ calculated for $\Delta H^o = 7.1$ kJ/mol from Eq. 7
	α_1	α_2	$\ln(\alpha_2/\alpha_1)$ exp.	α_1	α_2	$\ln(\alpha_2/\alpha_1)$ exp.	
353–333	28.12	36.21	0.15	39.53	47.09	0.11	0.14
353–313	22.85	36.21	0.27	28.76	47.09	0.30	0.31
353–293	16.00	36.21	0.47	19.91	47.09	0.51	0.50
333–313	22.85	28.12	0.12	28.76	39.53	0.19	0.16
333–293	16.00	28.12	0.32	19.91	39.53	0.40	0.35
313–293	16.00	22.85	0.21	19.91	28.76	0.21	0.19

Table 3
Composition of resin phases and apparent equilibrium constants of ternary Na^+–Mg^{2+}–Ca^{2+} exchange determined from artificial sea water at different temperatures

T (K)	Lewatit R 250-K				Lewatit R 249-K			
	Y_{Ca}	Y_{Mg}	Y_{Na}	k	Y_{Ca}	Y_{Mg}	Y_{Na}	k
283	0.33	0.50	0.17	9.54	0.31	0.47	0.22	7.35
293	0.31	0.56	0.13	12.89	0.33	0.57	0.10	16.31
313	0.32	0.59	0.09	18.23	0.34	0.59	0.07	23.04
333	0.34	0.58	0.08	22.27	0.35	0.59	0.06	31.02
353	0.34	0.60	0.06	29.09	0.36	0.59	0.05	37.89

described by the following equation:

$$4\,R{-}COONa + Ca^{2+} + Mg^{2+} \rightleftharpoons 2\,R{-}COOCa + 2\,R{-}COOMg + 4\,Na^+ \quad (13)$$

The apparent constant, k, of the above tri-ionic-equilibrium can be written as follows [36–38]:

$$(k)^4 = \frac{Y_{Ca}\,Y_{Mg}}{Y_{Na}^4} \times \frac{X_{Na}^4}{X_{Ca}\,X_{Mg}} \quad (14)$$

where X and Y have the same meaning as in Eq. 1.

The values of k determined by using artificial sea water at different temperatures are collected in Table 3.

Equation 13 can be represented as a superposition of the two equations describing the binary Na^+–Ca^{2+} and Na^+–Mg^{2+} exchanges. Consequently, the standard enthalpy (ΔH_{tot}^o) of ion-exchange reaction 13 is equal to the sum of ΔH^o values for the exchange of the respective ion couples. Following this, an estimation of $\ln(k_2/k_1)$ for different temperature intervals using Eq. 11 and assuming $y_1 \approx 1$ and $\Delta H_{ap} \approx \Delta H_{tot}^o$ can be obtained. The values of ΔH_{tot}^o can be taken from the above references [18,32], i.e. (1) $\Delta H_{tot}^o = 13$ kJ/equiv and (2) $\Delta H_{tot}^o = 15.5$ kJ/equiv. The results of these calculations are presented in Table 4.

Table 4
Calculated and experimentally determined $\ln(k_1/k_2)$ for Na^{2+}–Ca^{2+}–Mg^{2+} equilibrium on carboxylic resins at different temperatures (see text)

T_2-T_1	Calculated		Experimental	
	(1)	(2)	Lewatit R 250-K	Lewatit R 249-K
353-333	0.27	0.32	0.27	0.20
353-313	0.57	0.68	0.47	0.50
353-293	0.91	1.08	0.81	0.84
353-283 [a]	1.10	1.31	1.12	1.64
333-313	0.30	0.36	0.20	0.30
333-293	0.64	0.76	0.55	0.64
333-283 [a]	0.83	0.99	0.85	1.44
313-293	0.34	0.41	0.35	0.34
313-283 [a]	0.53	0.63	0.65	1.14
293-283 [a]	0.19	0.22	0.30	0.20

(1) $\Delta H_{tot} = 13$ kJ/mol; (2) $\Delta H_{tot} = 15.5$ kJ/mol.
[a] The data refered to the temperature intervals involving 283 K have been included to illustrate that the deviations of Y_{Ca} and Y_{Mg} from the constant values (see Table 4) result in the stronger disagreement of experimental and calculated results (see text).

Comparison of the results shown in Table 4 testifies to the correction of the approach proposed and to the validity of the assumptions made. As seen from Table 4 the values of $\ln(k_1/k_2)$ calculated from $\Delta H^{\circ}_{tot} = 13$ kJ/equiv are in a better agreement with those determined experimentally. This indicates that ΔH° values determined for the binary Na^{+}–Ca^{2+} and Na^{+}–Mg^{2+} exchanges in concentrated solutions [18] are most appropriate for the description of the temperature dependence of ion-exchange equilibrium in the ternary system under study.

With respect to Ca^{2+}–Mg^{2+} exchange, the temperature dependences of α^{Ca}_{Mg} for Lewatit R 250-K and R 249-K resins are presented in Fig. 2 where α^{Ca}_{Mg} is obtained by direct and indirect methods. The problem of elucidating the temperature influence on Ca^{2+}–Mg^{2+} exchange is complicated because of the weak temperature effect obtained (much weaker than in the previous two cases discussed) which was expected from the corresponding value of $\Delta H = 3$ kJ/equiv [18]. As seen from the data shown in Fig. 2, α^{Ca}_{Mg} values determined by indirect method demonstrate a slight increase with the increase of temperature for both ion-exchange resins studied while the direct method does not allow to distinguish any clear influence of temperature on α. This disagreement of α values determined by different methods may be associated with one feature of the indirect method which makes it advantageous in comparison with the direct one. Determination of α by indirect method is carried out *without separation of phases* after equilibration, which is known to be the source of additional and hardly measurable experimental errors [24]. This is particularly true for the ion-exchange equilibrium on carboxylic resins at different temperatures, since equilibrium, in this case, may be easily shifted due to either hydrolysis of ion exchanger (in applying rinsing technique) or indefinite change of the temperature inside the column (evacuating solution with water pump is accompanied by filtration of cool air through the resin bed). For a better elucidation of the temperature dependence on the separation of magnesium and calcium, some additional information has been applied. This information can be extracted from concentration–volume histories (breakthrough curves) obtained in each experiment carried out for phases equilibration, see Fig. 3. As seen in Fig. 3, the sorption front of

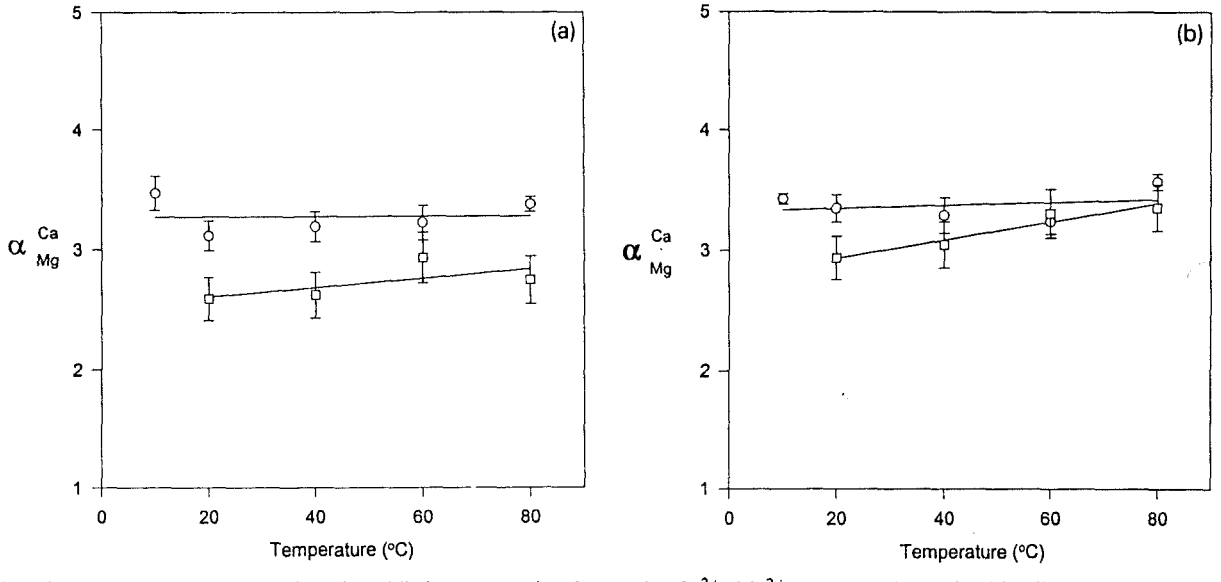

Fig. 2. Temperature dependencies of equilibrium separation factors for Ca^{2+}–Mg^{2+} exchange determined by direct (squares) and indirect (circles) methods from artificial sea water by Lewatit R 250-K (a) and Lewatit R 249-K (b) resins.

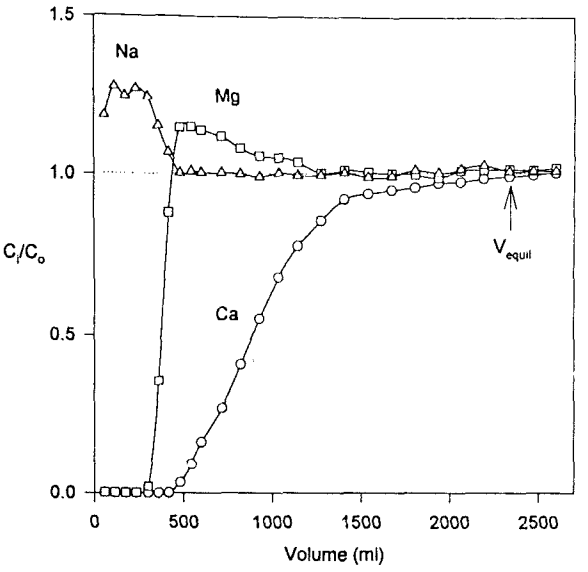

Fig. 3. Concentration–volume history of frontal separation of Mg^{2+} and Ca^{2+} by Lewatit R 250-K resin in Na^+-form at 80°C. $Q = 57$ meq.

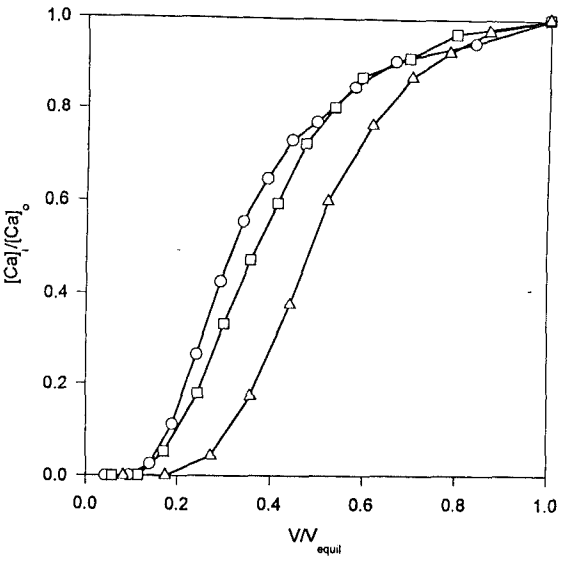

Fig. 4. Influence of temperature on relative length of calcium sorption fronts for artificial sea water on Lewatit R 249-K: 20°C (circles), 40°C (squares) and 80°C (triangles).

Ca^{2+} can be chosen as one of the parameters for characterization of Mg^{2+} and Ca^{2+} separation at different temperatures. Since the experimental conditions influencing the length of this front, such as solution concentration and flow rate, were kept constant in all the experiments, any alteration of the front position can be evidently attributed to the change of the temperature of the system. This is clearly observed from the data shown in Fig. 4 where the relative lengths of calcium sorption fronts at different temperatures are shown for Lewatit R 249-K. A similar effect was observed for Lewatit R 250-K. In this figure, V_{equil} was obtained from the corresponding concentration–volume histories by determining the volume of solution passed through the column before achieving the equilibrium. The values of V_{equil} applied to calculate the data plotted in Fig. 4 were 1220 ml for Lewatit R 250-K ($Q = 32$ meq)[4] 600 ml for Lewatit R 249-K ($Q = 13$ meq). The relative error for the determination of V_{equil} was around 5%. The variations of V_{equil} with the temperature lied within the corridor of experimental errors.

The data shown in Fig. 4 demonstrate that the front of Ca^{2+} shifts remarkably to the right with the increase of the temperature. This shift will result on the increase of the separation degree of Mg^{2+} and Ca^{2+} (which can be determined as the ratio of their concentrations in the respective solutions samples) in the head part of the breakthrough curve (see Fig. 3). This is confirmed by the data presented in Fig. 5 where the separation degrees of Mg^{2+} and Ca^{2+} for the head parts of concentration–volume histories obtained on Lewatit R 250-K at different temperatures are shown.

3.1.2. Natural sea water

Ion-exchange equilibrium. Experiments on studying ion-exchange equilibrium in Mg^{2+}–Ca^{2+}–Na^+ system on Lewatit R 250-K and Lewatit R 249-K resins from natural sea water were carried out at two temperatures: 10°C and 80°C assuming the temperature dependences of α_{Na}^{Ca}, α_{Na}^{Mg} and α_{Mg}^{Ca} to be practically linear as was demonstrated in the experiments with artificial sea water. Re-

[4] Note that the capacity of the resin bed used in this series of experiments was approximately twice less than that applied in the frontal separation of Ca^{2+} and Mg^{2+} shown in Fig. 3.

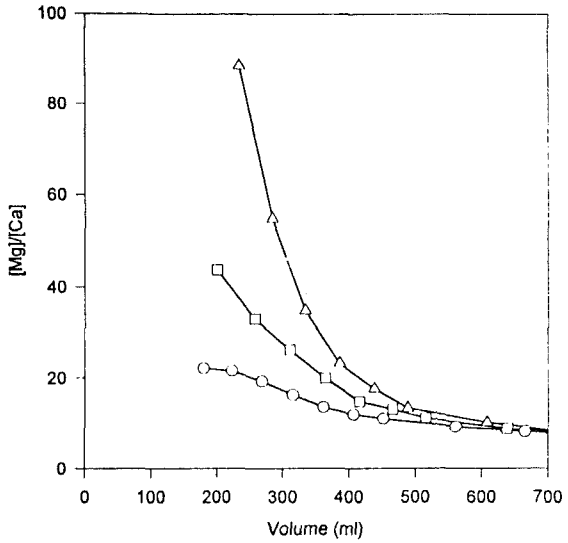

Fig. 5. Ratios of Mg^{2+} and Ca^{2+} concentrations (Mg^{2+} purification degree) in solution samples collected in frontal separation from artificial sea water by Lewatit R 250-K in Na^+-form at different temperatures: 20°C (circles), 60°C (squares) and 80°C (triangles).

sults of this series of experiments are presented in Table 5 where the values of α for the three ion couples studied for the ternary system and k are tabulated. For α_{Mg}^{Ca} the values were determined by both the direct and the indirect methods.

As seen in Table 5, α values for Ca^{2+}–Na^+ and Mg^{2+}–Na^+ exchanges determined from samples of natural sea water are much smaller than those determined from artificial sea water (cf. Fig. 1) while for Ca^{2+}–Mg^{2+} exchange they are similar to these shown in Fig. 2 for artificial solutions. This difference can be attributed

Table 5
Values of α for the binary exchanges Ca^{2+}–Na^+, Mg^{2+}–Na^+ and Ca^{2+}–Mg^{2+} and k for the ternary Na^+–Ca^{2+}–Mg^{2+} exchange on carboxylic resins from natural sea water at 10 and 80°C

Lewatit resin	t (°C)	α_{Na}^{Ca}	α_{Na}^{Mg}	α_{Mg}^{Ca}		k
				direct	indirect	
R 249-K	10	21.8	7.41	2.94	2.79	6.04
	80	32.8	9.90	3.31	3.46	8.01
R 250-K	10	31.0	10.2	3.05	2.60	8.09
	80	40.2	12.6	3.19	3.28	9.78

to the higher total ionic concentration in natural sea water samples received, in particular sodium concentration, in comparison with that in artificial sea water[5] prepared by following the reported data in the literature (see, e.g. [2, p. 26]). Therefore the decrease of α_{Na}^{Ca} and α_{Na}^{Mg} can be ascribed to the electroselectivity effect [39]. As follows from Eq. 7 the increase of N_{tot} results to the decrease of α values. Nevertheless, the trend in changing α values with temperature for different ion couples is similar to that observed in artificial sea water and also follows the order of differential enthalpy values for the respective ion-exchange reactions (see above). Comparison of α_{Mg}^{Ca} values determined by different methods (see Table 5) demonstrates that the indirect method allows for a better elucidation of temperature dependence of α than the direct method (as discussed above).

The influence of temperature on the separation of Ca^{2+} and Mg^{2+} from natural sea water by Lewatit R 250-K resin under dynamic conditions in column is illustrated by the data presented in Fig. 6, where the positions of calcium sorption front at 10°C and 80°C (a) and magnesium purification degree (b) are shown. As seen in Fig. 6a the increase of temperature in the system leads to remarkable retardation of calcium front that results in a more effective separation of Ca^{2+} from Mg^{2+} (see Fig. 6b).

The results obtained for the ion-exchange equilibrium of the ternary Ca^{2+}–Mg^{2+}–Na^+ system on carboxylic resins both acrylic and methacrylic ion exchangers from artificial and natural sea water can be used to carry out a dual-temperature ion-exchange concentration. The higher capacity of the acrylic resin provides with a better characteristics for this application.

Kinetics of thermodesorption. The results of studying kinetics of thermodesorption of Ca^{2+} and Mg^{2+} in eluting with natural sea water at 10°C from Lewatit R 250-K pre-equilibrated

[5] Chronologically samples of natural sea water have been received after carrying out experiments with artificial solutions.

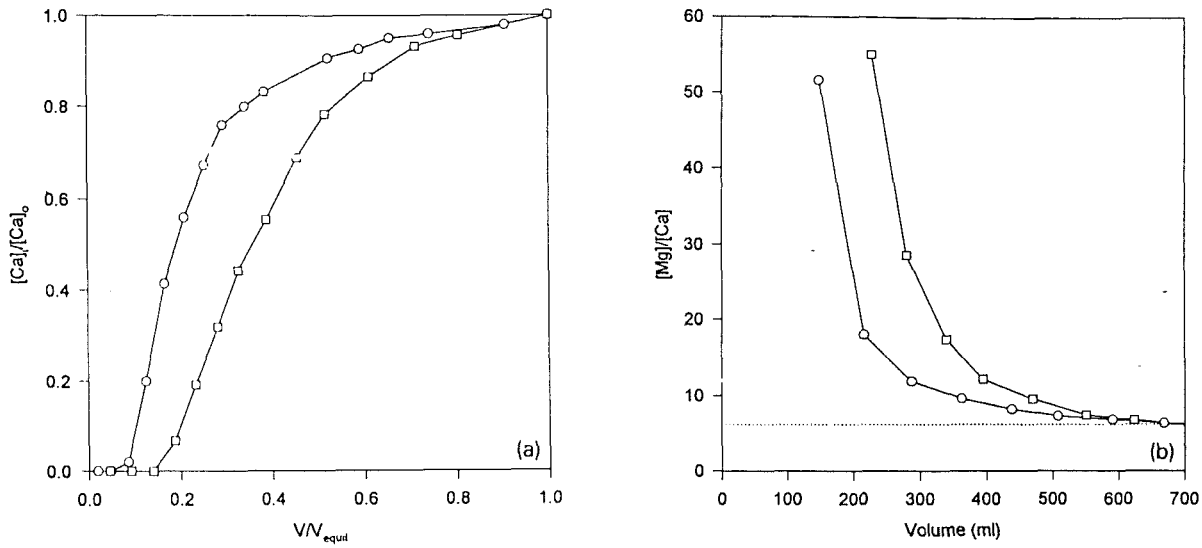

Fig. 6. Influence of temperature on relative length of calcium sorption fronts, (a), and Mg^{2+} purification degree (see Fig. 5), (b), in frontal separation of Ca^{2+} and Mg^{2+} from natural sea water by Lewatit R 250-K resin in Na^{+}-form at 10°C (circles) and 80°C (squares).

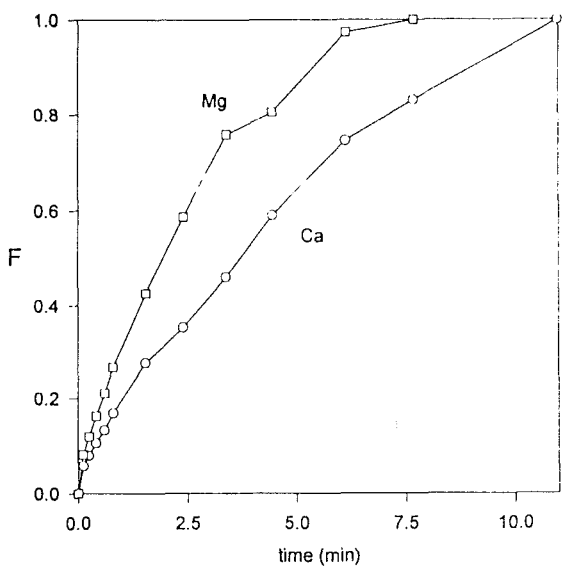

Fig. 7. Kinetics of thermodesorption of Ca^{2+} and Mg^{2+} from Lewatit R 250-K with natural sea water (see text).

with sea water at 80°C are presented in Fig. 7 where the kinetics curves for ions under study are shown. As seen in Fig. 7 Mg^{2+} demonstrates a higher rate of release than Ca^{2+}. The values of the time of half conversion ($t_{0.5}$) estimated from the respective kinetic curves appeared to be 114 s for Mg^{2+} and 222 s for Ca^{2+}. The diffusion coefficients, $\overline{D}$, of Ca^{2+} and Mg^{2+} in the resin phase have been estimated assuming the kinetics of thermodesorption to be controlled by the intraparticle diffusion and by applying the following equation [40]:

$$\overline{D} = 0.03\frac{r_o^2}{t_{0.5}} \tag{15}$$

where r_o is the radius of the resin beads in a swollen state = 0.0265 cm for the resin fraction used.

The calculated values have been found to be $\approx 1.0 \times 10^{-7}$ cm^2 s^{-1} for Mg^{2+} and 1.9×10^{-7} cm^2 s^{-1} for Ca^{2+}, which correlates with the respective data for alkali-earth metal ions [26, p. 90]. The results obtained indicate that no kinetic difficulties in carrying out the thermostripping of Ca^{2+} and Mg^{2+} from the resin can be expected.

3.2. Dual-temperature ion-exchange concentration

Concentration–volume histories obtained by thermostripping at 10°C from Lewatit R 250-K equilibrated at 80°C with natural and artificial

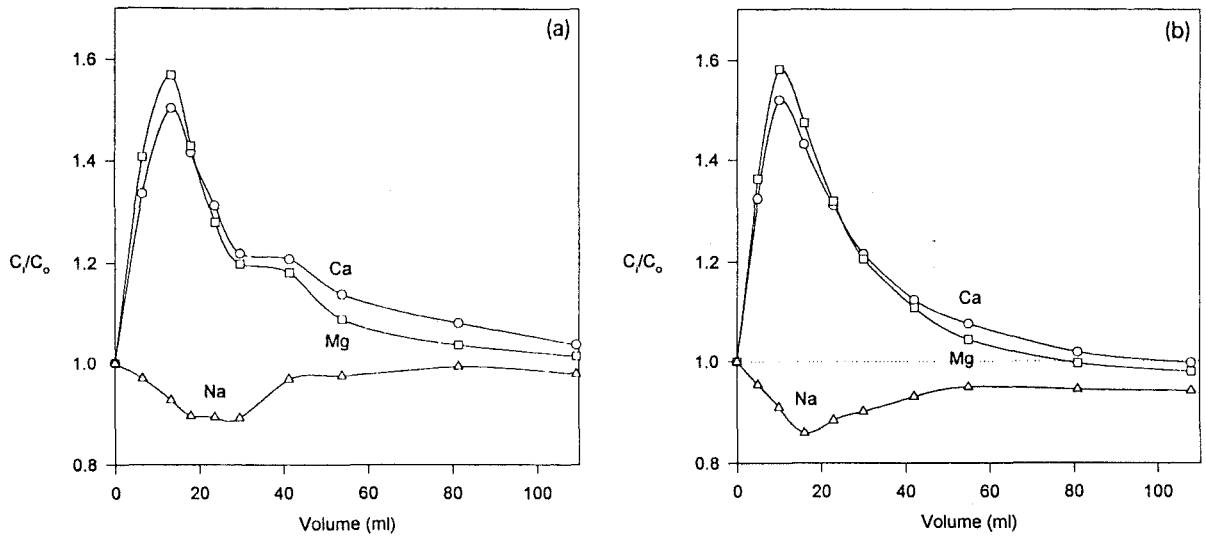

Fig. 8. Thermostripping breakthrough curves for natural (a) and artificial (b) sea water from Lewatit R 250-K resin. Na^+ (triangles), Ca^{2+} (circles) and Mg^{2+} (squares).

sea water are shown in Fig. 8a and b, respectively. The total capacity of the resin bed used in this series of experiments was 57 mg-equiv. Cooled sea water was passed at 1.5 cm^3/min of flow rate. As seen in Fig. 8 thermostripping leads to a selective desorption of both Ca^{2+} and Mg^{2+} from the resin while Na^+ ions are sorbed. This results in the increase of divalent metal ions concentration in eluate and decrease of sodium concentration. This situation may be considered as unique in polythermal concentration in comparison with, e.g. conventional evaporation technique which allows for increasing the concentration of all components of the solution under treatment.

In the case of Lewatit R 249-K resin, results of thermostripping have shown that the maximum concentration degree (C_i/C_o) of Ca^{2+} and Mg^{2+} for this ion exchanger do not exceed 38% while for Lewatit R 250-K this parameter is much higher (see Fig. 8). This confirms the conclusion given above about the better applicability of the acrylic resin for dual-temperature ion-exchange concentration.

After the thermostripping, the resin phase appears unloaded with Ca^{2+} and Mg^{2+} and becomes able to sorb them again without any additional treatment (regeneration). Passing hot sea water through the resin bed depleted after thermostripping leads to thermosorption of Ca^{2+} and Mg^{2+} as shown in Fig. 9.

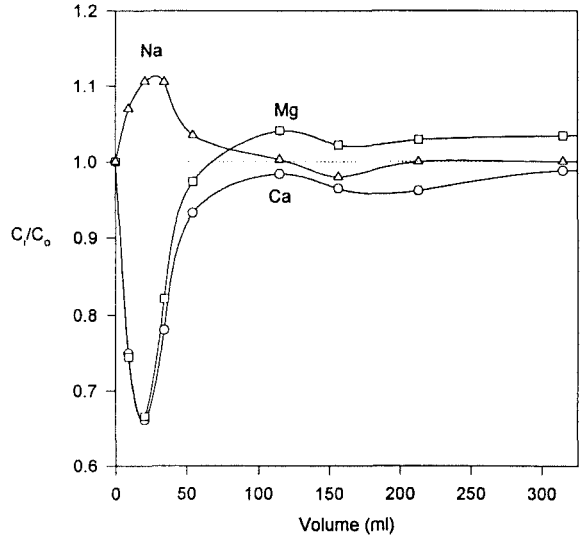

Fig. 9. Thermosorption breakthrough curve for natural sea water on Lewatit R 250-K resin. Na^+ (triangles), Ca^{2+} (circles) and Mg^{2+} (squares).

Solution collected during thermostripping (with increased concentration of Ca^{2+} and

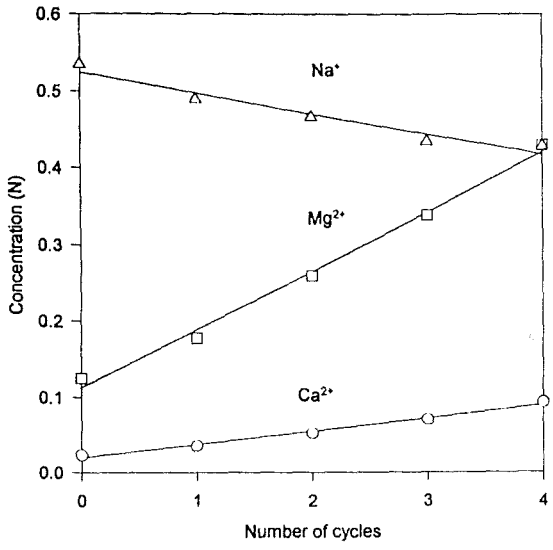

Fig. 10. Concentrations of Ca^{2+}, Mg^{2+} and Na^{+} obtained in consecutive thermo-sorption-stripping cycles vs number of cycle.

Mg^{2+}) can be underwent the repetitive thermosorption–thermostripping cycle where the next concentrate of Ca^{2+} and Mg^{2+} is yielded. Carrying out several concentration cycles has to result to the further increase of Ca^{2+} and Mg^{2+} and decrease of Na^{+} concentrations. The results of 4 consecutive thermo-sorption–stripping cycles carried out are shown in Fig. 10. As seen in Fig. 10 both Ca^{2+} and Mg^{2+} concentration grows practically linear while also a linear decrease of Na^{+} concentration takes place. This allows for the following description of the dual-temperature ion-exchange concentration process observed:

$$c_i = \prod_{i=1}^{i} a_i c_o \tag{16}$$

where a_i is the concentration factor; c_o and c_i are the concentrations of Ca^{2+}, Mg^{2+} or Na^{+} in the initial sea water and in the stripping solution after "i" cycle, respectively. The values of concentration factor a_i determined for Ca^{2+}, Mg^{2+} and Na^{+} in consecutive thermo-sorption–stripping cycles are tabulated in Table 6, where the products of a_i values for each metal ion are also presented.

Table 6
Concentration factors (a_i) for Ca^{2+}, Mg^{2+} and Na^{+} obtained by consecutive thermo-sorption–stripping cycles on Lewatit R 250-K resin

Cycle	Ca^{2+}	Mg^{2+}	Na^{+}
1	1.64	1.69	0.95
2	1.44	1.43	0.95
3	1.30	1.27	0.94
4	1.27	1.22	0.97
$\prod_{i=1}^{4} a_i$	3.90	3.74	0.82

As follows from the data given in Table 6 the concentration factors of Ca^{2+} and Mg^{2+} demonstrate a clear trend to decrease from cycle to cycle while this parameter remains practically constant in the case of Na^{+}. On the other hand, the values of a_i can be predicted from the results of the first cycle in the following way:

$$a_i = \frac{C_i}{C_i - 1} = \frac{C_o + N\Delta C}{C_o + (N-1)\Delta C} \tag{17}$$

After rearrangements one obtains:

$$a_i = 1 + \frac{\Delta C}{C_o + (N-1)\Delta C} \tag{18}$$

where ΔC is the absolute increase of a given metal ion concentration in thermostripping solution after the first cycle, C_o is the same as in Eq. 16, and N is the number of cycles carried out.

As follows from Fig. 10, ΔC values remain constant for both Ca^{2+}, Mg^{2+} and for Na^{+}. This allows for computing a_i vs N dependences for each component of the sea water. The results of these calculations and the experimental a_i values are shown in Fig. 11. Comparison of the computed (curves) and the experimental (points) results shows that Eq. 18 can be successfully applied for predicting concentration degrees for all metal ions under study after any thermosorption–thermostripping cycle. The decrease of concentration factors in the case of Ca^{2+} and Mg^{2+} can be attributed to the increase of their concentration in solution after each cycle that results in the decrease of α_{Na}^{Ca} and α_{Na}^{Mg} values (see above). This can be observed from the data given in Table 7, where α values for Ca^{2+}–Na^{+},

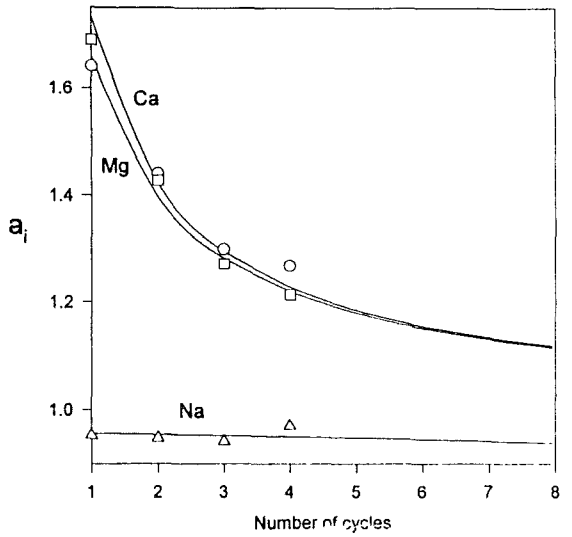

Fig. 11. Computed (curves) and experimental (points) values of concentration factors vs number of thermosorption (80°C)/thermostripping (10°C) cycles. Na^+ (triangles), Ca^{2+} (circles) and Mg^{2+} (squares), using Lewatit R 250-K.

Table 7
Separation factors of Ca^{2+}–Na^+, Mg^{2+}–Na^+ and Ca^{2+}–Mg^{2+} exchanges on Lewatit R 250-K from thermostripping concentrates obtained t = 10°C.

No. cycle	α_{NaCa}	α_{Na}^{Mg}	α_{Mg}^{Ca}	Total concentration (g-equiv/dm^3)
1	38.2	11.03	3.47	0.72
2	33.2	9.79	3.39	0.78
3	26.4	7.95	3.32	0.84
4	21.3	6.66	3.33	0.95

Mg^{2+}–Na^+ and Ca^{2+}–Mg^{2+} ion-exchange reactions on Lewatit R 250-K resin at 10°C from the respective thermostripping solutions (artificially prepared) are tabulated.

3.3. Separation of Mg^{2+} and Ca^{2+}

As follows from the data shown in Table 7 α_{Mg}^{Ca} values remain practically constant (and sufficiently high) in all thermostripping solutions obtained. This allows to carry out the final purification of Mg^{2+} from Ca^{2+} which can be carried out in applying frontal separation on acrylic cation exchanger in Na^+-form. The concentration–volume history of this process is similar to that shown above in Fig. 3 and is characterized by the formation of a solution zone containing pure Mg^{2+} free from Ca^{2+} impurities. Several experiments carried out with stripping solutions on frontal separation of Mg^{2+} and Ca^{2+} have shown similar results to those presented in Fig. 3. The width of pure Mg^{2+} zone depends on the height of the resin bed and could be easily increased, e.g. by carrying out the process in the counter current column [41].

One additional problem has to be solved for carrying out the final separation of Mg^{2+} and Ca^{2+}. This problem deals with the preparation of the resin in Na^+-form, i.e. the resin regeneration. This process can be fulfilled in two stages: (1) removal of all ionic species from the resin with acid solution, and (2) conversion of the resin from H^+ into Na^+-form by treatment with alkali solution. The completeness of each stage can be followed by controlling pH of solution leaving the column.

The results of the experiment on the regeneration of Lewatit R 250-K resin after carrying out the separation of Mg^{2+} and Ca^{2+} from thermostripping solution concentrate (3rd cycle) are presented in Fig. 12.

As seen, in Fig. 12a the complete removal of all metal ions sorbed (Na^+, Ca^{2+} and Mg^{2+}) needs practically equivalent expenditure of HCl solution. As follows from the data shown in Fig. 12b the final conversion of the resin into Na^+-form needs also equivalent amount of NaOH solution.

The composition of the solution yielded after regeneration with acid allows for mixing it with thermostripping solution used in separation of Mg^{2+} and Ca^{2+} so it can be returned back into the process. This means that even during the regeneration of the resin practically no wastes are produced.

Acknowledgements

This work has been carried out with the financial support of CICYT, the Spanish Com-

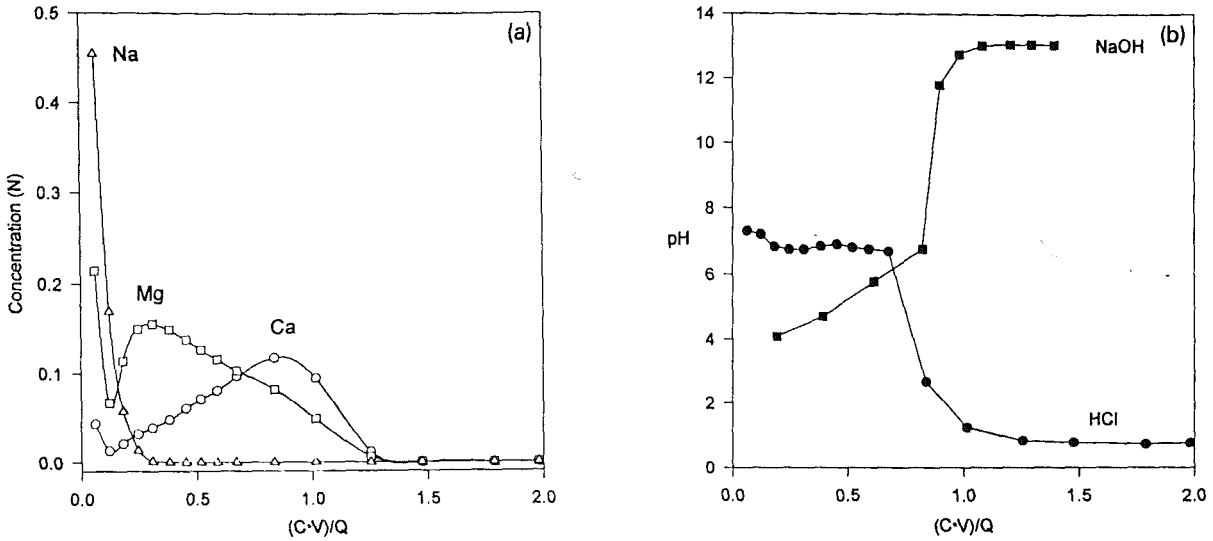

Fig. 12. Regeneration of Lewatit R 250-K with HCl and NaOH solutions after thermostripping (see text): V and C are volume and concentration of the regenerant solution; Q is the capacity of the resin bed.

mission for Research and Development, project PTR930009. The authors are indebted to Mrs. Maria Oleinikova for her assistance in preparation of the manuscript. Bayer Hispania Industrial, S.A. is gratefully acknowledged for supplying with samples of Lewatit resins.

References

[1] R. Khamizov, D. Muraviev and A. Warshawsky. In: J. Marinsky and I. Marcus (Eds.) Ion Exchange and Solvent Extraction, Vol. 12. Marcel Dekker, New York, 1995, p. 93.
[2] J.L. Mero. The Mineral Resources of the Sea. Elsevier Publishing Co., New York, 1965, p. 34.
[3] M. Marhol and K.L. Cheng, Anal. Chem., 42(6) (1970) 652.
[4] M.D. Arguello and J.S. Fritz, Anal. Chem., 49(11) (1977) 1595.
[5] D. Barba, V. Brandani and P.U. Foscolo, Desalination, 48 (1983) 133.
[6] H.T. Chen. In: P.A. Schweitzer (Ed.) Handbook of Separation Techniques for Chemical Engineers. McGraw-Hill, New York, 1979, p. 467.
[7] G. Grevillot. In: N.P. Cheremisinoff (Ed.) Handbook for Heat and Mass Transfer. Gulf Publ., West Orange, NJ USA, 1985, p. 427.
[8] D. Tondeur and G. Grevillot. In: A.E. Rodrigues (Ed.) Ion Exchange: Science and Technology, NATO ASI Vol. 107. Martinus Nijhoff, Dordrecht, 1986, p. 369.
[9] P.C. Wankat. In: A.E. Rodrigues and D. Tondeur (Eds.), Percolation Processes, Theory and Applications. Sijthoff and Noordhoff, Alphen aan den Rijn, 1978, p. 443.
[10] T. Szanya, L. Hanak and R. Mohila, Zhur. Prikl. Khim., 56, (1986) 2194 (in Russian).
[11] T. Szanya, L. Hanak and R. Mohila, Hung. J. Ind. Chem. Veszp., 16 (1988) 21.
[12] B.M. Andreev, G.K. Boreskov and S.G. Katalnikov, Khim. Prom., 6 (1961) 389 (in Russian).
[13] V.I. Gorshkov, A.M. Kurbanov and N.V. Apolonnik, Zhur. Fiz. Khim., 45 (1971) 2969 (in Russian).
[14] V.I. Gorshkov, M.V. Ivanova, A.M. Kurbanov and V.A. Ivanov, Vestnik Moskov. Univ., Ser. Khim., 5 (1977) 535 (in Russian); English translation in Moscow Univ. Bull., 32 (1977) 23.
[15] M. Bailly and D. Tondeur, J. Chromat., 201 (1980) 343.
[16] M. Bailly and D. Tondeur, J. Chem. E. Symp. Ser., 54 (1978) 111.
[17] G. Klein, M. Villena-Bianco and T. Vermeulen, Process Design Develop., 3 (1964) 280.
[18] V.D. Timofeevskaya, V.A. Ivanov and V.I. Gorshkov, Russ. J. Phys. Chem., 62(2) (1988) 1314.
[19] V.A. Ivanov, V.D. Timofeevskaya, V.I. Gorshkov and T.V. Eliseeva, High-Purity Substances, 4(2) (1990) 309.
[20] V.A. Ivanov, V.D. Timofeevskaya, V.I. Gorshkov and T.V. Eliseeva, Russ. J. Phys. Chem., 65(9) (1991) 1296.
[21] V.A. Ivanov, V.D. Timofeevskaya and V.I. Gorshkov, React. Polym., 17 (1992) 101.
[22] Lewatit Product Information, Edition Jan. 1993, Bayer, Leverkusen.
[23] F.H. Spedding, J.E. Powell and H.J. Svec, J. Am. Chem. Soc., 77 (1955) 6125.
[24] V.I. Gorshkov, In: B. Nykolsky (Ed.) Thermodynamics of Ion Exchange, Nauka, Minsk, 1968, p. 122 (in Russian).
[25] D.N. Muraviev, A.V. Chanov, A.M. Denisov, F. Omarova and S.R. Tuikina, React. Polym., 17 (1992) 29.

[26] K. Dorfner. In: K. Dorfner (Ed.) Ion Exchangers. Walter de Gruyter, Berlin–New York, 1991, p. 94.
[27] K. Dorfner. In: K. Dorfner (Ed.) Ion Exchangers. Walter de Gruyter, Berlin–New York, 1991, p. 339.
[28] D. Muraviev, Chem. Scripta, 29 (1989) 9.
[29] E. Ekedahl, E. Högfeldt and L.G. Sillén, Acta Chem. Scand., 4 (1950) 556.
[30] E. Högfeldt, Arkiv Kemi, 5 (1952) 147.
[31] E. Högfeldt. In: K. Dorfner (Ed.) Ion Exchangers. Walter de Gruyter, Berlin–New York, 1991, p. 581.
[32] Z.A. Samchenko, E.F. Nekrjach and O.D. Kurilenko, Zhur. Fiz. Khim., 41(10) (1975) 1042.
[33] K.A. Kraus and R.J. Raridon. J Phys. Chem., 63 (1959) 1901.
[34] O.D. Bonner and J.R. Overton, J. Phys. Chem., 65 (1961) 1599.
[35] G.L. Starobinets and V.S. Soldatov, Zhurn. Fiz. Khimii. 37 (1963) 294.
[36] V.S. Soldatov and V.A. Bychkova. Ion Exchange Equilibria in Multicomponent Systems. Nauka i Tekhnika, Minsk, 1988, p. 86.
[37] P. Fletcher and R.P. Townsend, J. Chem. Soc. Farad. Trans. 2, 77(6) (1981) 955.
[38] P. Fletcher and R.P. Townsend, J. Chem. Soc. Farad. Trans., 77(11) (1981) 2077.
[39] F. Helfferich. Ion Exchange. McGraw-Hill. New York, 1962.
[40] F.G. Helfferich and Hwang Yng-Long. In: K. Dorfner (Ed.) Ion Exchangers. Walter de Gruyter, Berlin–New York, 1991, p. 1288.
[41] V.I. Gorshkov. In: J. Marinsky and I. Markus (Eds.) Ion Exchange and Solvent Extraction, Vol. 12. Marcel Decker, New York, 1995, p. 29.

ANEXO II

ELSEVIER SCIENCE B.V.

Log-In Department

Molenwerf 1
1014 AG Amsterdam
The Netherlands

P.O. Box 2759
1000 CT Amsterdam
The Netherlands

Tel (+31) 20 485 3911

gopher.elsevier.nl
URL: http://www.elsevier.n

Dr. M. Valiente
Universitat Autonoma de Barcelona
Dept. de Quimica
E-08193 Bellaterra(Barcelona)
Spain

Tel: [not available]
Fax: 34 3 5811985
E-mail: iqan3@cc.uab.es

Amsterdam, 8 July 1996

Re: **Application of the reagentless dual-tempaerature ion-exchange techniqu**
to be published in: **Hydrometallurgy**
editor reference: **NJS1064**

Our reference: **HYDROM 1493**

Dear Dr. Valiente,

We have just received your article for publication. On behalf of Elsevier Science, I would like to take this opportunity to thank you for choosing our journal as your publishing medium.

From the details supplied by the journal editor, we have logged your address, telephone, fax and E-mail numbers (if available). Please check that the details are correct and complete so that we can contact you quickly if necessary.

Enclosed you will find a copyright transfer and offprint order form:

Copyright transfer: Articles are accepted for publication on the understanding that authors will transfer copyright to the publisher - please read and complete the form, and return the original by mail.
Offprint order: With this form you can claim your free offprints and order additional copies at the prices given. Your article is estimated to be 16 printed pages. Even if you only want free offprints you must return the order form.

If any questions or problems arise, please do not hesitate to contact us by fax or E-mail.

Yours sincerely,
Elsevier Science

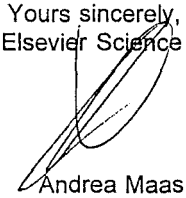

Andrea Maas
Desk Editorial Assistant

P.O. Box 2759
1000 CT Amsterdam
Fax: (+31-20) 485 3239
E-mail: a.maas@elsevier.nl

[HPLAS4.ARM 13-09-95]

Imprints:
Elsevier
Pergamon
North-Holland
Excerpta Medica

Bankers: Hollandsche Bank-U
Rotterdam 62.30.60.493
HR Amsterdam 33158992

APPLICATION OF THE REAGENTLESS DUAL-TEMPERATURE ION-EXCHANGE TECHNIQUE TO A SELECTIVE SEPARATION AND CONCENTRATION OF COPPER VERSUS ALUMINUM FROM ACIDIC MINE WATERS

Dmitri Muraviev[1], Joan Noguerol and Manuel Valiente[*]

Departament de Química (Química Analítica), Universitat Autònoma de Barcelona,

E-08193 Bellaterra (Barcelona), Spain.

Fax: 34-3-5811985, E-mail: IQAN3@CC.UAB.ES

---

[*]Author for correspondence.

[1]On Sabbatical leave from Dept. of Physical Chemistry. Moscow State University (Russia).

ABSTRACT

Acidic mine waters represent natural effluents from pyritic ore deposits and they are mainly characterized by a low pH and a high concentration of metal ions such as Fe^{3+}, Zn^{2+}, Cu^{2+}, Mn^{2+}, Al^{3+}, Ca^{2+}, Mg^{2+} and Na^{+}. The treatment of these waters is of great economical and ecological importance. The present study was targeted to the development of reagentless and wasteless dual-temperature ion-exchange technique for concentrating copper from the natural acidic mine waters of Rio Tinto area (Huelva, Spain). The work has been performed in applying carboxylic ion exchanger (Lewatit R 250-K) and iminodiacetic resin (Lewatit TP-207). Values of the resin capacity towards mine water metal ions and the equilibrium separation factors (α) for different metal ion couples have been determined at different temperatures in the range from 20°C to 80°C. Acrylic resin has been found selective towards Al^{3+} and iminodiacetic resin demonstrates high selectivity towards Cu^{2+}. Furthermore, the sorbability of Al^{3+} increases while that of Cu^{2+} decreases with temperature for both resins. This effect gives the possibility for a selective thermostripping of Cu^{2+} from the resins pre-equilibrated with cold mine water (at 20°C) using hot mine water at 80°C. The increase of Cu^{2+} concentration in the eluate is 30% for acrylic resin and 20% for iminodiacetic resin. The concentration of Al^{3+} in stripping solution drops to 50% level in the first case and to 70% level in the second.

INTRODUCTION

The treatment of acidic metal-bearing effluents is both of economical and of ecological importance. This means that not only the most valuable or toxic constituents must be removed and recovered from the water under treatment, but also the technology applied for this purpose has to satisfy both economical requirements and ecological standards. In other words, this particular technology must be (1) adapted for the selective recovery of certain ionic species and (2) be ecologically clean, i.e. be practically wasteless.

There are a number of processes which are commonly exploited for removal and/or recovery of metals from waters and waste waters [1-7]. These processes can be classified into two groups:

1) non-specific treatment technologies such as precipitation and evaporation; and

2) recovery technologies involving extraction, membrane separation, electrowinning and ion-exchange.

The main pros and contras of all the techniques mentioned have been discussed in the literature [see, e.g. ref. 6,7]. The primary disadvantages of ion-exchange relate to the resin regeneration step which is known to be the main source of wastes in ion-exchange technology. Hence, ion-exchange separation methods providing the ability to exclude the regeneration step are of particular interest. The group of methods of this type includes parametric pumping [8-11], thermal ion-exchange fractionation [12,13] and dual-temperature ion-exchange processes [14-18]. Although the advantages of the above techniques are quite obvious the practical applications of these methods is still very limited. This fact can be attributed to the lack of information on real systems (ionic mixtures, effluents, waste waters, etc.) appropriate for the treatment (e.g. for separation

or concentration of certain components from the mixture) within dual-temperature ion-exchange separation techniques. In this context accumulation of the data on ion-exchange equilibrium at different temperatures from the native metal-bearing solution such as acidic mine waters for example can stimulate the further development and wider application of ecologically clean ion-exchange recovery technologies.

The present study was undertaken (1) to obtain information on ion-exchange equilibrium of acidic mine water metal ions on carboxylic and iminodiacetic resins over a wide temperature range and (2) to demonstrate the possibility to concentrate copper from native mine waters by reagentless ion-exchange technique.

EXPERIMENTAL

Samples of the native acidic mine waters of Rio Tinto area (Huelva, Spain) were kindly supplied by Rio Tinto Minera, S.A. These mine waters represent the natural generic metal-bearing effluents originating from the pyritic ore deposits typical for the southern provinces of Spain and Portugal. Iminodiacetic ion exchanger, Lewatit TP-207 and polyacrylic resin, Lewatit R 250-K (both of macroporous type) were kindly supplied by Bayer Hispania Industrial, S.A.. NaOH, HCl and H_2SO_4 of p.a. quality were purchased from Probus (Spain) and used as received. The concentration of metal and sulfate ions were determined by ICP technique using an ARL model 3410 spectrometer (Fisons, USA) with minitorch. The uncertainty of spectrochemical analysis was always less than 1.5%. pH was controlled using a Crison pH-meter 507 (Spain) supplied with a combined glass electrode. Jacketed glass columns (1.4 cm inner diam.) connected with a thermostatic bath (Haake D1, Germany) were used for studying ion exchange equilibrium at different temperatures. The construction of columns provided the

heating/cooling of both resin and feed solution phases [19].

The preliminary treatment of Rio Tinto water (RTW) samples aiming at the selective oxidative precipitation of Fe(III) hydroxide was carried out as described elsewhere [19]. Artificial RTW samples were prepared from $Al_2(SO_4)_3$, $ZnSO_4$, $CuSO_4$, Na_2SO_4 (Probus, Spain) of p.a. quality used as received. The composition of RTW samples before and after treatment and that of artificial RTW are shown in Table 1.

Table 1

PROCEDURE

Ion-Exchange Equilibrium

The ion-exchange equilibrium was studied under dynamic conditions in thermostatic columns. The columns were loaded with a certain portion of the ion exchanger which remained constant during a given series of experiments. The total capacity of the resin portions used was determined prior to the equilibrium studies and after each equilibrium cycle applying a standard technique [17-19]. After equilibration of the resin bed with RTW at a certain temperature, the solution phase was separated from the resin by evacuating with a water pump followed by the stripping with 1.5 M HCl solution. Then the analysis of RTW metal ions in the eluate collected was carried out. After stripping, the resin was converted back into the initial Na^+ form and prepared for the next run. Concentrations of metal ions stripped were used to determine both the values of resin capacity towards each RTW component and to calculate the equilibrium separation factors (α) for different ion couples as follows:

$$\alpha_{Me_1}^{Me_2} = \frac{Y_{Me_2}}{Y_{Me_1}} \cdot \frac{X_{Me_1}}{X_{Me_2}} \qquad (1)$$

where Y and X are the equivalent fractions of ions under consideration in the resin and initial solution phases, respectively; indices 1 and 2 are chosen so that $\alpha>1$.

The repetitive determination of the total ion-exchange capacity of the resin bed at different temperatures was fulfilled by summarizing the values of partial resin capacities towards each RTW metal ion.

Thermostripping and Thermosorption

Thermostripping and thermosorption experiments were carried out as follows; after equilibration of the resin with RTW at a certain temperature the excess of the solution over the resin bed was removed so that its level coincided with that of the resin bed. Then, the temperature was decreased/increased to the preselected value. After equilibration of the system under given thermal conditions, feed solution (RTW of the same composition) was passed through the column at constant flow rate and collected in portions where concentrations of metal ions were determined. In the series of experiments of consecutive thermostripping-sorption cycles, the composition of the initial solution used in each cycle corresponded to that of the sample of thermostripping solution obtained during the previous cycle which contained the highest concentration of Cu^{2+}.

The resin bed heights were kept constant in all experiments (otherwise it is stated): 5 cm for R 250-K and 0.5 cm for TP-207. These conditions were chosen because of the remarkable kinetic differences to reach equilibrium in the metal adsorption process on the resins under study. The kinetics of metal ions sorption on TP-207 was found much slower than that on R 250-K. For the same reason the feed flow rate was 1.55 m/h (R 250-K) and 0.33 m/h (TP-207).

Results and Discussion

Ion-exchange equilibrium

1. Resin capacities

The relative capacities of Lewatit TP-207 and Lewatit R 250-K towards RTW metal ions after equilibration with sample 2 (see Table 1) at 20°C are shown in Fig. 1. As seen in Fig. 1a the capacities of the resins studied towards Zn^{2+}, Fe^{3+}, Mn^{2+}, Mg^{2+}, Ca^{2+} and Na^{+} do not differ remarkably from each other and are relatively low to the absolute value. The main difference observed in the affinity regards is found with Al^{3+} and Cu^{2+}. This is clearly shown in Fig. 1b from which it follows that TP-207 is highly selective towards Cu^{2+} while R 250-K has a preference for Al^{3+}, so that approximately 90% of the resin capacity is occupied by these ionic species.

The influence of RTW composition (which is known to vary significantly during the year [19]) on the capacity of TP-207 towards different metal ions is illustrated by the results shown in Fig. 2. As follows from Table 1 the main difference in compositions of the natural RTW samples used concerns Cu^{2+}, Al^{3+}, Na^{+}, Zn^{2+} and Fe^{3+} contents. As seen in Fig. 2a TP-207 is highly responsive to the concentration of Fe^{3+} in the feed solution that testifies to the high selectivity of the resin towards this ionic species (see below) and confirms the necessity to eliminate its content to mg/m^3 level. Alterations of the concentrations of other RTW metal ions do not result in significant changes of their sorbabilities. As follows from Fig. 2b, TP-207 is most sensitive to the content of Al^{3+} in the equilibrium solution. Indeed, the ~20% decrease of Al^{3+} concentration in the feed causes the drop of its relative content in the resin phase from 15.3 to 8.4%. This result is of particular interest, since the further elimination of Al^{3+} must result in the additional sorption of more valuable (than Al^{3+}) RTW metals, such as Cu^{2+} and Zn^{2+}

which can occupy the corresponding part of the resin capacity. This can improve the efficiency of Cu^{2+} and Zn^{2+} recovery from RTW.

The temperature dependence of relative TP-207 capacities towards RTW metal ions are shown in Fig. 3. The results in Fig. 3a show the affinity of TP-207 for Zn^{2+}, Mg^{2+} and Fe^{3+} to decrease slightly with the rise of temperature while the sorbabilities of Mn^{2+}, Ca^{2+} and Na^{+} remain practically constant within the same temperature interval. The most remarkable influence of temperature on the resin capacity is observed for Al^{3+} and Cu^{2+} (see Fig. 3b). Moreover, the sorbability of the former increases while that of the latter decreases at elevated temperature.

The data presented in Fig. 3 may serve to predict the behavior of the different ionic species in dual-temperature ion-exchange concentration. The concentration degree of any ion in the thermostripping solution obtained can be described in terms of C_i/C_o ratios, where C_o and C_i are the concentrations of the ion in the feed and in the "i" portion of thermostripping solution, respectively. Consider the case of "ideal displacement" which corresponds to the condition i=1, i.e. when the ion under displacement is concentrated in the first portion of the eluate. In this case:

$$C_i = \frac{\Delta q}{V_i} = \frac{q\ (T_1) - q\ (T_2)}{V_i} \qquad (2)$$

where V_i is the volume of the eluate, q is the capacity of the resin towards the ion under consideration, T_1 and T_2 are the temperatures of the loading and the stripping processes, respectively.

Under this condition, the concentration degree of the ion is directly proportional to the parameter **b**, which can be expressed as follows:

$$b = \frac{\Delta q}{C_o \, V_o} \qquad (3)$$

where V_o is the volume of the feed solution passed through the column at T_2 (see experimental part).

Δq, C_o (for RTW sample 1, see Table 1) and **b** values for TP-207 at T_1=20°C and T_2=80°C are collected in Table 2.

Table 2

As seen from **b** values given in Table 2, Cu^{2+} is the only ionic species which can be expected to be markedly concentrated by dual-temperature ion-exchange technique using Lewatit TP-207 resin.

On the other hand, the relative capacities of R 250-K towards different RTW metal ions vs temperature are shown in Fig. 4. In this case, the temperature dependence of metal adsorption is similar to that of Lewatit TP-207. The main differences are related to the capacities for Al^{3+} and Cu^{2+} which are found to be opposite to those of Lewatit TP-207, i.e. Al^{3+} is more highly adsorbed while Cu^{2+} is much less adsorbed. The **b** values calculated from the respective equilibrium data by using eq. (3) (Δq=q(20°C)-q(80°C), see eq. (2)) and C_o for RTW sample 2, (see Table 1) are given in brackets for the different RTW metal ions as follows: Cu^{2+}[**b**=74.36×10^{-3}]; Zn^{2+}[**b**=15.17×10^{-3}]; Mn^{2+}[**b**=4.94×10^{-3}]; Ca^{2+}[**b**=1.93×10^{-3}]; Mg^{2+}[**b**=0.96×10^{-3}]; Na^{+}[**b**=0.42×10^{-3}] and Al^{3+}[**b**=-59.05×10^{-3}].

The difference in the absolute values of parameter **b** obtained for R 250-K and for TP-207 (see Table 2) can be ascribed to the difference of the resin volumes used. The height of the R 250-K resin bed was 10 times higher than for TP-207.

The results of the above estimation of **b** values for R 250-K testify to the similarity of the behavior of both resins TP-207 and R 250-K in dual-temperature concentration of RTW metal ions, i.e. thermostripping from R 250-K must lead to a predominant concentration of Cu^{2+}. Since this conclusion does not obviously follow the results shown in Fig. 3 and 4, we have carried out experimental confirmation of its validity as given below.

2. Resin selectivity

Temperature dependencies of α_{Me2}^{Me1} determined for different RTW ion couples in the experiments with RTW sample 1 on TP-207 (using equation (1)) are shown in Fig. 5. As seen in Fig. 5a, the absolute values of α_{Me}^{Fe} significantly exceed those for other RTW metal ion couples (cf. Fig. 5b, 5c, etc.) Which testifies to the high selectivity of TP-207 towards Fe^{3+} and confirms the above conclusion concerning the need for the complete removal of this particular ionic species from the feed solution prior to the ion-exchange treatment by TP-207 resin. As follows from Fig. 5b the resin manifests high affinity towards Cu^{2+} in comparison with other RTW metal ions. A remarkable increase of α with temperature is observed only for α_{Mg}^{Cu} while for the other ion couples a weaker temperature effect is found. The most significant temperature dependence is observed for α_{Al}^{Cu} which drops from 45.5 at 20°C to 17 at 80°C. As seen in Fig. 5c all ion couples involving Al^{3+} are characterized by far stronger influence of temperature on α_{Me}^{Al} than those shown, e.g. in Figs. 5d and 5e. This feature of $\alpha_{Me}^{Al} = f(T)$ dependencies can be better visualized as follows: consider the ratio of two α values determined at two different temperatures for a given ion couple. As follows from eq. (1), the ratio **a** for the equilibrium solution of the same composition can be written as follows:

$$a = \frac{Y_{Me_1}(T_1)}{Y_{Me_1}(T_1) - \Delta Y_{Me_1}} \cdot \frac{Y_{Me_2}(T_1) - \Delta Y_{Me_2}}{Y_{Me_2}(T_1)} \qquad (4)$$

where T_1 and T_2 are chosen so that **a**>1, and $\Delta Y_{Me}=Y_{Me}(T_1)-Y_{Me}(T_2)$.

The value of parameter **a** achieves a maximum (at a determined value of T_1 and T_2) if $\Delta Y_{Me1}<0$ and $\Delta Y_{Me2}>0$, i.e. when the sorbabilities of metal ions under consideration depend on the temperature in an opposite manner. As follows from Figs. 3 and 4, Al^{3+} is the only RTW ionic species which demonstrates the rise of its sorbability in both resins with the increase of temperatures. On the other hand, the deviation of **a** from 1 can be considered as a measure of α changes caused by the rise of temperature, hence both resins under study are characterized by strong temperature dependencies of α_{Me}^{Al}. Such a difference can be interpreted in terms of the respective thermodynamic characteristics of corresponding chemical reaction i.e. $\Delta H°$ values of the complex formation reaction between metals and compounds containing iminodiacetic groups. In this case, the enthalpy changes are positive for Al^{3+} and negative for Cu^{2+} and the other RTW metal ions [20].

3. Thermostripping and Thermosorption.

The typical concentration-volume histories obtained in thermostripping with natural RTW at 80°C from Lewatit TP-207 and R 250-K resins equilibrated at 20°C with the same RTW sample are shown in Figs. 6a and 6b, respectively. The total capacities of the resin beds used were 2.63 mequiv. for TP-207 and 11.58 mequiv. for R 250-K. The bed height of the former resin was 0.5 cm and that of the latter was 5 cm. Because of that, hot RTW was passed at 0.34 cm^3/min of flow rate in the first case and at 1.6 cm^3/min in the second. The breakthrough curve shown in Fig. 6b was obtained after the

repetitive equilibration of R 250-K with RTW at 20°C to exclude the first thermostripping cycle. The first cycle was carried out at 80°C after loading the resin in the initial Na-form with RTW metal ions at 20° and resulted in an exceptional increase of Cu^{2+} concentration in the eluate by factor of ~3 [19].

As seen in Fig. 6 thermostripping from both resins leads to selective concentration of Cu^{2+} while the content of the remaining RTW metal ions in the eluate obtained remain practically at the feed level. This confirms the correctness of the above predictions (see Table 2 and related comments). The significant decrease of Al^{3+} concentration in the thermostripping solution testifies to the increased sorption of this ionic species which proceeds with the simultaneous desorption of the other RTW components, i.e. Al^{3+} in fact acts as a displacer towards the other RTW cations.

Thus, this thermostripping process characterizes the system under study by a maximum on both the concentration degree of Cu^{2+} and the depletion degree of Al^{3+} occurring simultaneously.

Several factors can influence (both positively and negatively) the effectivity of the thermostripping process, such as the resin bed height and the temperature range.

As seen in Fig. 7, the increase of the bed height of the TP-207 resin from 0.5 cm to 2.5 cm allows achievement of a higher concentration degree of Cu^{2+} and also a wider zone where the effective separation of Cu^{2+} and Al^{3+} occurs. Similar results are obtained for R 250-K resin as reported elsewhere [19]. An opposite trend is observed in narrowing the range of the working temperatures. As follows from the results shown in Fig. 8a the decrease of the stripping temperature leads to a remarkable drop of the stripping efficiency. Also, the RTW metal sorption presented in Fig. 8b shows a mirror image of the corresponding thermostripping and shows the influence of the temperature

range. The effectivity of the thermosorption process also depends on the temperature of the prior thermostripping cycle as clearly seen from the corresponding breakthrough curves shown in Fig. 8b.

The results given in Fig. 8 are the consequence of changes of Al^{3+} and Cu^{2+} sorbabilities at different T_1 and T_2 (see above) and could be predicted from the respective equilibrium data. For example, parameter **a** can be used for this purpose. The values of **a** (see equation (6)) calculated for Cu^{2+}-Al^{3+} exchange on TP-207 at T_2=20°C and different T_1 are collected in Table 3 where the maximum concentration degrees (C_i/C_o) for Cu^{2+} obtained in the thermostripping cycles carried out at different temperature (see Fig. 8a) are also given.

Table 3

A comparison of **a** and C_i/C_o values presented in Table 3 shows that they are practically directly proportional to each other, which suggests that concentration process has a strong correlation with the selectivity characteristics of the resin, and which shows the chemical reaction to be a key factor in the overall ion-exchange process.

As follows from the results shown in Fig. 8a and 8b after the thermostripping, the resin phase appears unloaded with Cu^{2+} and becomes able to sorb it again from cold RTW without any additional treatment (regeneration).

Solution collected during thermostripping (with increased Cu^{2+} concentration and decreased content of Al^{3+}) can be sent to consecutive thermosorption-thermostripping cycles to achieve higher concentrations. Experiments of consecutive thermo-sorption-stripping cycles were carried out with R 250-K resin (total capacity of the resin bed 11.58 mequiv.) and artificial RTW samples. The primary composition of artificial RTW

(given in Table 1) has been shown to model adequately the behavior of RTW components during the dual-temperature ion-exchange concentration cycle. The results of 4 thermo-sorption-stripping cycles carried out are shown in Fig. 9. The concentration factor of Cu^{2+} achieved after the fourth cycle equals ~2.7 while the depletion factor of Al^{3+} (C_o/C_i) reaches ~10. The final concentrate contained 324 mg/l Cu^{2+} and 51 mg/l Al^{3+}. The content of Zn^{2+} and Na^{+} remained practically constant and did not change from cycle to cycle. As follows from the above discussion the composition of the last (fourth) concentrate is suitable for the recovery of Cu^{2+} which can be carried out with TP-207 resin. The final recovery of copper from this concentrate was carried out by loading the resin bed followed by rinsing with water and stripping with 1 M H_2SO_4. The purity vs amount of Cu^{2+} stripped is shown in Fig. 10. An average purity of $CuSO_4$ obtained (for the total eluate volume collected) has been estimated to be ~86%. As seen in Fig.10, this value can be markedly improved by the differential collecting of the product. Thus, an average of Cu^{2+} purity of 93.5% will be obtained, if the first portion of the eluate, containing the highest level of impurities, is collected separately avoiding the mixing with the rest of the product solution.

Finally, we propose a possible flowsheet for a process of dual-temperature ion-exchange concentration of Cu^{2+} from acidic mine waters of RTW type. The simplified block-scheme of the process is shown in Fig. 11 and refers to continuous counter-current mode operation . The unit comprises several two-sectional countercurrent columns which are operated at different temperatures T_1 and T_2 ($T_2 > T_1$) [6]. The first column is fed by the native RTW and produces the first concentrate which is directed to the bottom section of the second column and so on. The heating of the solution under treatment up to T_2 can be provided using cheap facilities such as, e.g. solar

boiler systems, known to be very effective in the areas with high level of solar irradiation (e.g. in southern provinces of Spain and Portugal). The resin in all columns circulates in a practically closed cycle and does not need regeneration, i.e. the process is absolutely free of wastes.

ACKNOWLEDGMENTS

This work has been carried out with the financial support of European Commission (EV5V-CT94-0556) and CICYT, the Spanish Commission for Research and Development, project PTR930009. Bayer Hispania Industrial, S.A. is gratefully thanked for supplying with samples of Lewatit resin. The help of Rio Tinto Minera S.A. is also gratefully acknowledged for supplying samples of acidic mine waters. The Spanish Ministry for Education and Science is acknowledged for providing financial support to D. Muraviev for a sabbatical stay at U.A.B. (SAB95-0073).

REFERENCES

1) Tiravanti, G., Di Pinto, A.C., Macchi, G., Marani, D., Santori, M. and Wang, Y. Heavy Metals Removal: Pilot Scale Research on the Advanced Mexico Precipitation Process, in: Metals Speciation, Separation and Recovery (Patterson, J.W. and Passino, R., eds.), Lewis Publ., Chelsea, 1987, p. 665.

2) Ritcey, G.M. and Asbrook, A.W. in: Solvent extraction, principles and applications to process metallurgy, part II, Elsevier, 1979, p. 605.

3) Högfelt, E. Liquid ion exchangers, in: Ion Exchangers, (Dorfner, K., ed.), Walter de Gruyter, Berlin, 1990, p. 573.

4) Patterson, J.W. in: Metals Speciation, Separation and Recovery (Patterson, J.W. and Passino, R., eds.) Lewis Publ., Chelsea, 1987, p. 63.

5) Streat, M. Ion Exchange Processes in Hydrometallurgy, in: Ion Exchangers, (Dorfner, K., ed.), Walter de Gruyter, Berlin, 1990, p. 1061.

6) Khamizov, R. , Muraviev, D. and Warshawsky, A. Recovery of Valuable Mineral Components from Seawater by Ion-Exchange and Sorption Methods, in: Ion Exchange and solvent Extraction (Marinsky, J.A. and Marcus, Y. eds.), v. 12, Marcel Dekker, New York, 1995, p.93.

7) Ritcey, G.M. in: Tailing Management, problems and solutions in the mining industry, Elsevier, 1989, p. 446.

8) Chen, H.T. in: Handbook of Separation Techniques for Chemical Engineers, (Schweitzer, P.A., ed.) McGraw-Hill, New York, 1979, p. 467.

9) Grevillot, G. in: Handbook for Heat and Mass Transfer (Cheremisinoff, N.P., ed.) Gulf Publ., West Orange, NY USA, 1985, Ch. 36.

10) Tondeur, D. and Grevillot, G. in: Ion Exchange: Science and Technology,

(Rodrigues, A.E., ed.) NATO ASI, v. 197, Martinus Nijhoff, Dordrecht, 1986, p. 369.

11) Wankat, P.C. in : Percolation Process, Theory and Application, (Rodrigues, A.E. and Tondeur, D., eds.), Sijthoff and Noordhoff, Alphen aan den Rijm, 1978, p. 443.

12) Bailly, M. and Tondeur, D. Thermal fractionation by moving-bed ion exchange: principles and experiments. J. Chromatogr., **201**, 343, 1980.

13) Bailly, M. and Tondeur, D. Continuous counter-current thermal ion-exchange fractionation. J. Chem. Eng. Symp. Ser., **54**, 111, 1978.

14) Andreev, B.M., Boreskov, G.K. and Katalnikov, S.G. Dual-temperature method for ions separation using fixed bed of ion exchanger. Khim. Prom., **6**, 389, 1961 (Russ).

15) Gorshkov, V.I., Kurbanov, A.M. and Apolonnik, N.V. Counter-current ion-exchange separation without auxiliary ions. Zhur. Fiz. Khim., **45**, 2969, 1971 (Russ.)

16) Gorshkov, V.I., Ivanova, M.V., Kurbanov, A.M. and Ivanov, V.A. New method for ion-exchange separation. Vestnik Moskov. Univ., Ser. Khim., **5**, 535, 1977 (Russ.). English translation in: Moscow Univ. Bull., **32**, 23, 1977.

17) Muraviev, D., Noguerol, J. and Valiente, M. Separation and concentration of calcium and magnesium from seawater on carboxylic resins with temperature induced selectivity. Reactive Polymers, **28**, 111, 1996.

18) Muraviev, D., Gonzalo, A. and Valiente, M. Ion exchange equilibrium of Cu^{2+} and Zn^{2+} on iminodiacetic and aminomethylphosphonic resins at different

temperatures. Anal. Chem., **67**(17), 3028, 1995.

19) Muraviev, D., Noguerol, J. and Valiente, M. Seawater as auxiliary reagent in dual-temperature ion-exchange processing of acidic mine waters. Environmental, Science & Technology, submitted.

20) Christensen, J. J. and Izatt, R. M. in: Handbook of Metal Ligands Heats, Dekker, M., New York, 1983.

LEGENDS TO FIGURES

Fig. 1 Relative capacities of Lewatit R 250-K (white bars) and Lewatit TP-207 (grey bars) resins for RTW metal ions.

Fig. 2 Influence of the composition on the relative capacity of Lewatit TP-207 resin for RTW metal ions. Sample 1 (white bars) and sample 2 (grey bars).

Fig. 3 Temperature dependencies of relative capacities of Lewatit TP-207 resin for RTW metal ions a) (○) Zn^{2+}, (□) Mn^{2+}, (◇) Fe^{3+}, (●) Ca^{2+}, (■) Mg^{2+}, (▲) Na^{+}; and b) (Δ) Cu^{2+}, (▽) Al^{3+}.

Fig. 4 Temperature dependencies of relative capacities of Lewatit R 250-K resin for RTW metal ions a) (○) Zn^{2+}, (□) Mn^{2+}, (Δ) Cu^{2+}, (◇) Fe^{3+}, (●) Ca^{2+}, (■) Mg^{2+}, (▲) Na^{+} and b) (▽) Al^{3+}.

Fig. 5 Temperature dependencies of equilibrium separation factors for ion couples: a) (○) Fe^{3+}/Zn^{2+}, (□) Fe^{3+}/Mn^{2+}, (Δ) Fe^{+3}/Mg^{2+}, (▽) Fe^{3+}/Al^{3+}, (◇) Fe^{3+}/Ca^{2+}, (●) Fe^{3+}/Na^{+}; b) (●) Cu^{2+}/Mg^{2+}, (■) Cu^{2+}/Mn^{2+}, (▲) Cu^{2+}/Na^{+}, (▼) Cu^{2+}/Ca^{2+}, (◆) Cu^{2+}/Zn^{2+}, (○) Cu^{2+}/Al^{3+}; c) (○) Al^{3+}/Mg^{2+}, (□) Al^{3+}/Mn^{2+}, (Δ) Al^{+3}/Na^{+}, (▽) Al^{3+}/Ca^{2+}, (◇) Al^{3+}/Zn^{2+}; d) (●) Fe^{3+}/Cu^{2+}, (■) Zn^{2+}/Mn^{2+}, (▲) Zn^{2+}/Mg^{2+}, (▼) Zn^{2+}/Ca^{2+}, (◆) Zn^{2+}/Na^{+} and e) (○) Mn^{2+}/Mg^{2+}, (□) Mn^{2+}/Ca^{2+}, (Δ) Mn^{2+}/Na^{+}, (◇) Na^{+}/Ca^{2+}, (●) Ca^{2+}/Mg^{2+} on Lewatit TP-207.

Fig. 6 Thermostripping breakthrough curves for RTW from Lewatit TP-207 a) and Lewatit R 250-K b) resins; (○) Zn^{2+}, (□) Mn^{2+}, (Δ) Cu^{2+}, (▽) Al^{3+}, (◇) Fe^{3+}, (●) Ca^{2+}, (■) Mg^{2+}, (▲) Na^{+}.

Fig. 7 Influence of the height of the TP-207 resin bed on the thermostripping process;

(○) 2.5 cm and (□) 0.5 cm.

Fig. 8 Thermostripping (a) and thermosorption (b) breakthrough curves for RTW from Lewatit TP-207 at different temperatures; (○) 40°C, (□) 60°C and (Δ) 80°C.

Fig. 9 Concentrations of (○) Cu^{2+} and (□) Al^{3+} obtained in consecutive thermo-sorption-stripping cycles vs number of cycle with artificial RTW on Lewatit TP-207 resin.

Fig. 10 Purity vs amount of copper stripped with 1 M H_2SO_4 from Lewatit TP-207 resin loaded with RTW concentrate obtained after four concentration cycles.

Fig. 11 Flowsheet of the reagentless process for ion-exchange treatment of RTW.

Table 1. *Composition of Rio Tinto water samples before and after the oxidative Fe precipitation treatment, natural and artificial.*

C (mg/l)	SO_4^{2-}	Fe	Cu	Zn	Al	Mn	Mg	Ca	Na	pH
Sample 1 (initial)	16,450	5,050	239	912	399	75	751	326	19	1.9
Sample 1 (treated)	16,300	3	235	890	386	73	735	319	4,175	3.5
Sample 2 (treated)	17,350	0.3	115	1,275	530	90	950	475	3,550	3.5
Sample 2 (artificial)	17,250	0	120	4,700	530	0	0	0	3,500	3.5

Table 2. Δq, Co and **b** values for different RTW metal ions sorbed by Lewatit TP-207 at T_1=20°C and T_2=80°C.

Me	Cu	Zn	Mn	Mg	Ca	Na	Al
Δq^* (mequiv.)	0.057	0.016	0.001	0.017	-0.007	0	-0.398
Co (mequiv/dm^3)**	8.60	34.00	3.19	74.40	19.20	193	47.90
$bx10^{3***}$	6.63	0.47	0.31	0.23	-0.36	0	-8.31

* The values refer to the difference of the resin bed capacity.
** C_o values refer to RTW sample 1, treated (see Table 1).
*** For simplicity V_o values for different ions are presumed to be the same and equal to 1.

Table 3. Values of parameter **a** for Cu^{2+}- Al^{3+} exchange on Lewatit TP-207 and maximum concentration factors for Cu^{2+} (see Fig.8a) at different T_1, with T_2=20°C.

T_1 (°C)	**a**	C_i/C_o
80	2.68	1.195
60	1.86	1.125
40	1.36	1.053

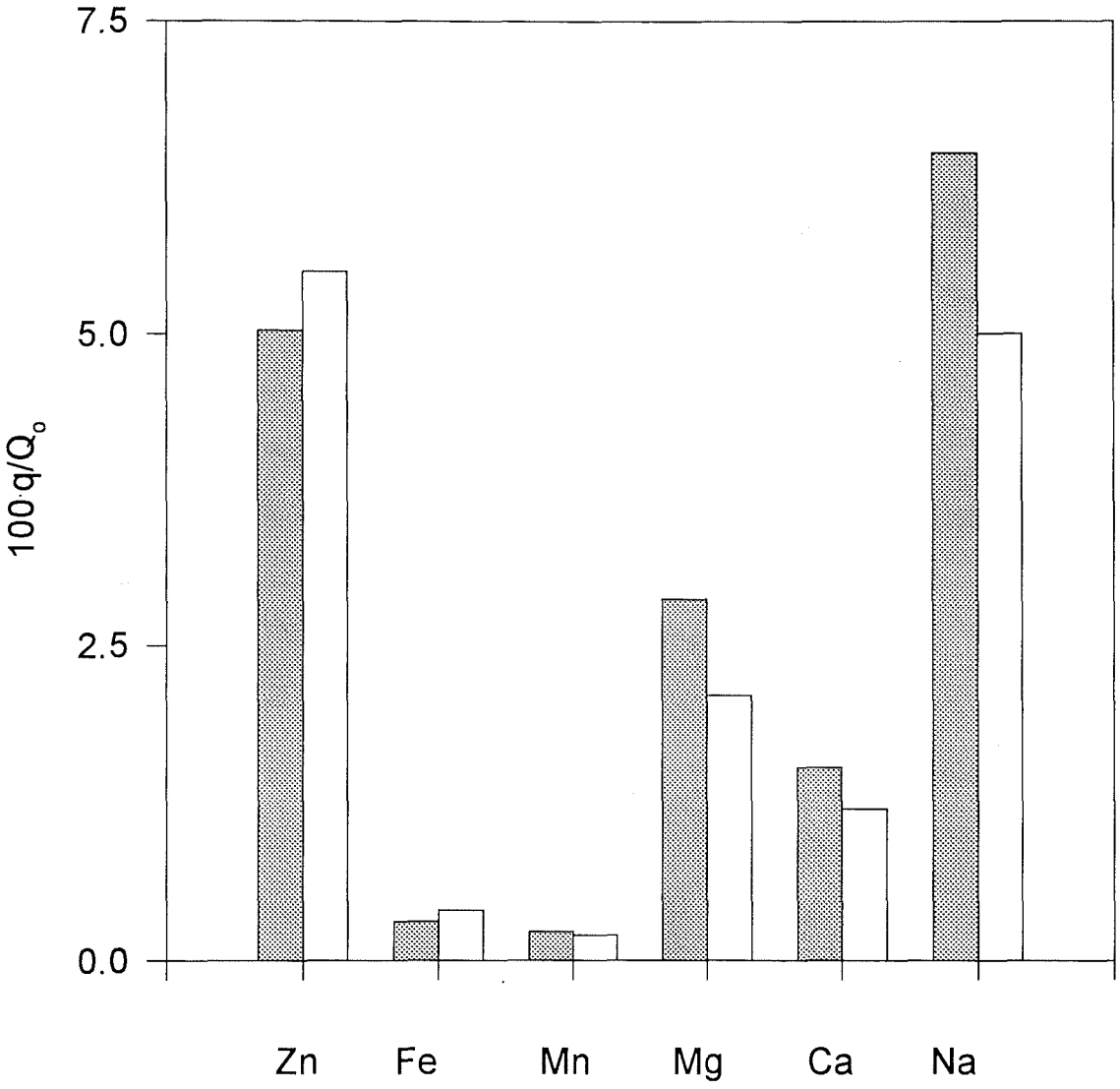

Fig. 1a

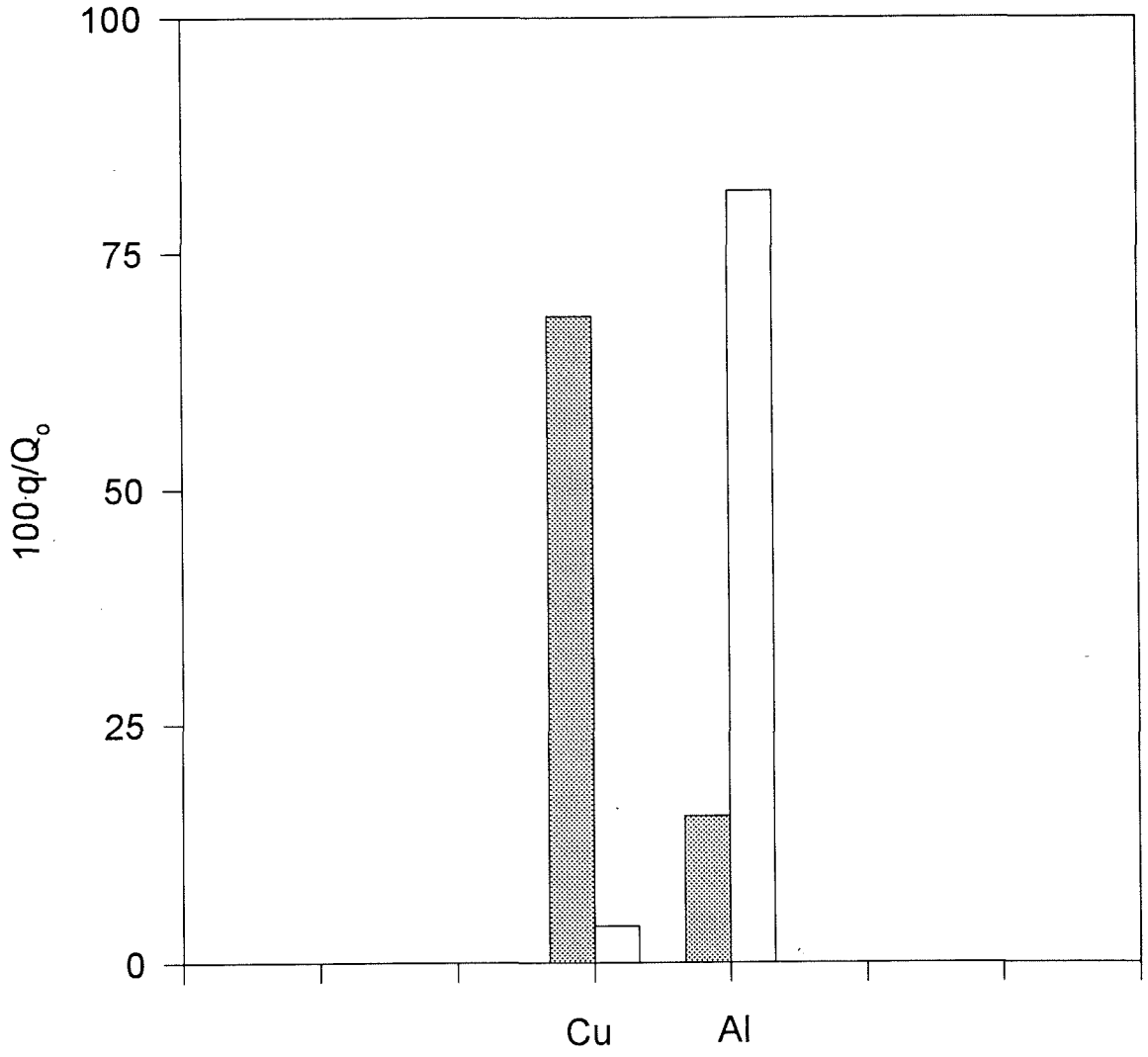

Fig. 1b

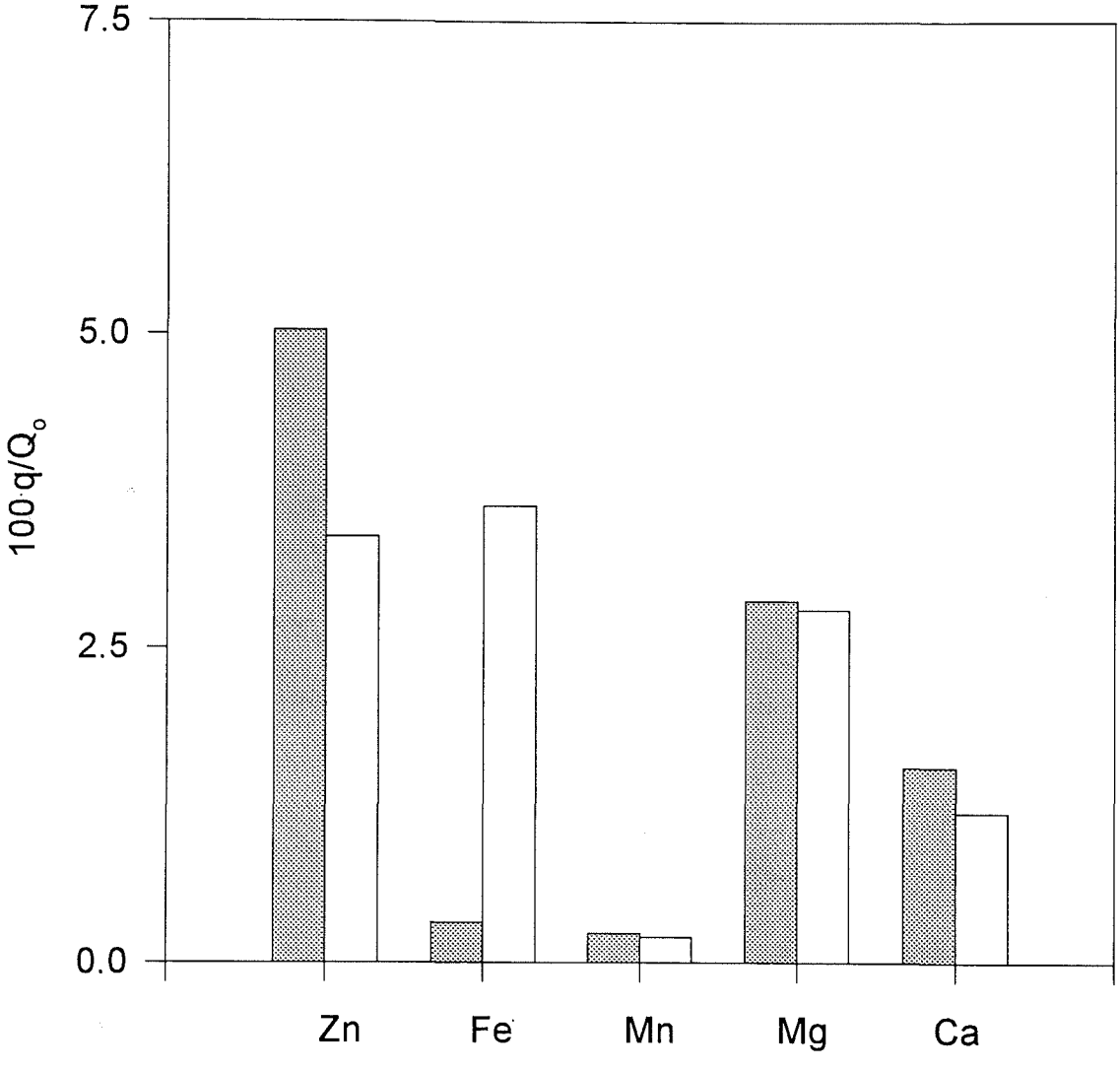

Fig. 2a

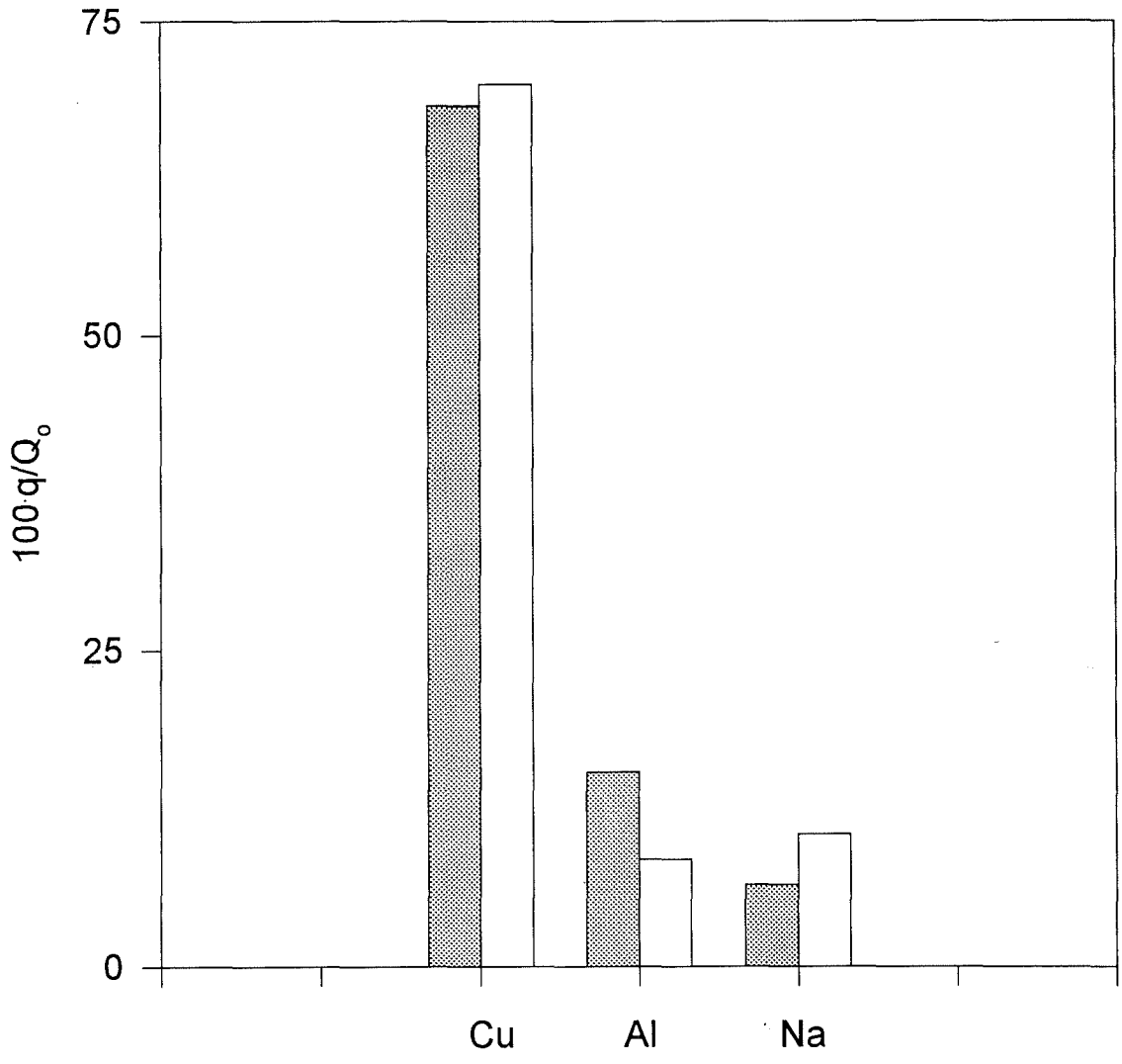

Fig. 2b

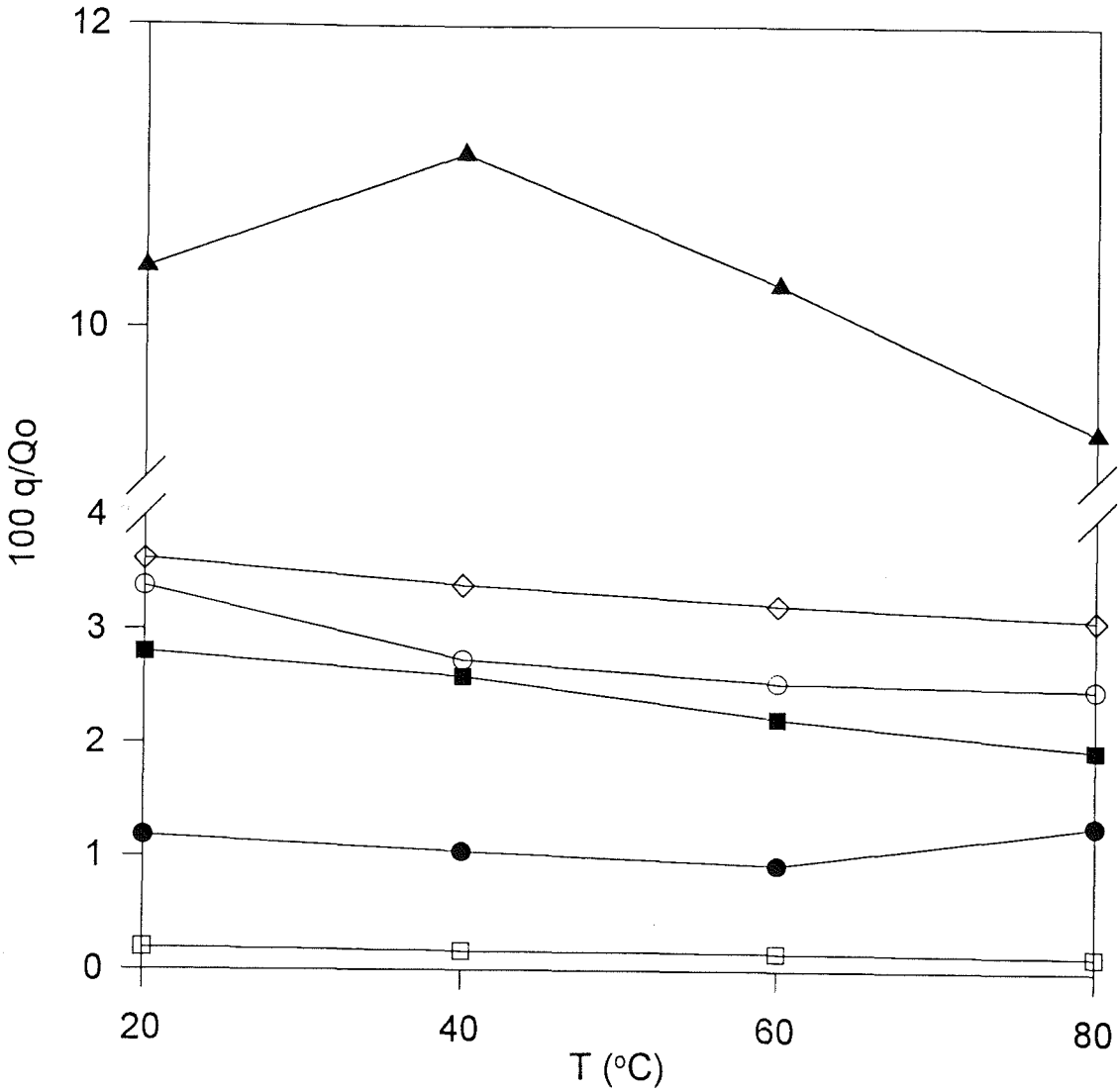

Fig. 3a

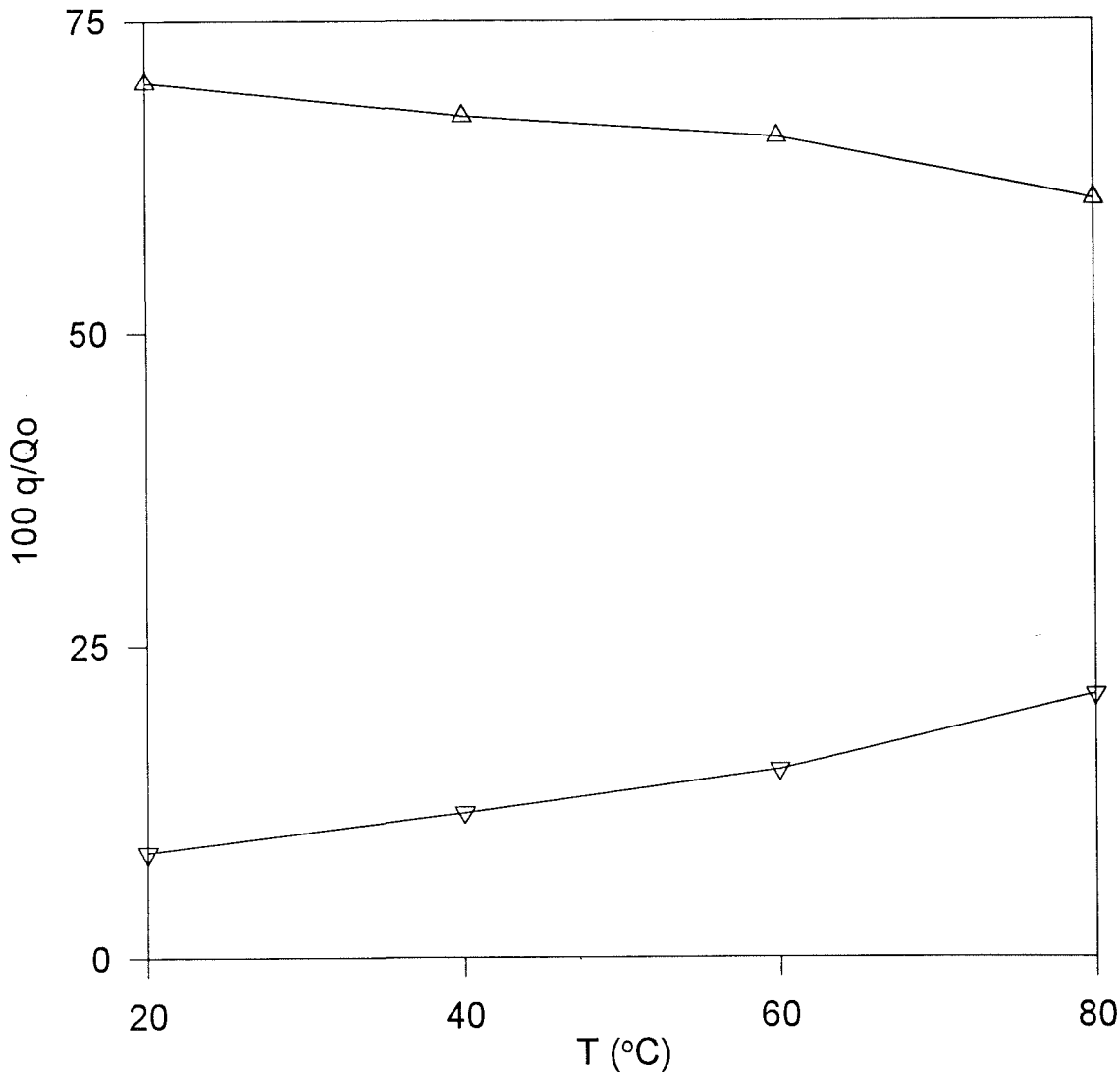

Fig. 3b

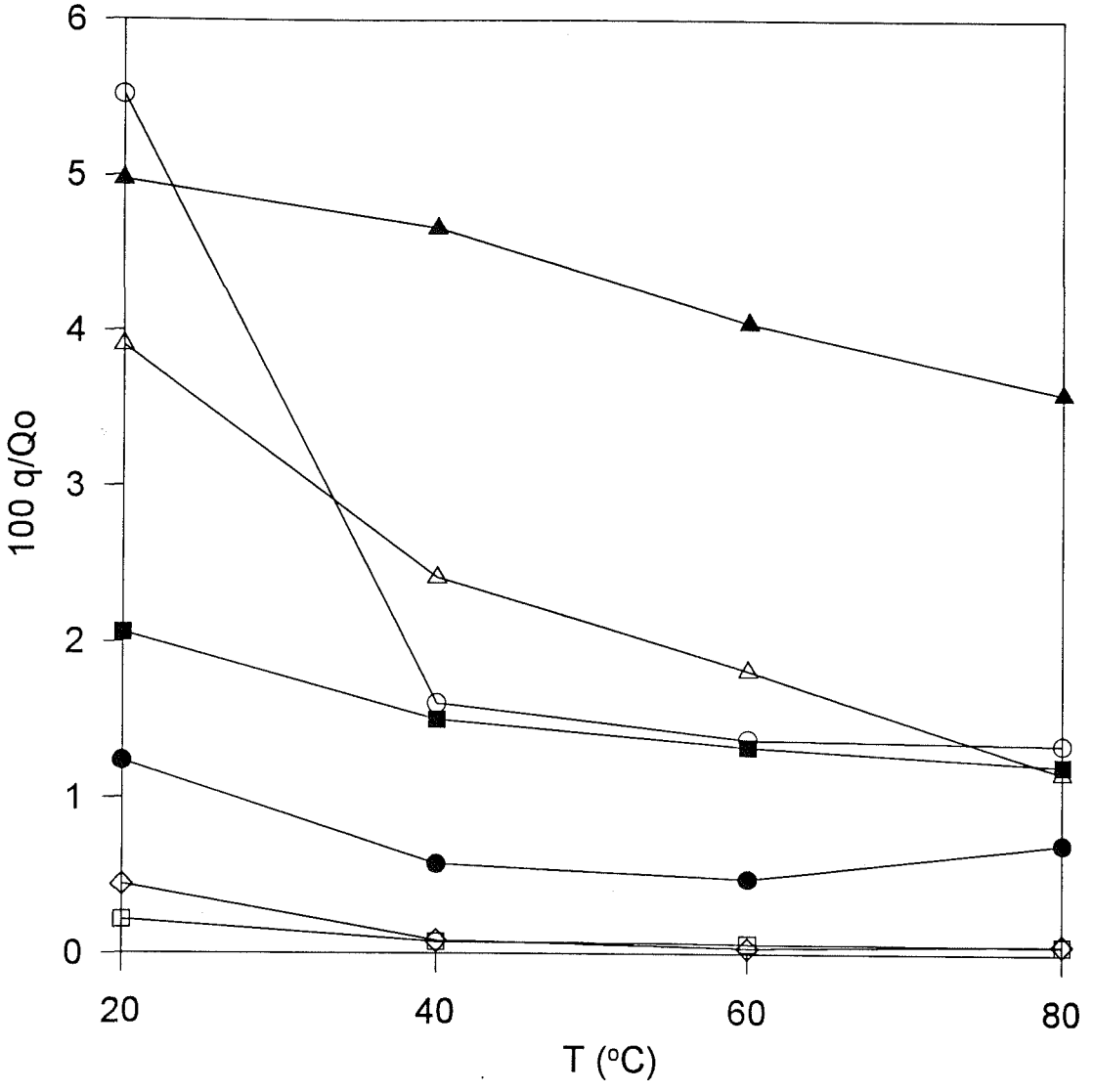

Fig. 4a

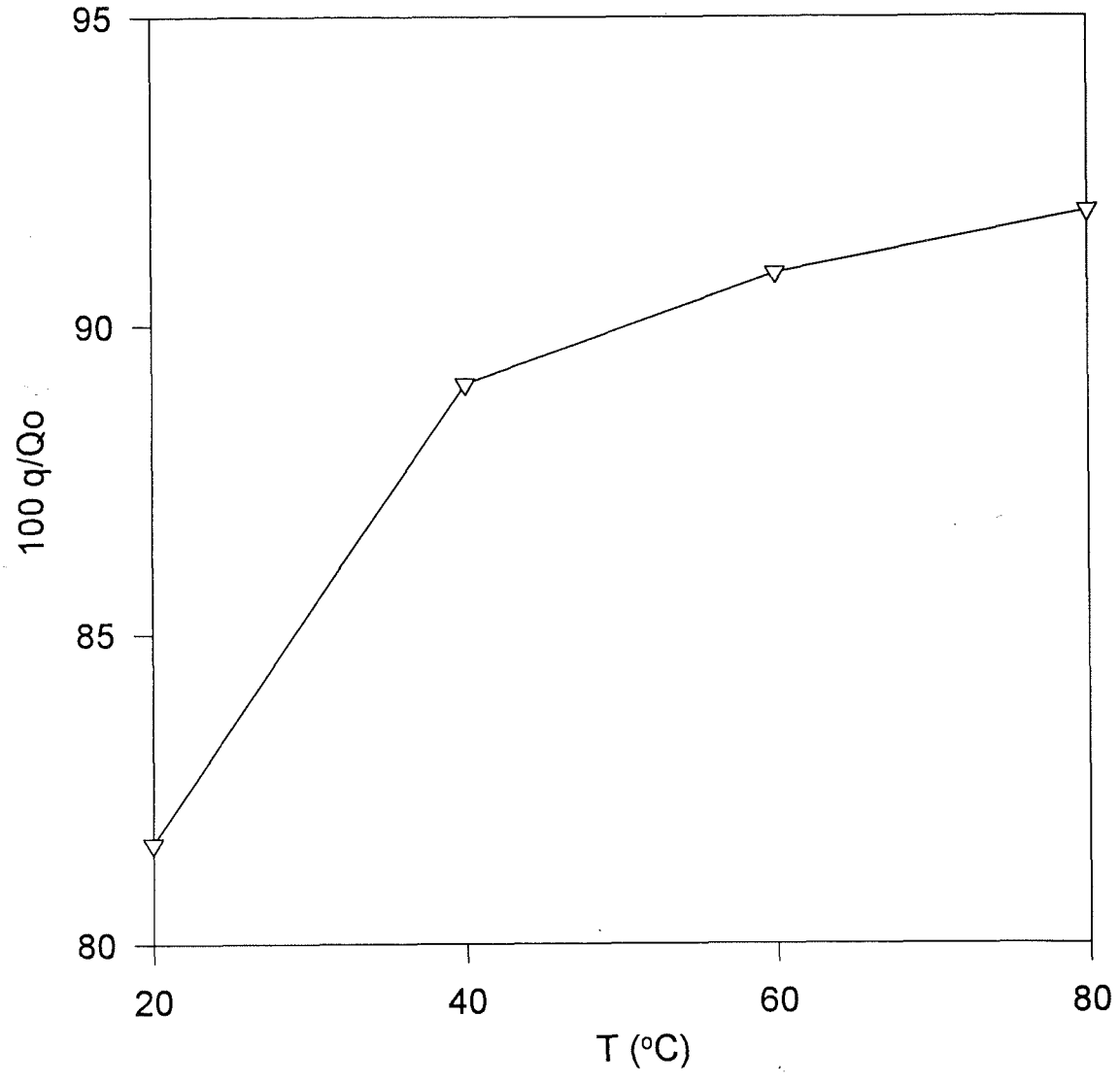

Fig. 4b

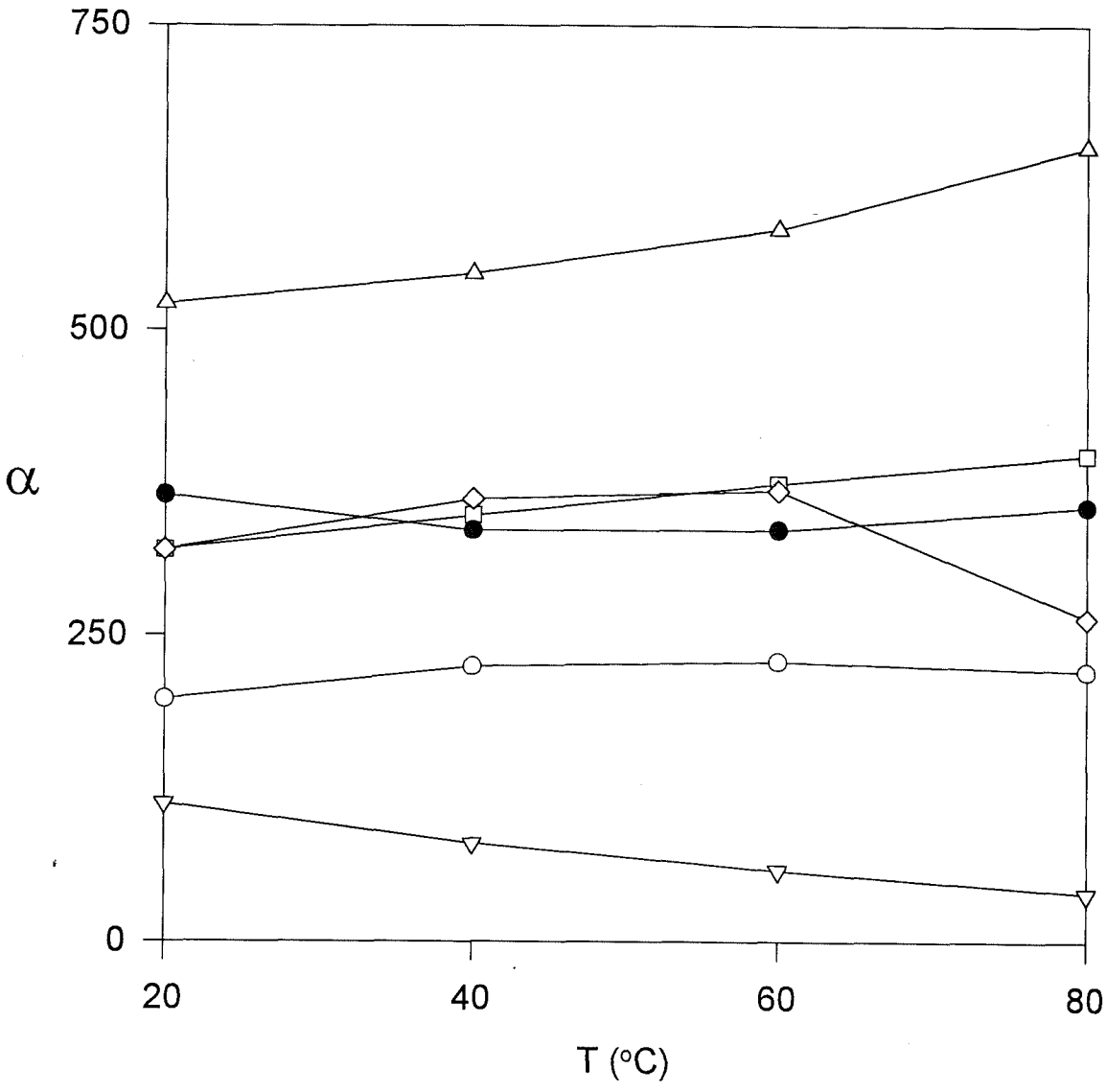

Fig. 5a

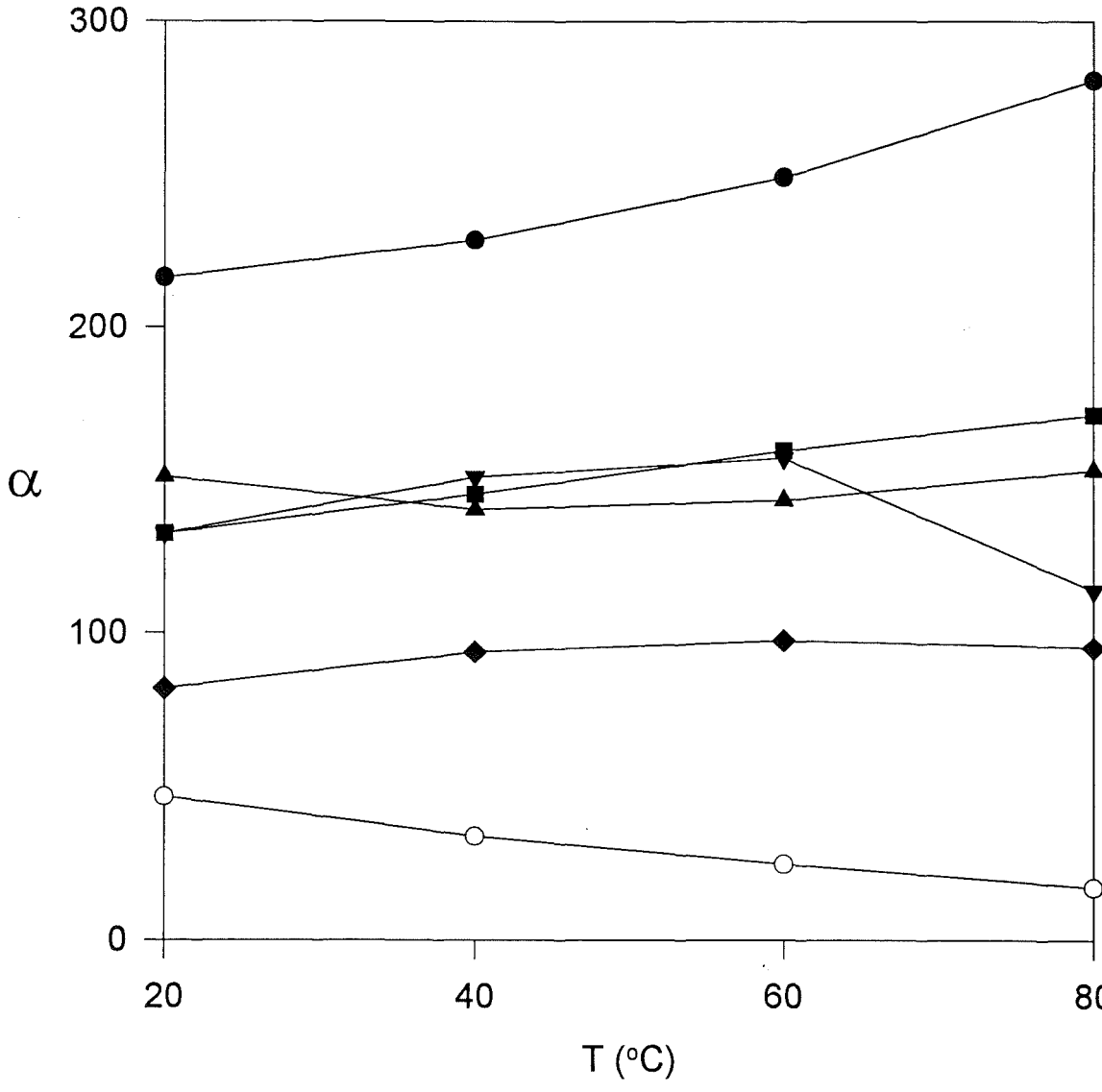

Fig. 5b

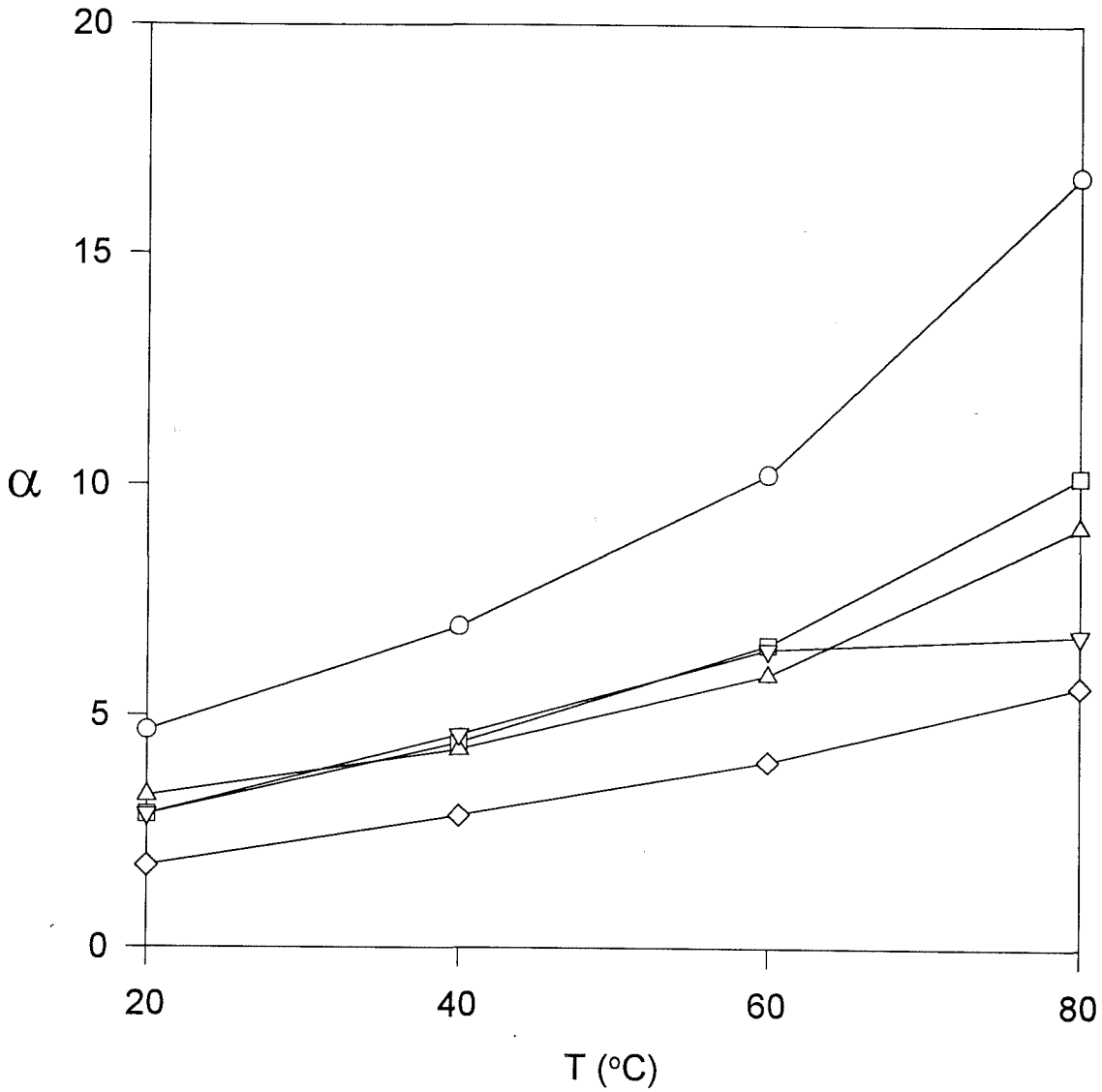

Fig. 5c

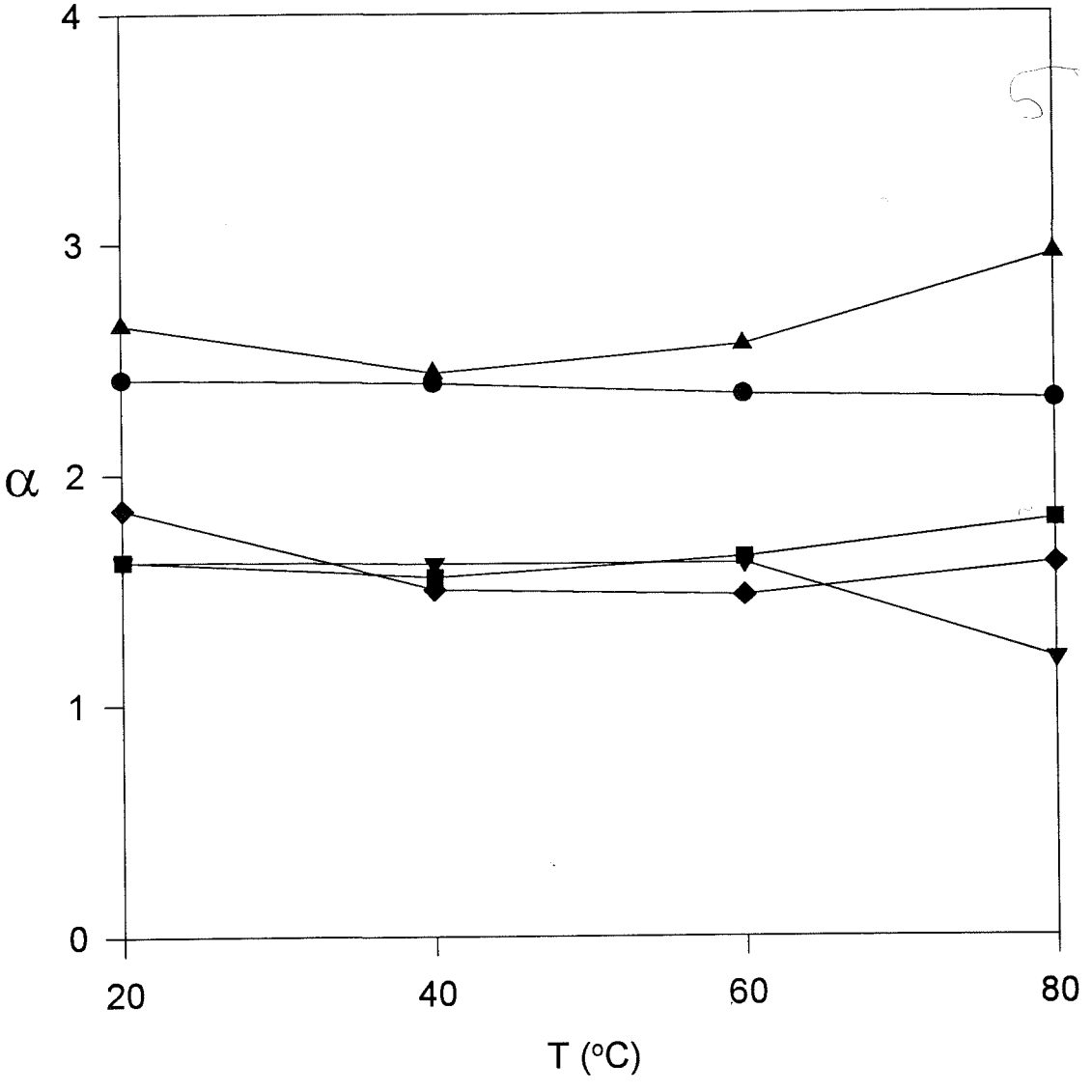

Fig. 5d

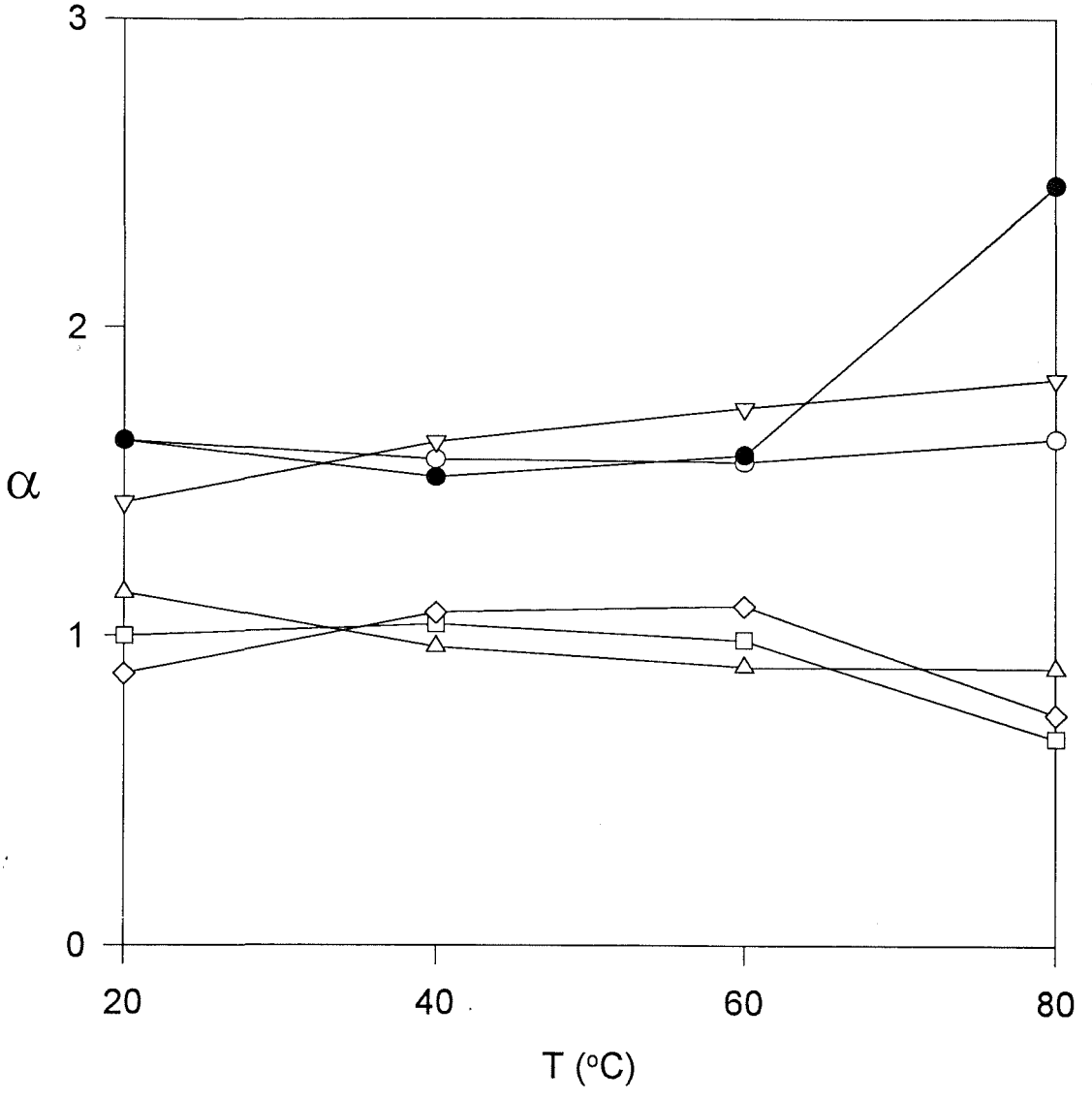

Fig. 5e

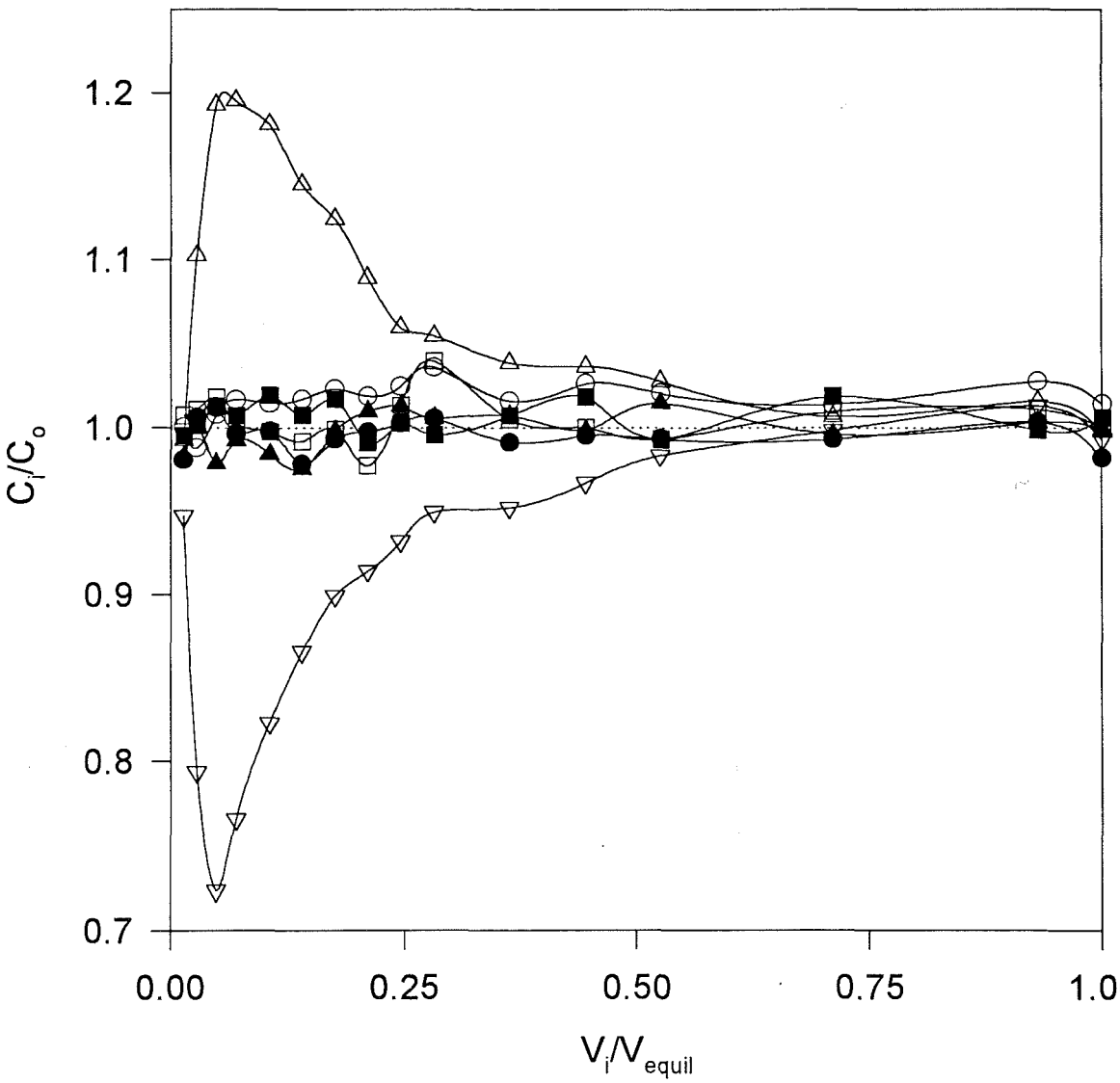

Fig. 6a

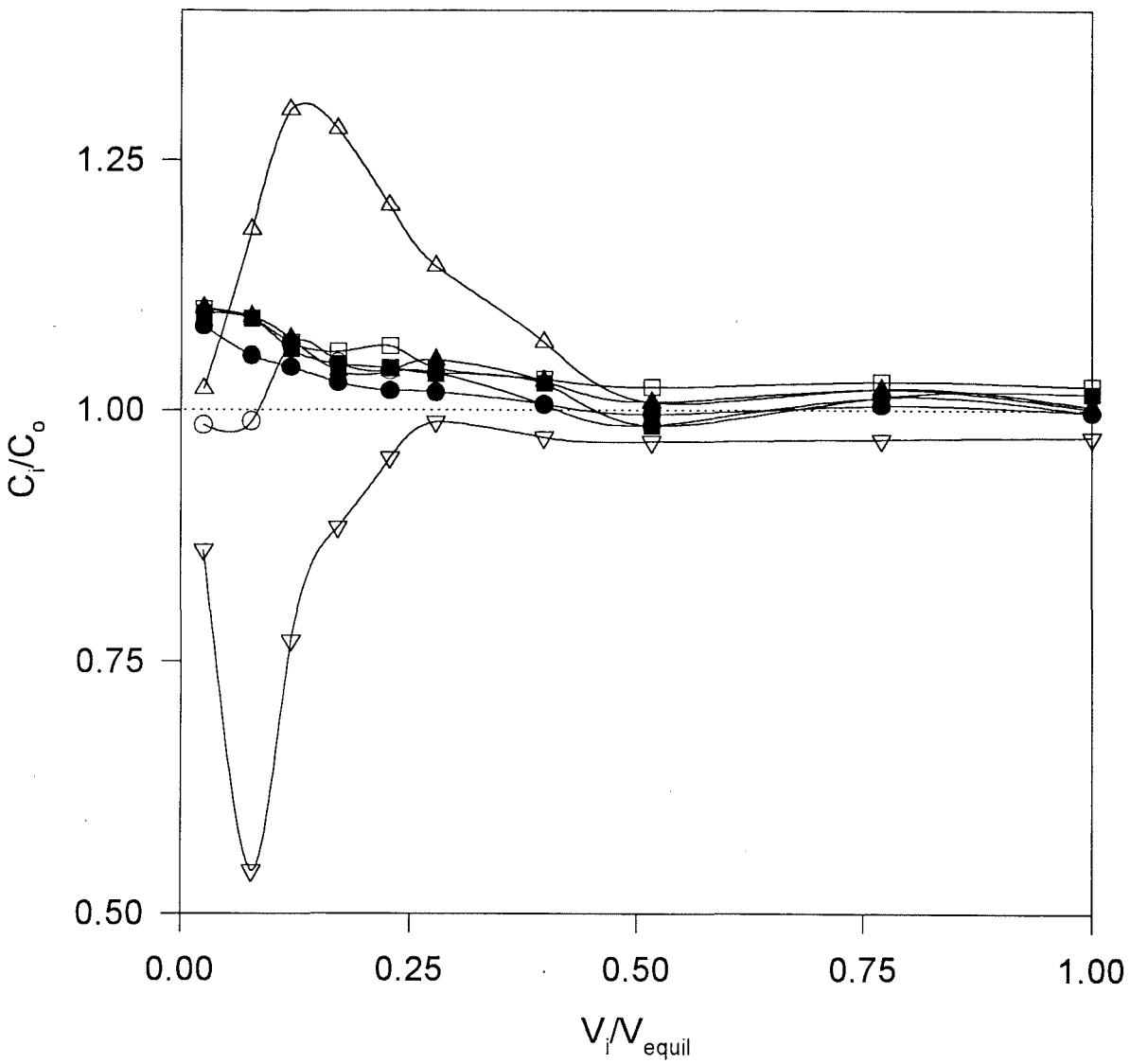

Fig. 6b

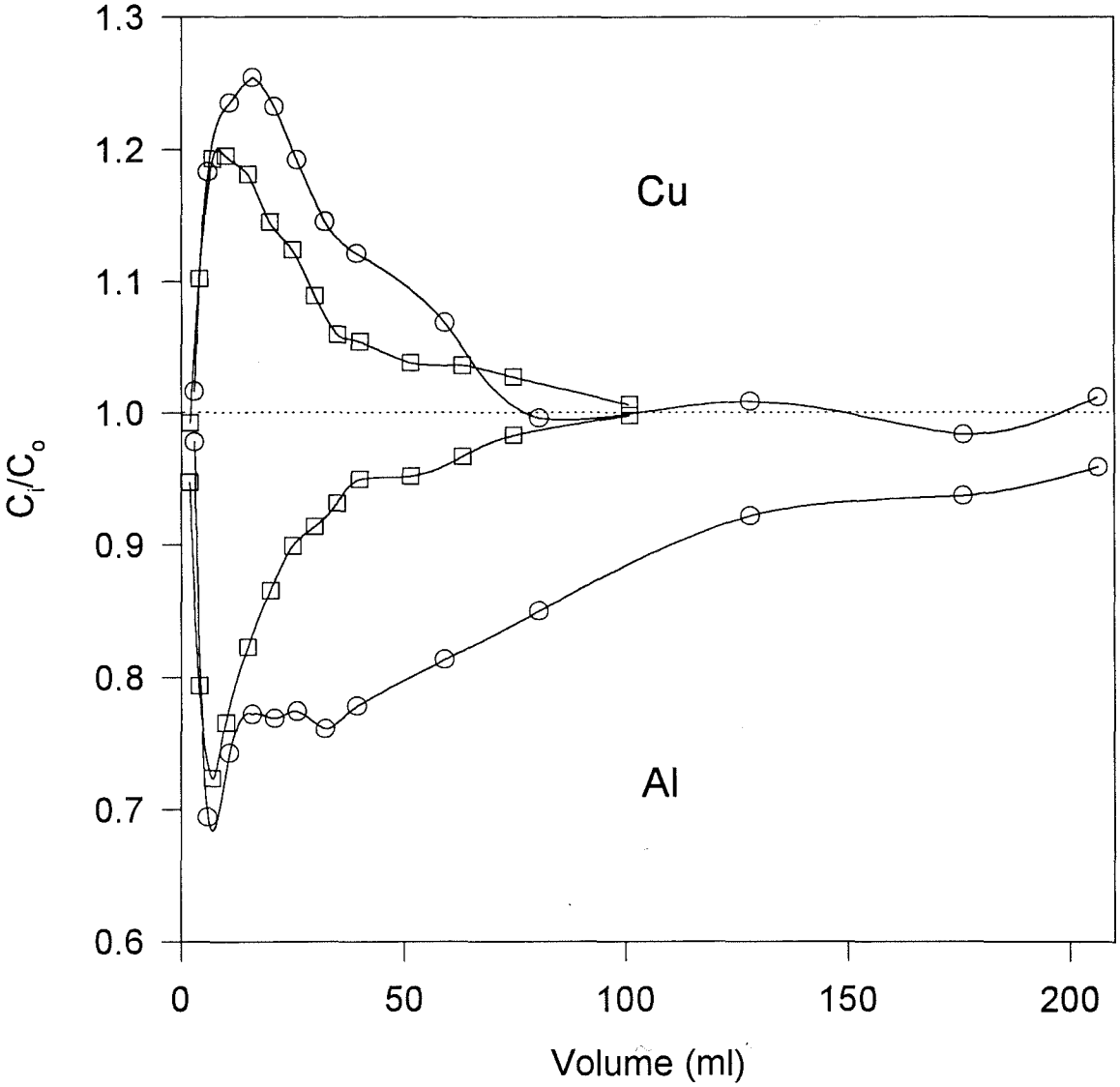

Fig. 7

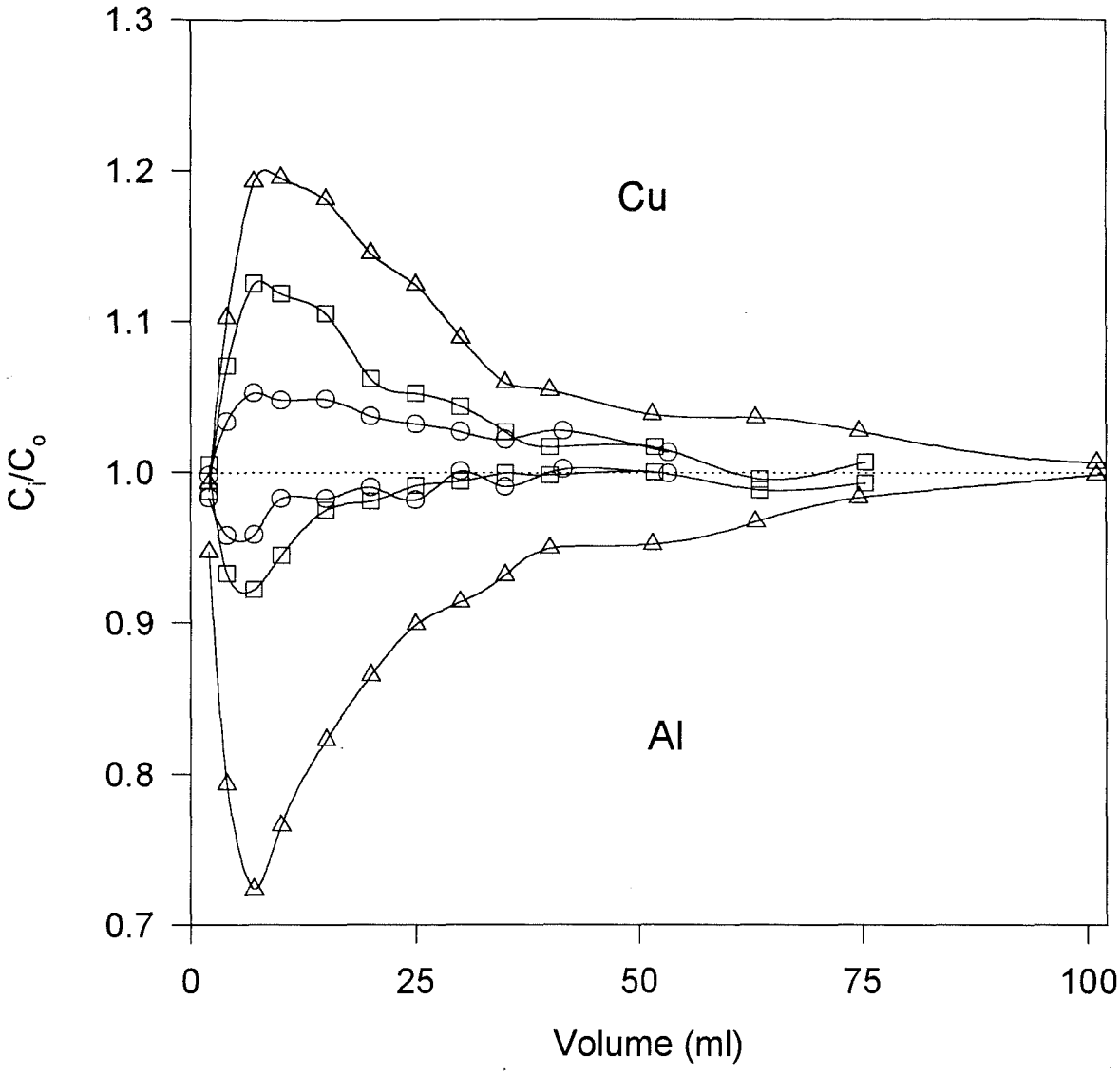

Fig. 8a

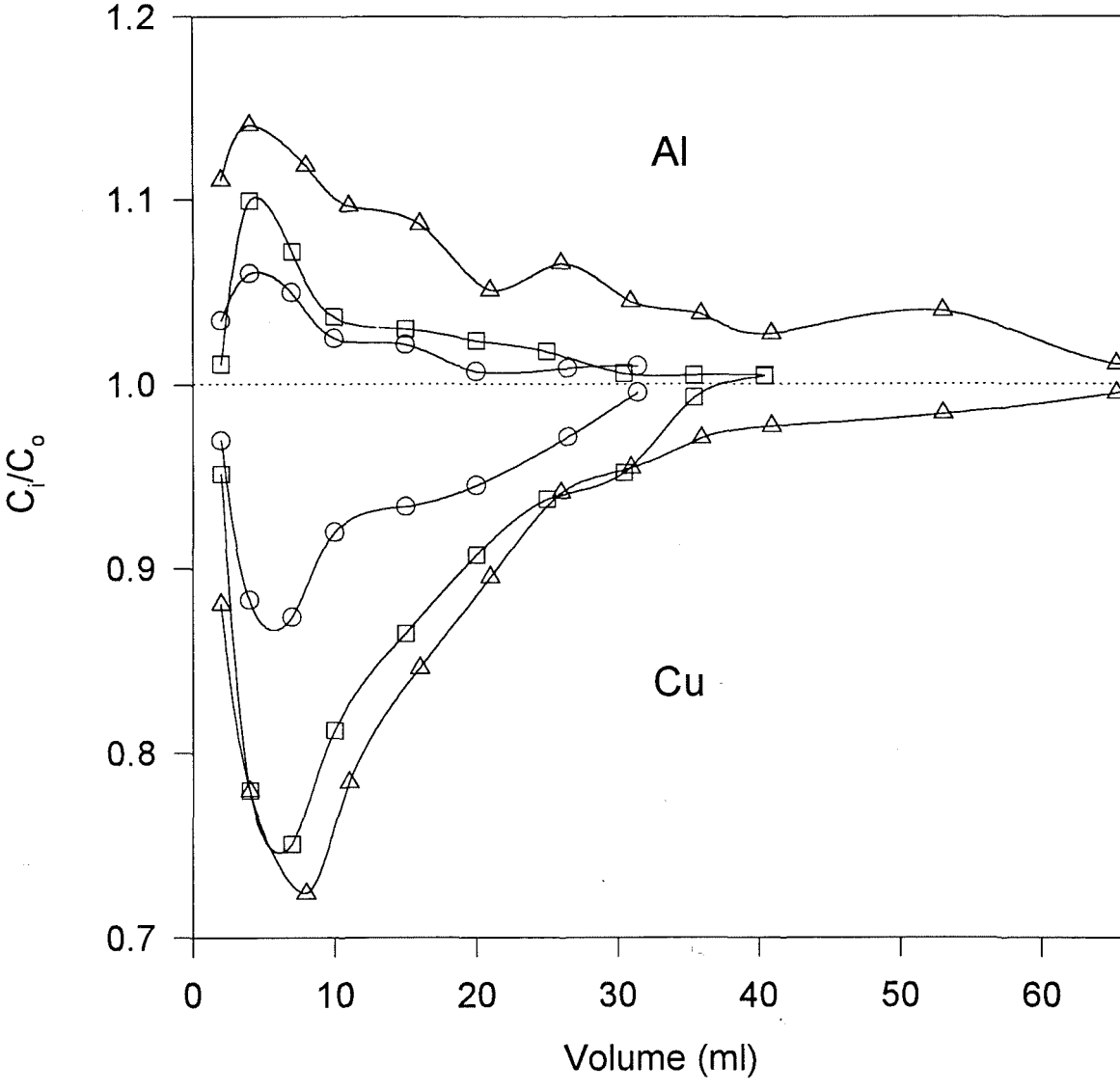

Fig. 8b

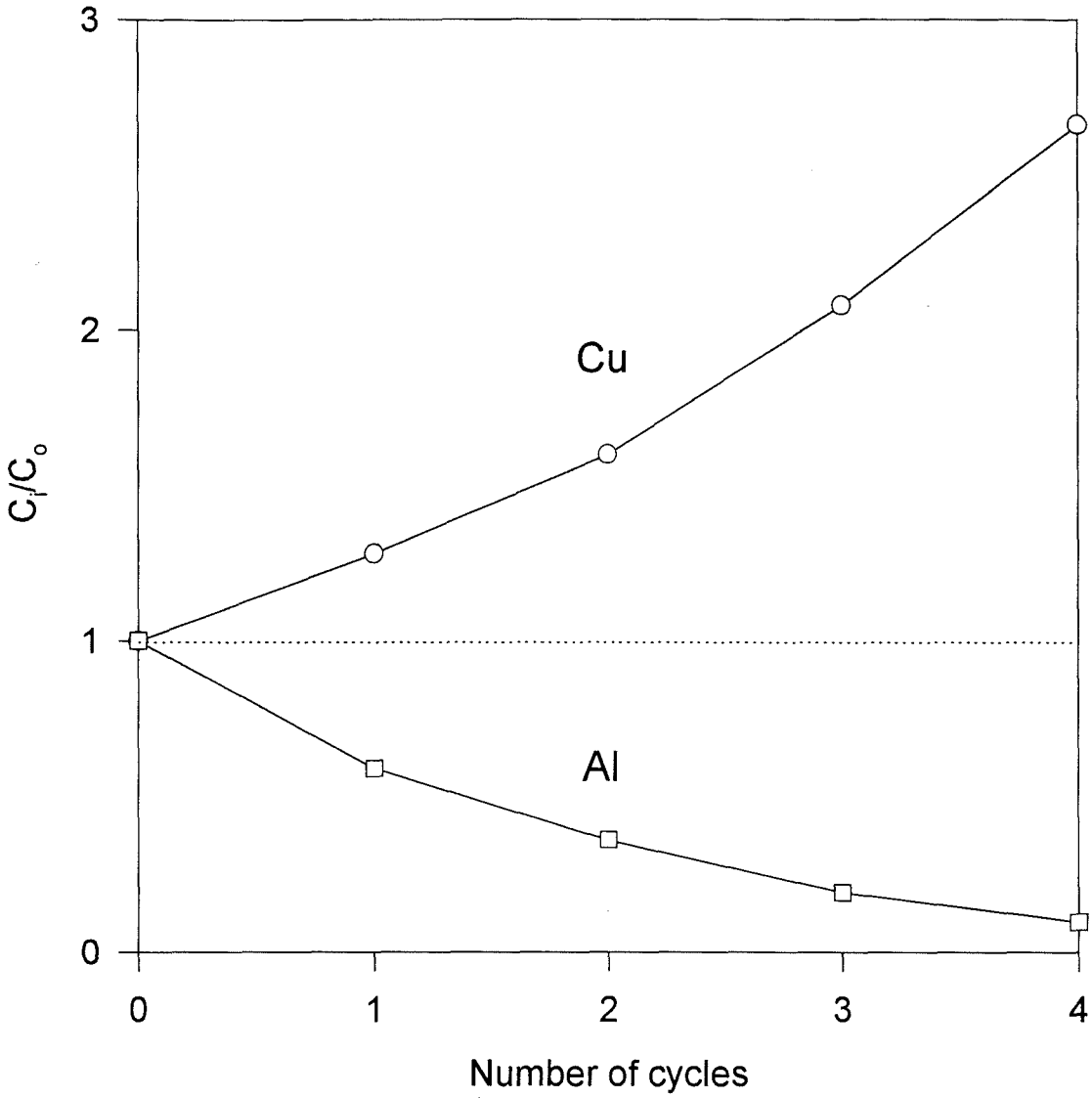

Fig. 9

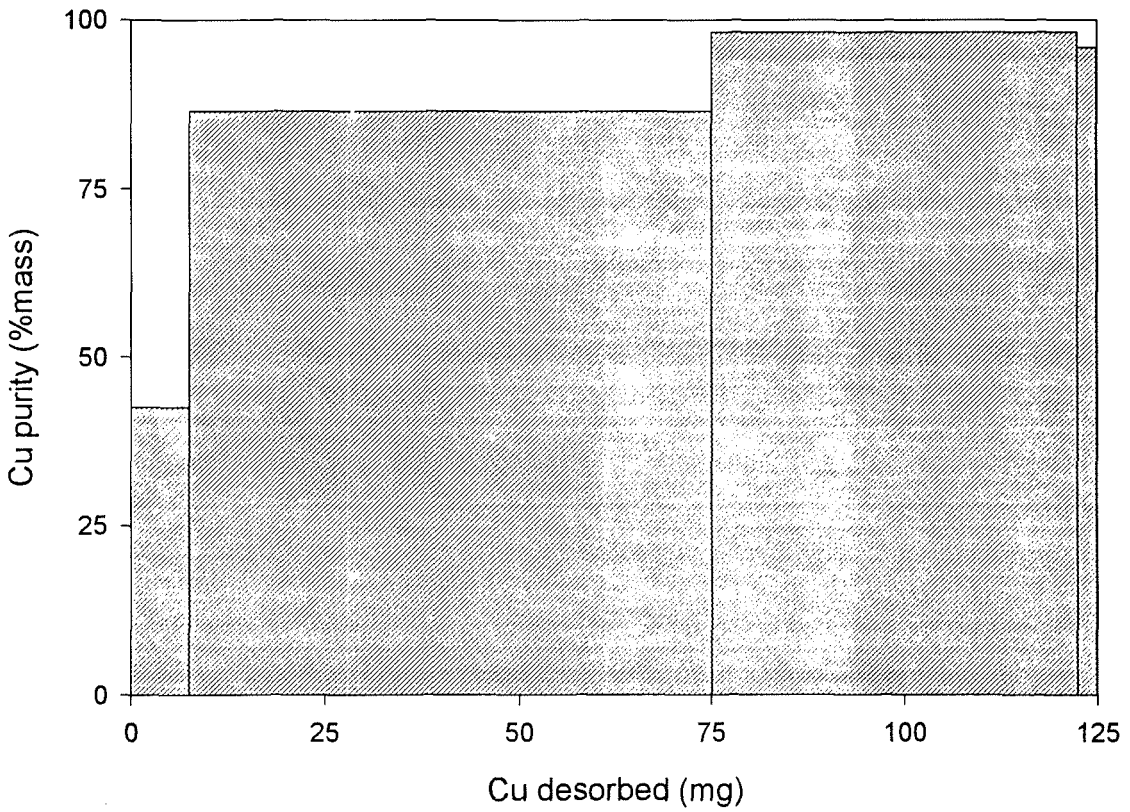

Fig. 10

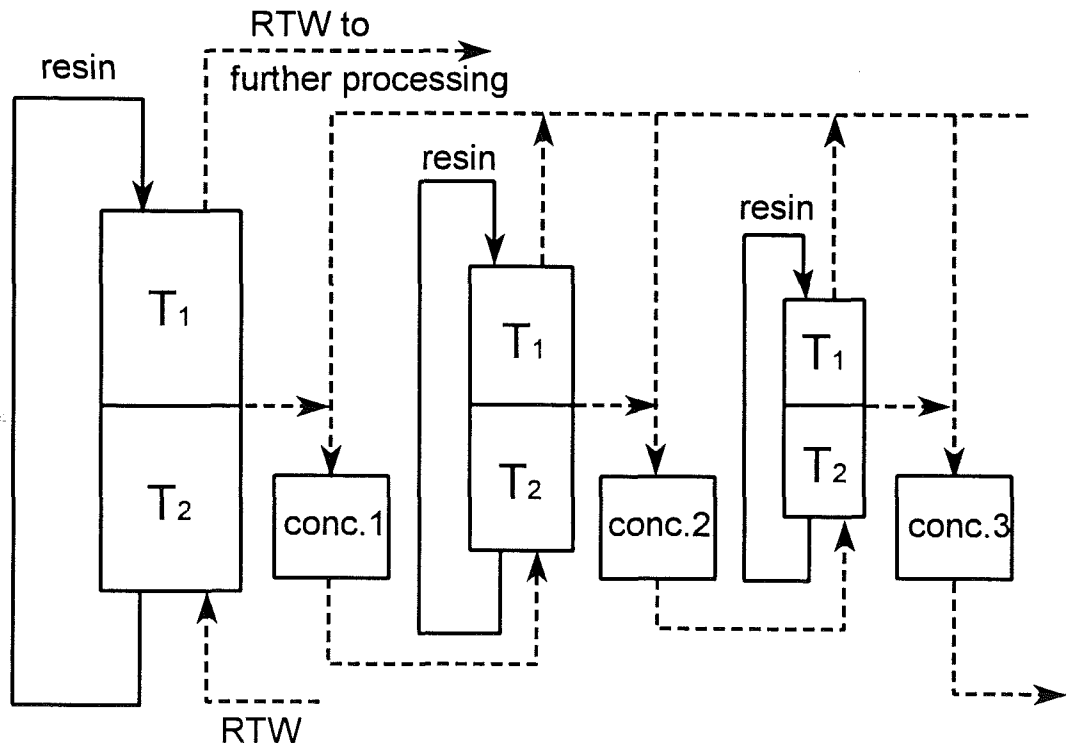
RTW to
further processing
resin
resin
resin
T1
T2
T1
T2
T1
T2
conc.1
conc.2
conc.3
RTW

Fig . 11

ANEXO III

FORECASTING DEGREES OF CONCENTRATION FOR METAL IONS IN DUAL-TEMPERATURE ION EXCHANGE PROCESSING OF ACIDIC MINE WATERS.

Dmitri Muraviev[1], Joan Noguerol and Manuel Valiente*.

Departament de Química, Química Analítica, Universitat Autònoma de Barcelona,

E-08193 Bellaterra (Barcelona), Spain.

Fax: 3435811985, E-mail: IQAN3@CC.UAB.ES

*Author for correspondence.

[1]On sabbatical leave from Moscow State University. Dept. of Physical Chemistry.

ABSTRACT

This paper reports the results on the development of a novel approach for predicting concentration degrees of acidic mine water metal ions such as Cu^{2+}, Zn^{2+}, Al^{3+}, Mn^{2+}, Ca^{2+}, Mg^{2+}, Fe^{3+} and Na^{+} in the reagentless dual-temperature ion exchange process on acrylic resin Lewatit R 250-K . The values of resin capacity towards all ionic species and equilibrium separation factors (α) for different metal ion couples have been determined from the native mine water of Rio Tinto area (Huelva, Spain) in the temperature range from 20°C to 80°C. It has been shown that the capacity of the resin towards Al^{3+} increases while that towards the rest of the metal ions decreases at elevated temperatures. As a result, significant growth of α values for ion couples involving Al^{3+} with increase of temperature is observed. Thermostripping from the resin equilibrated at 20°C with mine water at 80°C leads to sorption of Al^{3+} while the other metal ions are desorbed, resulting in the increase of their concentration in the eluate. Concentration degrees of different metal ions predicted from the equilibrium data have been shown to follow the sequence: $Cu^{2+}>>Zn^{2+}>Mn^{2+}>Ca^{2+}>Mg^{2+}>Na^{+}$. Experimental results obtained agree well with the predictions made, testifying to the validity of the approach proposed.

Key words: ion-exchange equilibrium; temperature dependence; acidic mine water; metal ions; carboxylic resin; dual-temperature ion-exchange concentration.

INTRODUCTION

Acidic mine water is a common problem in many mining situations but it is particularly important in pyritic areas. Interaction of pyrite and other sulfide minerals with water and atmospheric oxygen produces acid solutions which can cause serious problems in the environment. Acid mine drainage is perhaps the most serious environmental impact of mining activity. Although efficient and modern engineering design are now incorporated into the mines, ecological problems related to acidic mine water persist, especially after mining activity has stopped. The origin of acidic water from pyritic areas is the oxidation of sulfide minerals. A rapid oxidation of sulfide minerals occurs where such minerals in contact with water are exposed to the atmosphere. The sulfide components in pyrite are oxidized to sulfate by acidity generation and release of iron. Both Fe(II) and Fe(III) plays a key role in this mineral alteration. These oxidation processes are dynamically accelerated by bacterial activity (Ritcey, 1989; Smith, 1974). Acidic mine water pollution in areas associated with mining can be seen at Rio Tinto (Spain), Neves-Corvo (Portugal), Chuquicamata (Chile), Katanga (Zaire), etc.

Rio Tinto area (Huelva, Spain) is one of the most important pyritic area of the world. The mines are rich in deposits of iron pyrite, copper, zinc, manganese and some precious metals and is one of the best examples of acidic mine waters production. The name Rio Tinto is due to the spectacular reddish color of the river due to the high concentration of Fe(III) hydroxide produced by pyrite oxidation. The acidic mine water production is independent of the mining activity. Although the pyritic ore deposits are scarcely exploited actually, these continue producing approximately several tens of million m^3 of acidic mine waters every year. These waters flow to Rio Tinto and Odiel

rivers that have their origin in the pyritic area and flow into Huelva estuary. In densely populated areas like, e.g. Huelva and other southern provinces of Spain and Portugal, high priority is needed to prevent escaping toxic substances into the environment, and contamination, as a result, of fresh water sources, the number of which is limited. Thus, the ecological impact of the acidic effluents produced in Rio Tinto mines is evident and its treatment is necessary. The composition and pH of different Rio Tinto water samples withdraw at different periods (during January-May 1993) are shown in Table 1.

Table 1

The treatment of the acidic metal-bearing effluents is both of economical and ecological importance. This means that not only the more valuable and toxic constituents must be removed and recovered from the water under treatment, but also the technology applied has to satisfy both economical and ecological standards. From this viewpoint, information on ion-exchange equilibrium of metal ions at different temperatures is essential for further development and wider practical applications of the reagentless ion-exchange separation methods such as dual-temperature ion-exchange processes (e.g. Andreev et al., 1961; Gorshkov et al., 1971; Gorshkov et al., 1977; Muraviev et al., 1996 a; Muraviev et al., 1995; Khamizov et al., 1995) and associated techniques (e.g. Chen et al., 1972; Grevillot et al., 1980; Tondeur and Grevillot, 1986; Wankat, 1978; Szanya et al., 1988; Szanya et al., 1986). This information is of particular interest when obtained from the real metal-bearing effluents, (i.e. acidic mine waters) since it may be helpful in the design of the wasteless and ecologically clean process for the removal and recovery of toxic and/or valuable metals from the effluent under treatment. One of the important economic factors, that need to be considered is the reduction in energy expenditure for heating solution under

treatment. In the countries with high level of solar radiation such as, e.g., Mediterranean countries, this problem can be successfully solved by using conventional or concentrated sunlight as the principal and ecologically clean energy source (sun-boiler systems).

This paper commences a series of investigations on dual-temperature ion-exchange processing of acidic mine waters. The present study was undertaken (1) to investigate the ion-exchange equilibrium of acidic mine water metal ions on a carboxylic resin at different temperatures; (2) to develop a method for selective concentration of copper from the native acidic mine water by applying a reagentless dual-temperature ion-exchange technique, and (3) to develop a novel approach for predicting concentration degrees for different metal ions in a dual-temperature ion-exchange process from the data on ion-exchange equilibrium at different temperatures.

EXPERIMENTAL

Materials, Apparatus and Analytical Methods

The work was performed with samples of the native acidic mine waters of the Rio Tinto area, known to be the natural generic metal-bearing effluents originated from the pyritic ore deposits typical for the southern provinces of Spain and Portugal.

The ion exchanger, a macroporous polyacrylic resin bearing carboxylic groups, Lewatit R 250-K, was kindly supplied by Bayer Hispania Industrial, S.A., NaOH and H_2SO_4 of A.G. were purchased from Probus (Spain) and used as received. The concentration of metal ions was determined by atomic emission spectroscopy (ICP-AES technique) using ARL Model 3410 spectrometer (Fisons, USA) provided with minitorch. The uncertainty of metal ions determination was less than 1.5%. Determination of H^+

and OH^- ions was carried out by potentiometric titration using a Crison pH-meter 507 (Spain) provided with a combined glass electrode. Thermostatic glass columns (of 1.4 cm i. d.) connected with a thermostat (Haake D1, Germany) were used to study the ion-exchange equilibrium at different temperatures. The construction of these columns provides simultaneously the heating (or cooling) of both resin and entering solution phases.

The necessary conditioning of Rio Tinto water samples (RTW) included the adjustment of pH and the removal of iron (Muraviev et al., 1996 b). This was carried out by a preliminary treatment of RTW samples that involved the adjustment of pH to 3.4-3.5 with concentrated NaOH solution and the bubbling of air through the solution during several days. Under those conditions the oxidation of Fe(II) to Fe(III) and selective precipitation of Fe(III) hydroxide took place. These processes are known to be significantly accelerated by *Thiobacillius Ferrooxidans* so that the complete oxidation of Fe(II) (and precipitation of Fe(III) hydroxide as a result) can be reduced to several hours (Ritcey, 1989). The final removal of the precipitate was carried out by filtration using a sintered glass filter and a water-pump. The composition of RTW samples, before and after this treatment, are shown in Table 2.

Table 2

Methods

Ion-Exchange Equilibrium

The ion-exchange equilibrium was studied under dynamic conditions in the thermostatic columns previously described. The columns were loaded with a certain portion of the ion exchanger which remained constant during all the series of experiments. The total capacity of the resin bed was determined prior to the equilibrium

studies by applying a standard technique (e.g. Muraviev et al., 1996 a). Then, the resin was converted into Na-form and equilibrated at a selected temperature. Conditioned RTW was passed through the column in a fluidized mode (from bottom to top) at constant flow rate of 40 cm^3/min to prevent clogging of the resin bed with $Al(OH)_3$ precipitate which appeared in the first portions of solution passing through the column.

Under these conditions, achievement of the ion-exchange equilibrium in the system was followed by a comparison of the metal concentration in the solution leaving the column with that of the feed as described elsewhere (Muraviev et al., 1995; Muraviev et al., 1996 a). After equilibration, the remaining solution phase was removed from the resin and a stripping process of the metal loaded resin was immediately stripped with 1.5 M HCl. Then, the resin was converted back into Na-form and prepared for the next run. Analysis of the eluate metal content during the loading process provided the corresponding breakthrough curves. The results of the stripping solution analysis were used to determine the values of the partial capacity of the resin towards each metal ion and to calculate the separation factors, α, for different ion couples by the use of the following expression:

$$\alpha_{Me_1}^{Me_2} = \frac{Y_{Me_2}}{Y_{Me_1}} \cdot \frac{X_{Me_1}}{X_{Me_2}} \qquad (1)$$

where Y and X are the equivalent fractions of ions under consideration in the resin and solution phases, respectively; indices 1 and 2 are chosen so that $\alpha>1$. The relative uncertainty of α values never exceed 7%.

Thermosorption and Thermostripping

Separate thermostripping and thermosorption experiments were carried out as follows: after equilibration of the resin with RTW at 80°C and 20°C respectively, the remaining solution over the resin bed was removed from the column. Then, either a cooling (for thermosorption) or a heating (for thermostripping) of the column was started. After reaching the temperature equilibrium, RTW was passed through the column at a constant flow rate and collected in portions to determine the corresponding metal ions content. RTW solution was passed until the ion-exchange equilibrium at each temperature was achieved.

RESULTS AND DISCUSSION

Ion-Exchange Equilibrium

The absolute partial capacities of Lewatit R 250-K towards RTW metal ions and the total capacity of the resin bed used vs temperature are shown in Table 3.

Table 3

As seen from the data presented in Table 3, the resin under study demonstrates a different behavior for Al^{3+} than for the rest of the RTW metal ions in terms of both partial capacity and temperature dependence. Indeed, the affinity of the resin towards Al^{3+} increases while that towards the other metal cations usually decreases with the increase of temperature. The most remarkable drop of the resin bed capacity (as observed, e.g. for Cu^{2+} and Zn^{2+}) does not exceed several tenth of mequiv. while the growth of that towards Al^{3+} is about 2 mequiv/g within the temperature interval studied. This results to the increase of the total capacity of the resin at elevated temperatures.

Temperature dependencies of α for different ion couples are shown in Fig.1. As

seen in Fig. 1a, a strong positive influence of temperature on α values is observed for ion couples involving Al^{3+}. As seen in Figs.1b and 1c an opposite trend (a negative temperature dependence of α) is observed for $\alpha^{Me1}_{Me2}=f(t)$, where $1=Zn^{2+}$ (see curves 1-4 in Fig. 1c), and for α^{Cu}_{Mg} and α^{Cu}_{Na} (curves 1 and 3 in Fig. 1b). Dependencies of α vs temperature for the rest of the ion couples are much weaker (see, e.g. curve 5 in Fig.1c and Fig.1d). A reversal of selectivity is observed at elevated temperature for Mn^{2+}-Ca^{2+} and Mn^{2+}-Na^{+} exchanges as seen in Fig. 1d (curves 4 and 5).

Temperature dependencies of α^{Me1}_{Me2} shown in Fig. 1 reflect the alteration of metal ion sorbabilities caused by the temperature change (see Table 3). Indeed, as follows from eq. (1) the ratio of two α values determined at different temperatures for a given ion couple (the composition of the equilibrium solution at two temperatures is presumed to be identical) can be written as follows:

$$a = \frac{\alpha^{Me_1}_{Me_2}(T_1)}{\alpha^{Me_1}_{Me_2}(T_2)} = \frac{Y_{Me_1}(T_1)}{Y_{Me_1}(T_2)} \cdot \frac{Y_{Me_2}(T_2)}{Y_{Me_2}(T_1)} \qquad \textbf{(2)}$$

where T_1 and T_2 are chosen so that ***a*** >1. Equation (2) can be rewritten in the following form:

$$a = \frac{Y_{Me_1}(T_1)}{Y_{Me_1}(T_1) + \Delta Y_{Me_1}} \cdot \frac{Y_{Me_2}(T_1) + \Delta Y_{Me_2}}{Y_{Me_2}(T_1)} \qquad \textbf{(3)}$$

where $\Delta Y_{Me}=Y_{Me}(T_1)-Y_{Me}(T_2)$. As follows from equation (3) ***a*** achieves the maximum

magnitude at $\Delta Y_{Me1}<0$ and $\Delta Y_{Me2}>0$, i.e. when metal ions under consideration are characterized by an opposite temperature dependence of their sorbabilities.

Parameter ***a*** is known to serve as a criterion of the efficiency of any dual-parametric ion-exchange separation including dual-temperature ion-exchange technique (e.g. Tondeur and Grevillot, 1986; Muraviev et al., 1996 b; Gorshkov, 1995). On the other hand, it may be also applied for predicting the metal ions which separation is expected to prevail in the system under study. This prediction is of particular importance in instances of multicomponent mixtures such as, e.g. RTW. As follows from Table 3 and from the above discussion the main separation effect in the system under consideration must be observed between Al^{3+} and the rest RTW metal ions. To quantify this conclusion a comparison of the values of parameter ***a*** given in Table 4 for Al^{3+} and other RTW cations has been carried out, taking T_2=80 °C and different values of T_1.

Table 4

As follows from the data collected in Table 4, the value of parameter ***a*** varies for the different ionic couples and a non linear decrease with the increase of T_2 is observed. The maximum ***a*** values are observed for Al^{3+}-Zn^{2+}, Al^{3+}-Mn^{2+} and Al^{3+}-Cu^{2+} (at T_1=20°C), hence, it is expected the maximum separation effect will occur for these ionic couples.

On the other hand, the degree of concentration by dual-temperature ion-exchange technique for any ion is (1) directly proportional to the variation of the corresponding resin capacity, Δq, between the loading temperature, T_1, and the stripping temperature, T_2, and (2) inversely proportional to the initial concentration of the ion in the feed solution, C_o. To predict the behavior of different ions when a dual-temperature ion-exchange concentration technique is applied to a multicomponent

mixture, a new parameter $\boldsymbol{b}_{equil}=\Delta q.m/C_oV_i$ (V_i is the solution volume passed and m is the mass of the resin) has been introduced. In our case, $\Delta q=q(20°C)-q(80°C)$, C_o and ***b*** values for different RTW ions are collected in Table 5.

Table 5

As seen from ***b*** values given in Table 5 for the series of ions under consideration, the relative order of their concentration degrees will follow the sequence:

$$Cu^{2+}>>Zn^{2+}>Mn^{2+}>Ca^{2+}>Mg^{2+}>Na^{+} \qquad (4)$$

Note that ***b*** values can not be applied for the quantitative prediction of the metal ion concentration degrees since they have been calculated for the conditions of "ideal displacement" without taking into account the real diffusivities of ionic species in the resin phase (Dorfner, 1991).

Thermostripping and Regeneration

One of the typical concentration-volume histories obtained by thermostripping at 80°C from Lewatit R 250-K equilibrated at 20° C with natural RTW is shown in Fig. 2. The total capacity of the resin bed used in this series of experiments was 8.4 mequiv/g (see Table 3). Hot RTW was passed at 1.6 cm^3/min of flow rate. As seen in Fig. 2, thermostripping leads to desorption of all RTW metal ions from the resin except Al^{3+} which is sorbed. This results in a decrease of Al^{3+} concentration in the eluate and to a increase of the rest metal ions concentration. The maximum relative concentration observed for each ion in fact correlates with the above sequence of concentration degrees. The only exception occurs for Mn^{2+} and Zn^{2+}. As seen in Fig. 2 the peak of the former is quite high and narrow while that of the latter is wide (with clearly seen tail)

and of lower height. This disagreement of the predicted and observed behavior of Mn^{2+} and Zn^{2+} can be ascribed to the difference in their diffusivities which is known to be around one order of magnitude (Dorfner, 1991). Zn^{2+} as a species of lower diffusivity, releases slower than Mn^{2+} and gives a wider and lower peak. On the other hand, the peak integral, I, for any RTW ion, "i", can be calculated from the data shown in Fig. 2 as follows:

$$I = \sum_{i}^{j} (C_i - C_o)\ V_i \qquad (5)$$

where C_o and C_i are the concentrations of the ion in the initial mixture and in the "i" eluate fraction, respectively, V_i is the volume of eluate portion "i"; "j" is the total number of eluate fractions where $C_i \neq C_o$.

From the mass balance in the system under consideration it follows that I is proportional to Δq, i.e. parameter $\boldsymbol{b}$ can be now expressed as follows:

$$b_{strip} = \frac{\sum_{i}^{j} (C_i - C_o)\ V_i}{C_o \sum_{i}^{j} V_i} \qquad (6)$$

A comparison of $\boldsymbol{b}$ values calculated from the equilibrium data ($\boldsymbol{b}_{equil}$) (see above) with those determined from the results of stripping experiments ($\boldsymbol{b}_{strip}$) is presented in Fig. 3. As seen in Fig. 3 the plot $\log(\boldsymbol{b}_{equil})$ vs $\log(\boldsymbol{b}_{strip})$ fits to a straight line that testifies to the direct proportionality between $\boldsymbol{b}_{equil}$ and $\boldsymbol{b}_{strip}$ values and confirms the validity of the approach proposed and the prediction made.

ACKNOWLEDGMENTS

This work has been carried out with the financial support of CICYT, the Spanish Commission for Research and Development, project PTR930009. Dr. D. Muraviev thanks to the Spanish Ministry for Education and Science to support his sabbatical stay at Universitat Autónoma de Barcelona (SAB95-0073). Bayer Hispania Industrial, S.A. is gratefully acknowledged for supplying with samples of Lewatit resins. Rio Tinto Minera S.A. is also gratefully acknowledged for supplying with samples of acidic mine waters.

REFERENCES

Andreev, B.M.; Boreskov, G.K. and Katalnikov, S.G. (1961) Dual-temperature technique for separation of ions on fixed bed of ion exchanger *Khim. Prom-st*, **6**, 389-395. (Russ.)

Chen, H.T., Rak, J.L., Stokes, J.P. and Hill, F.B. (1972). Separation via continuous parametric pumping. AICHE. J., **18(2)**, 356-361.

Dorfner, K. (1991). Introduction to ion exchange and ion exchangers. In *Ion Exchangers*; K. Dorfner, Ed.; Walter de Gruyter: Berlin, pp. 7-187.

Grevillot, G., Dodds, J. and Marques, S. (1980). Separation of silver-copper mixtures by ion-exchange parametric pumping. J. Chromatogr., **201**, 329-342.

Gorshkov, V.I.; Kurbanov, A.M. and Apolonnik, N.V. (1971). Counter-current ion-exchange separation without auxiliary ions. *Zhur. Fiz. Khim.*, **45**, 2969-2971. (Russ.).

Gorshkov, V.I.; Ivanova, M.V.; Kurbanov, A.M.; Ivanov, V.A. (1977). New ion-exchange separation techniques. *Vestnik Moskov. Univ., Ser. Khim.*, **32**, 535-545. (Russ.). *English translation in Moscow Univ. Bull.*, **32**, 23.

Gorshkov, V. I. (1995). Ion exchange in counter-current columns. In *Ion Exchange and Solvent Extraction*; Marinsky, J.A.; Marcus, Y., Eds.; Marcel Dekker: New York, Vol. 12, pp. 29-92.

Khamizov, R.; Muraviev, D.; Warshawsky, A. (1995). Recovery of valuable mineral components from seawater by ion exchange and sorption methods. In *Ion Exchange and Solvent Extraction*; Marinsky, J.A.; Marcus, Y., Eds.; Marcel Dekker: New York, Vol.12; pp. 93-148.

Muraviev, D.; Noguerol, J.; Valiente, M. (1996 a). Separation and concentration of calcium and magnesium from sea water by carboxylic resins with temperature-induced

selectivity. *React. Polym.*, **28**, 111-126.

Muraviev, D.; Gonzalo, A.; Valiente, M. (1995). Ion exchange on resins with temperature responsive selectivity. 1. Ion-exchange equilibrium of Cu^{2+} and Zn^{2+} on iminodiacetic and aminomethylphosphonic resins. *Anal. Chem.*, **67(17)**, 3028-3035.

Muraviev, D.; Noguerol, J.; Valiente, M. (1996 b). Application of the reagentless dual-temperature ion-exchange technique to selective separation and concentration of copper versus aluminium from acidic mine waters. *Hydrometallurgy*, in press.

Ritcey, G.M. (1989). *Tailings Management, Problems and Solutions in the Mining Industry*; Elsevier: Amsterdam, p. 270.

Smith, M.J. (1974). Acid production in mine drainage systems. In *Extraction of Minerals and Energy: Today's Dilemmas*; Dejn, R.A., Ed.; Ann Arbor Science: Ann Arbor, Michigan, pp. 57-75.

Szanya, T.; Hanak, L. and Mohila, R. (1988). Separation by ion-exchange and adsorption parametric pumping. III. Enrichment of alkali- and alkali earth ions from aqueous binary mixtures by batch thermal ion-exchange parametric pumping. *Hung. J. Ind. Chem. Veszp.*, **16**, 261-268.

Szanya, T.; Hanak, L. and Mohila, R. (1986). Separation of ions by thermal ion-exchange parametric pumping. *Zhur. Prikl. Khim.*, **56**, 2194-2199. (Russ.)

Tondeur, D. and Grevillot, G. (1986). Parametric ion-exchange processes (Parametric pumping and allied techniques). In *Ion-Exchange: Science and Technology*. NATO ASI series; Rodrigues, A.E. Ed.; Martinus Nijhoff: Dordrecht, Vol. 107, pp. 369-399.

Wankat, P.C. (1978). Cyclic separation techniques. In *Percolation Processes: Theory and Applications*; Rodrigues, A.E.; Tondeur, D., Eds.; Sijhoff and Noordhoff: Alpen aan den Rijm, p. 443-515.

LEGENDS TO FIGURES

Fig. 1 Temperature dependencies of equilibrium separation factors for ion couples:

a) Al^{3+}/Mg^{2+} (1), Al^{3+}/Mn^{2+} (2), Al^{+3}/Na^{+} (3), Al^{3+}/Ca^{2+} (4), Al^{3+}/Zn^{2+} (5), Al^{3+}/Cu^{2+} (6);

b) Cu^{2+}/Mg^{2+} (1), Cu^{2+}/Ca^{2+} (2), Cu^{2+}/Na^{+} (3), Cu^{2+}/Mn^{2+} (4),and Cu^{2+}/Zn^{2+} (5);

c) Zn^{2+}/Mg^{2+} (1), Zn^{2+}/Mn^{2+} (2), Zn^{2+}/Ca^{2+} (3), Zn^{2+}/Na^{+} (4), Mn^{2+}/Mg^{2+} (5);

d) Na^{+}/Mg^{2+} (1), Na^{+}/Ca^{2+} (2), Ca^{2+}/Mg^{2+} (3), Mn^{2+}/Ca^{2+} (4), Mn^{2+}/Na^{+} (5)

on Lewatit R 250-K.

Fig. 2 Thermostripping breakthrough curves for RTW from Lewatit R 250-K resin:

Zn^{2+} (1), Mn^{2+} (2), Cu^{2+} (3), Al^{3+} (4), Ca^{2+} (5), Mg^{2+} (6) and Na^{+} (7).

T=80°C, solution flow rate = 1.6 cm^3/min.

Fig. 3 Comparison of $\boldsymbol{b}$ values calculated from equilibrium data ($\boldsymbol{b}_{equil}$) with those determined from results of stripping experiments ($\boldsymbol{b}_{strip}$) for RTW metal ions:

(○) Zn^{2+}, (□) Mn^{2+}, (Δ) Cu^{2+}, (●) Ca^{2+}, (■) Mg^{2+}, (▲) Na^{+}.

Table 1. Composition (the concentration is expresed in ppm) and pH of different Rio Tinto water samples.

Date	Cu^{2+}	Fe^{2+}	Fe^{3+}	Zn^{2+}	Al^{3+}	SO_4^{2-}	pH
930105	110	6,479	2,121	1,600	490	26,125	1.80
930209	106	5,965	1,365	1,500	550	25,132	1.60
930310	90	5,764	1,436	1,500	480	23,720	1.70
930412	70	6,433	67	1,200	490	20,499	1.75
930519	260	4,155	945	1,100	550	20,662	2.00

Table 2. Composition of Rio Tinto water samples before and after treatment.

C (ppm)	pH	SO_4^{2-}	Fe^{3+}	Cu^{2+}	Zn^{2+}	Al^{3+}	Mn^{2+}	Mg^{2+}	Ca^{2+}	Na^{+}
Initial	1.8	17,430	4,527	117	1,217	560	87	940	480	22
Treated	3.5	17,350	3	115	1,275	530	90	950	475	3,550

Table 3. Temperature dependencies of partial (q) and total (Q_o) capacities expresed in mequiv/g of Lewatit R 250-K resin for RTW metal ions.

T (°C)	Fe^{3+}	Cu^{2+}	Zn^{2+}	Al^{3+}	Mn^{2+}	Mg^{2+}	Ca^{2+}	Na^{+}	Q_o
20	0.031	0.270	0.382	5.65	0.015	0.142	0.085	0.344	6.92
40	0.006	0.171	0.114	6.30	0.005	0.106	0.041	0.330	7.07
60	0.003	0.138	0.105	6.92	0.005	0.101	0.036	0.308	7.61
80	0.003	0.097	0.113	7.68	0.005	0.102	0.059	0.301	8.37

Table 4. Values of parameter ***a*** for ion couples involving Al^{3+} at T_2=80°C and different T_1.

T_1 (°C)	Cu^{2+}	Zn^{2+}	Mn^{2+}	Mg^{2+}	Ca^{2+}	Na^{+}
20	3.43	4.26	4.02	1.85	1.95	2.23
40	2.13	1.25	1.45	1.37	0.91	1.35
60	1.62	1.09	1.19	1.18	0.73	1.14

Table 5. Δq, C_o and ***b*** values for different RTW metal ions at T_1=20°C y T_2=80°C.

Me	Cu^{2+}	Zn^{2+}	Mn^{2+}	Mg^{2+}	Ca^{2+}	Na^{+}
Δq^{*} (mequiv/g)	0.17	0.27	0.010	0.040	0.026	0.043
Co^{**} (mequiv/dm^3)	3.90	29.66	3.44	70.78	22.75	170
$b_{equil} \times 10^{3***}$	74.36	15.17	4.94	0.96	1.93	0.42

* The values refer to the difference of the resin bed capacity (1.674 g).
** Recalcullated from the data given in Table II.
*** For simplicity V_i for different ions are presumed to be the same and equal to 1.

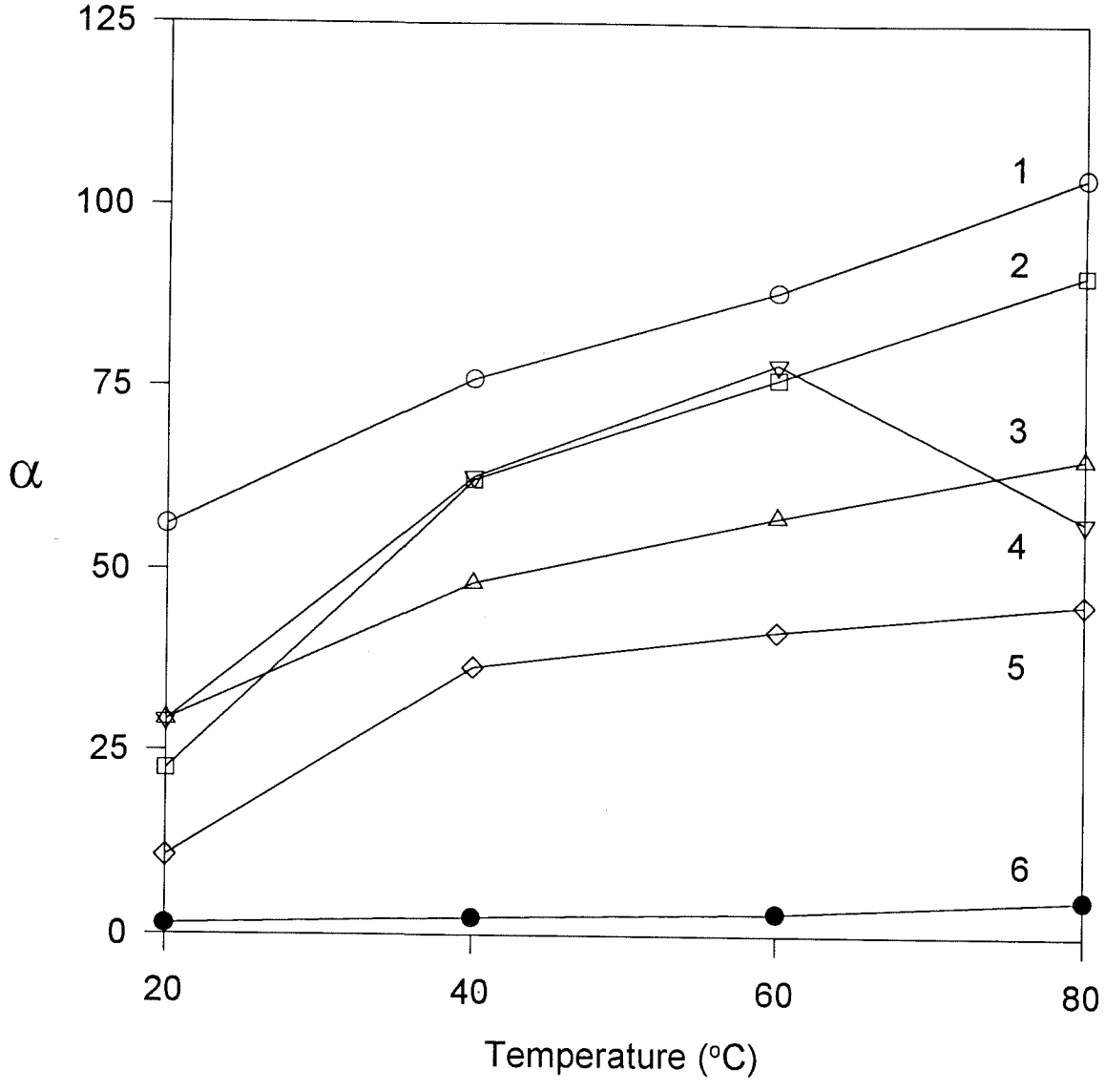

Fig. 1a

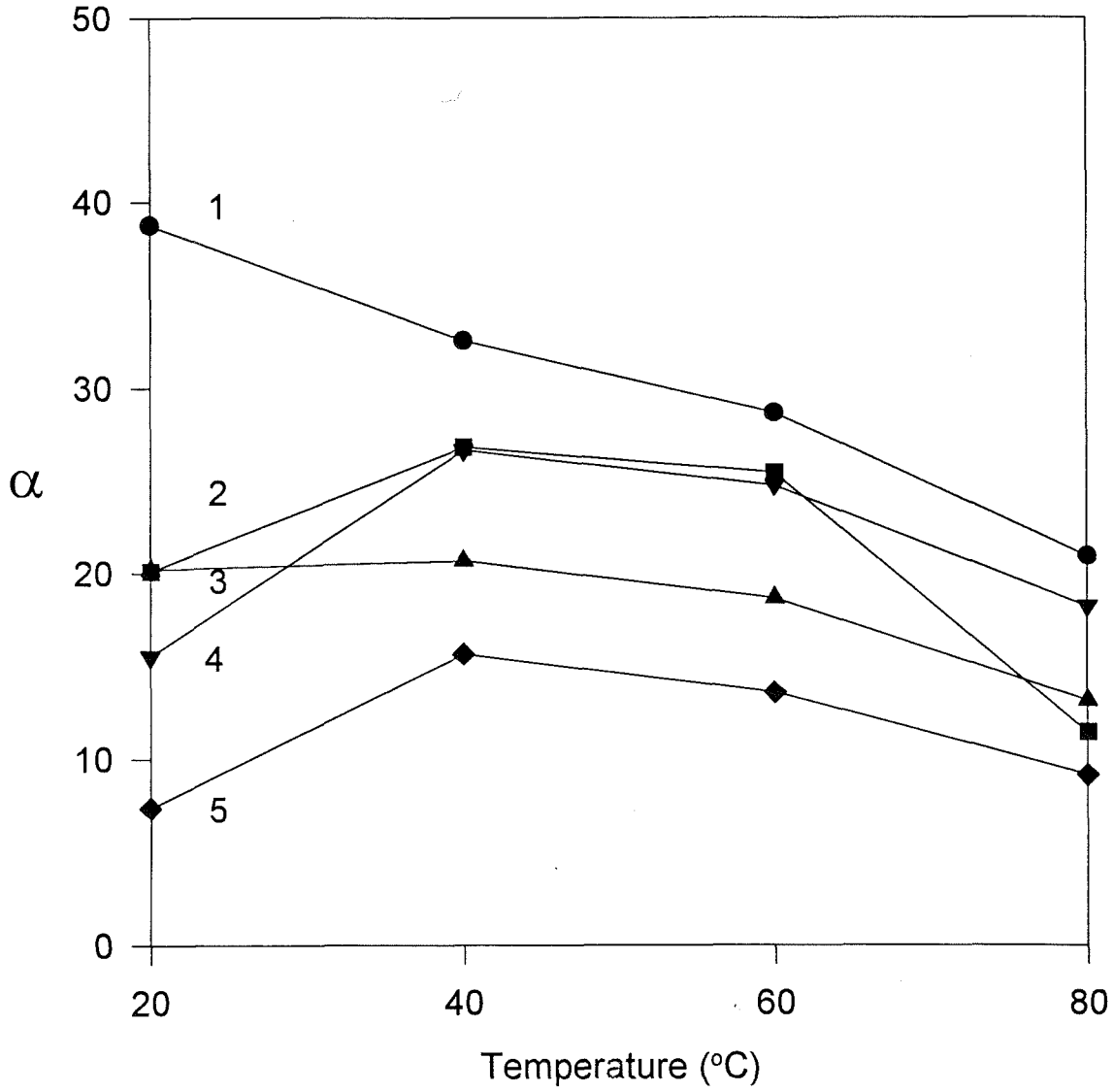

Fig. 1b

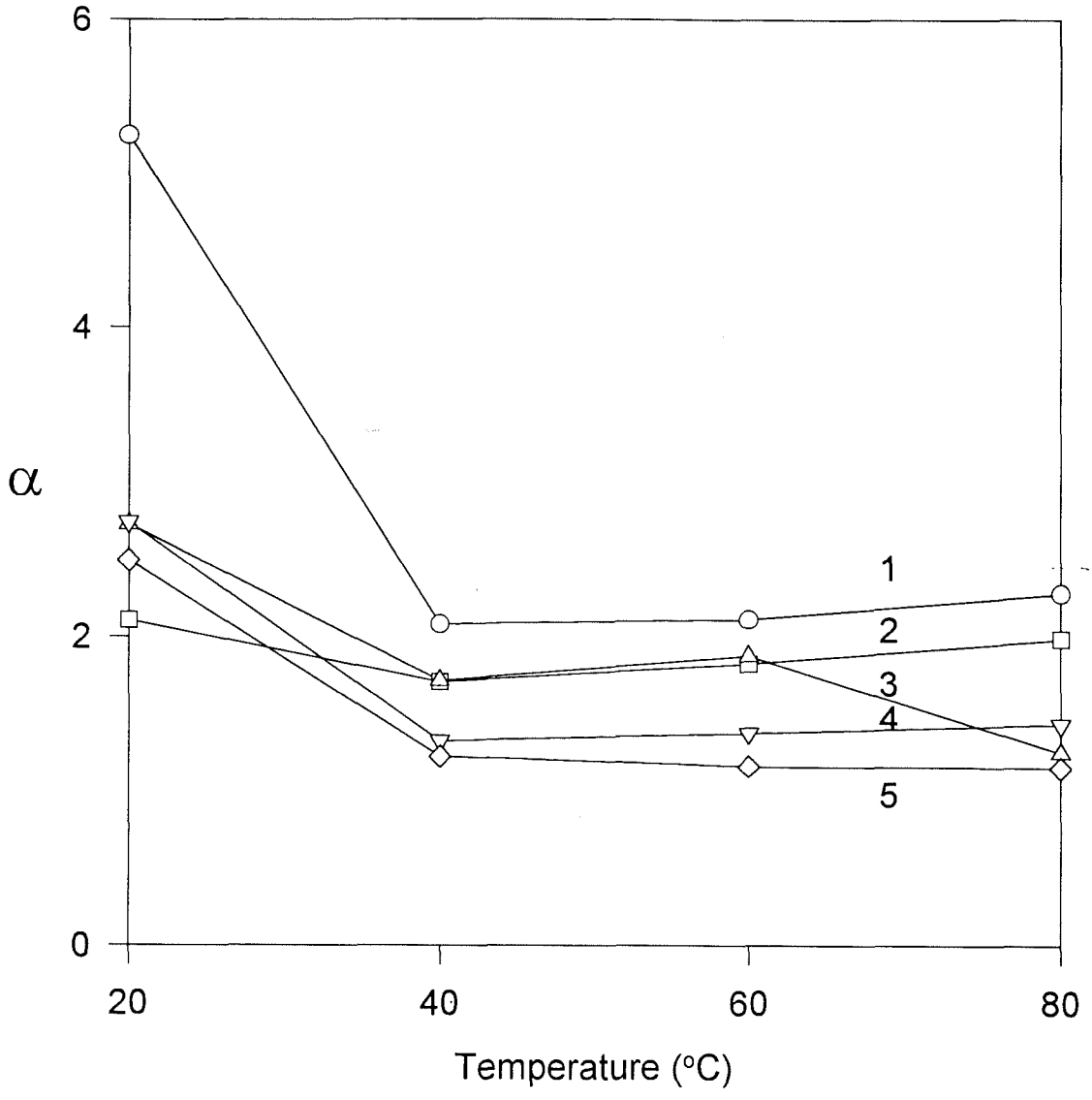

Fig. 1c

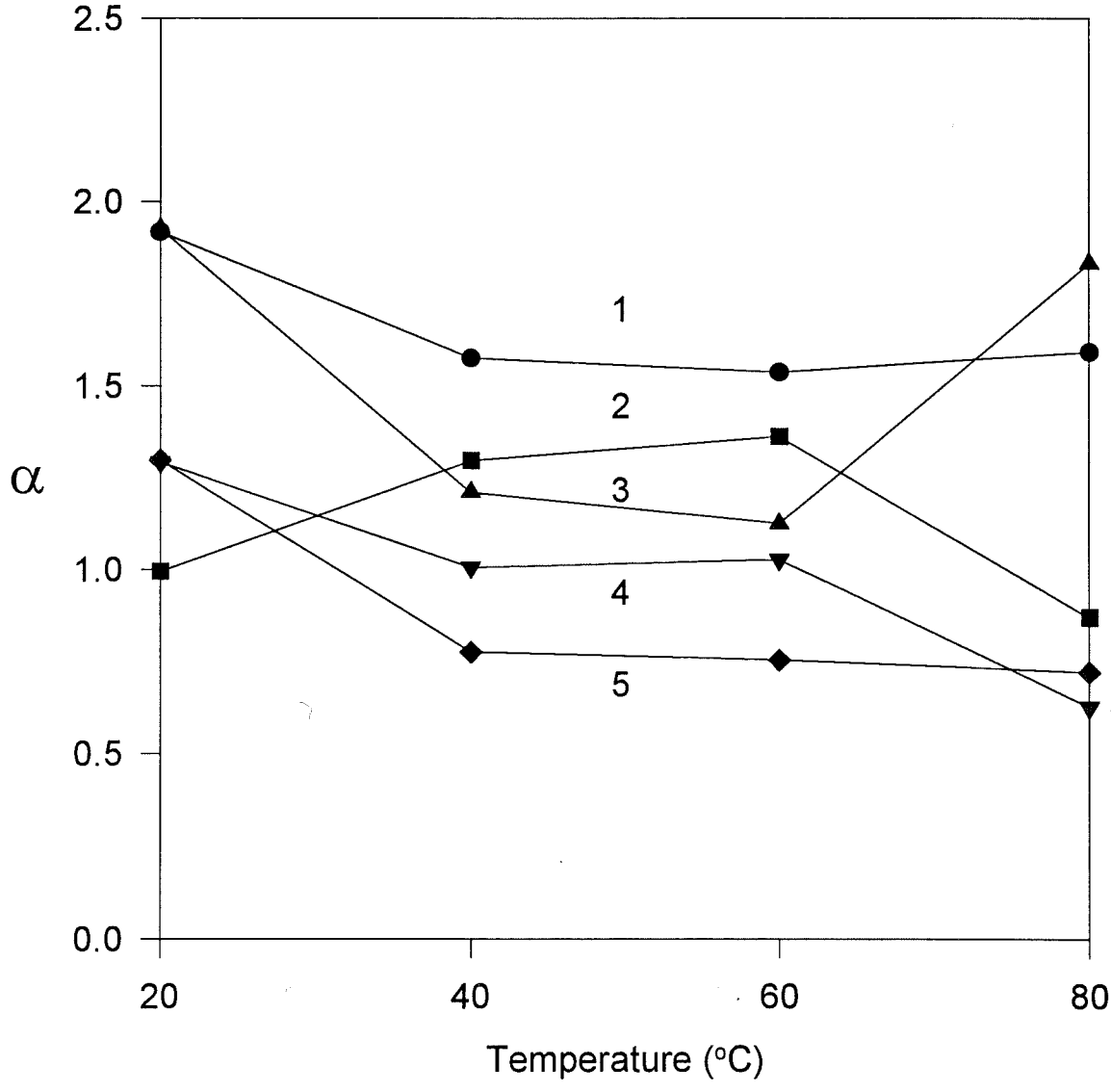

Fig. 1d

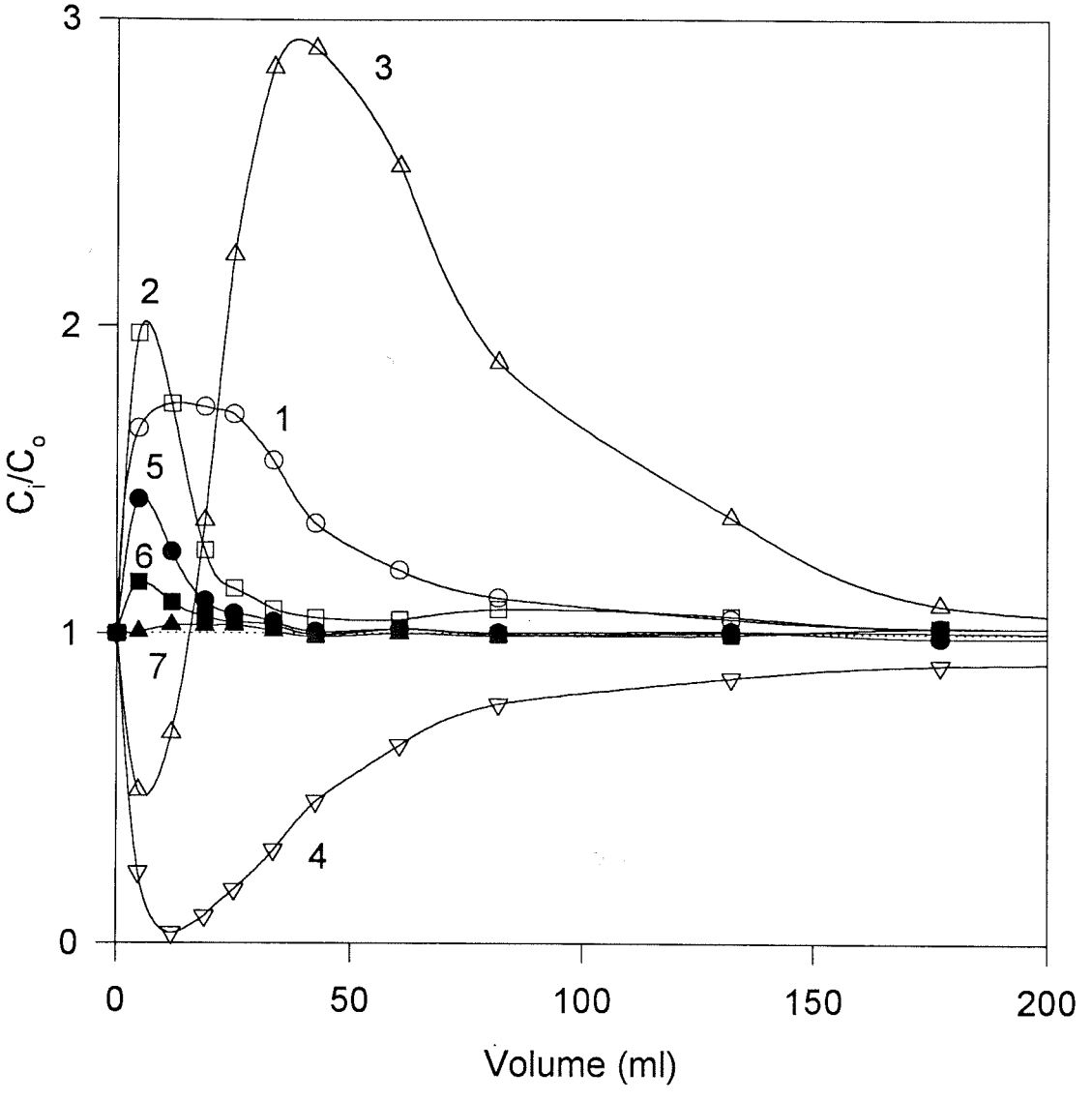

Fig. 2

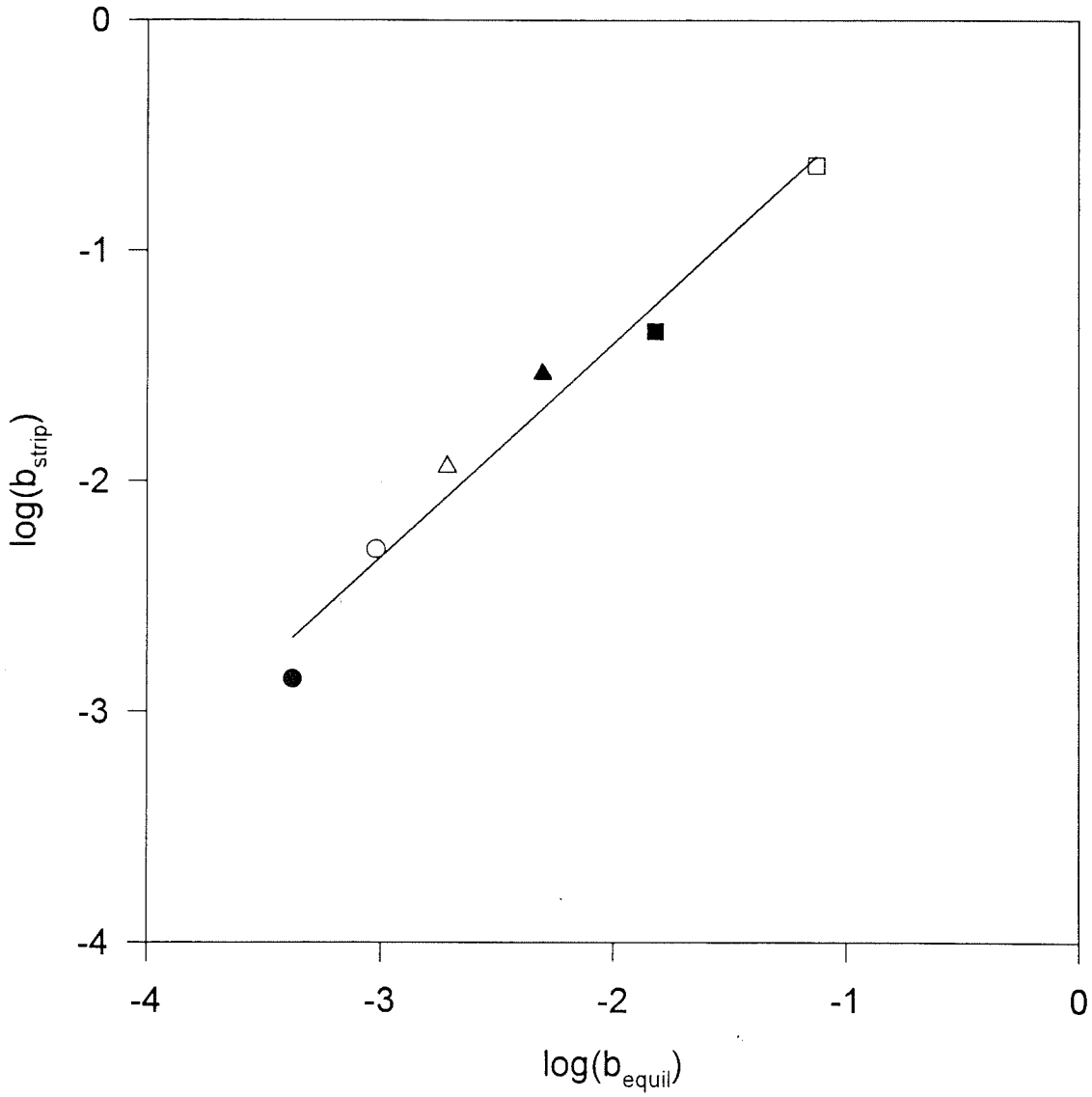

Fig. 3

ANEXO IV

ENVIRONMENTAL SCIENCE & TECHNOLOGY

PUBLISHED BY THE
AMERICAN CHEMICAL SOCIETY

Department of Environmental Science and Engineering
Oregon Graduate Institute of Science and Technology
P.O. Box 91000
Portland, OR 97291-1000
Phone: (503) 690-1507
FAX: (503) 690-1273
INTERNET: ES&T@ese.ogi.edu

September 27, 1996

Dr. Manuel Valiente
Departament de Quimica, Quimica Analitica
Universitat Autonoma de Barcelona
E-08193 Bellaterra (Barcelona)
SPAIN

Dear Dr. Valiente:

We are pleased to inform you that your manuscript entitled "Sea Water as Auxiliary Reagent in Dual-Temperature Ion-Exchange Processing of Acidic Mine Waters" (ES960178E). has been accepted for publication in *ENVIRONMENTAL SCIENCE & TECHNOLOGY.*

Your galley proof will be prepared by our staff in Columbus, Ohio, and, unless otherwise directed, will be sent to you at the address listed above. Since your paper is not yet scheduled for an issue, we cannot tell you the exact time you will receive the proof. As a general rule, galleys are mailed to authors at least eight weeks prior to publication of the issue in which the paper is scheduled to appear. Prompt return of your proof will be greatly appreciated.

If in the future you have questions about your paper, please contact the Columbus staff directly. The number is (614) 447-3665. We have enjoyed working with you on this paper and look forward to receiving other contributions from you in the future.

Sincerely yours,

James F. Pankow
Associate Editor

SEA WATER AS AUXILIARY REAGENT IN DUAL-TEMPERATURE ION-EXCHANGE PROCESSING OF ACIDIC MINE WATERS

Dmitri Muraviev[1], Joan Noguerol and Manuel Valiente*.

Departament de Química, Química Analítica, Universitat Autònoma de Barcelona,

E-08193 Bellaterra (Barcelona), Spain.

Fax: 3435811985, E-mail: IQAN3@CC.UAB.ES

Key words: dual-temperature ion-exchange concentration; copper; mine waters; carboxylic resin; sea water; regeneration.

---

*Author for correspondence.

[1]On sabbatical leave from Moscow State University. Dept. of Physical Chemistry.

ABSTRACT

This paper reports the results of studying dual-temperature ion-exchange concentration of Cu^{2+} from acidic mine waters on acrylic resin Lewatit R 250-K in applying sea water as a regenerant. Application of seawater as an auxiliary reagent has been shown to enhance selective concentration of copper. Loading of the resin in the initial seawater form with mine water at 20° C followed by thermostripping with hot mine water at 80° C has been shown to result in around three-fold increase of copper concentration in the first portions of the eluate. The repetitive thermosorption-thermostripping concentration cycles appear to be less efficient and give around 25 % increase of Cu^{2+} concentration. The applicability of seawater for regeneration of the resin in the course of ion-exchange treatment of mine water has been successfully demonstrated and the flowsheet of a proposed process is presented.

INTRODUCTION

The processes, which are commonly exploited for the treatment of metal bearing industrial waste waters and effluents to remove and/or to recover most valuable and/or toxic constituents *(1-7)*, can be classified into two groups:

1. *Non-specific technologies* such as precipitation and evaporation, and
2. *Recovery technologies* involving ion exchange, extraction, membrane separation, electrowinning and some others.

Current economic and ecological analyses of the various processes available for recovery of metals from waste waters favor in many instances ion exchange *(3, 6)*. Even though ion exchange is favored, one must take into account the primary disadvantage of this treatment technique, which relates to the resin regeneration step. This step requires application of aggressive chemicals (e.g., acid and/or alkali) and is known to be the main source of wastes in ion-exchange technology. Hence, ion-exchange methods providing the ability to exclude (at least partially) the regeneration step are of particular interest. The group of methods of this type include dual-temperature ion-exchange processes *(8-15)* and allied techniques *(16-18)*. Although the advantages of the above techniques are quite obvious the practical application of these methods is still very limited. The following factors can stimulate the development of the above techniques: (1) the possibility of their combination with conventional ion-exchange methods; (2) the application of non-aggressive and easily available auxiliary reagents, such as, e.g., seawater for regeneration of the ion exchanger, and (3) the reduction in energy expenditure for heating solution under treatment and the regenerant (e.g., seawater) applied. The last problem can be successfully solved by using conventional or concentrated sunlight (in the areas with high level of solar

radiation) as the principal and ecologically clean energy source (sun-boiler systems). An alternative solution can be the use of seawater in the cooling cycles of the steam power stations. An estimation shows, that in this case almost 50% of the overall power costs could be written off *(6)*.

In a recent communication *(11)* we reported the data on ion-exchange equilibrium of seawater metal ions on carboxylic resins at different temperatures. A significant increase of the equilibrium separation factor, α, at elevated temperatures was observed for Ca^{2+}-Na^{+} and Mg^{2+}-Na^{+} exchanges. These results provide a selective thermostripping of Ca^{2+} and Mg^{2+} from the resins equilibrated with sea water at 80°C by applying cold seawater at 10°C.

Although during the last two decades there has been a growing interest in the recovery of different valuable minerals from seawater (see, ref. *(6)* and references therein) practically no reports on applying seawater as an auxiliary agent in ion-exchange separation processes can be found in the literature.

In our recent communication *(15)* we have demonstrated the applicability of the reagentless dual-temperature ion exchange process for selective concentration of copper from the native acidic mine waters on a carboxylic cation exchanger Lewatit R 250-K. The present study was undertaken (1) to study the regeneration of a carboxylic ion exchanger in a form of mine water metal ions with natural sea water, and (2) to study the conditions for concentrating copper from acidic mine water by reagentless dual-temperature ion-exchange technique.

EXPERIMENTAL

Materials, Apparatus and Analytical Methods

The work was performed with samples of the native acidic mine waters of the Rio Tinto area, known to be the natural generic metal-bearing effluents originated from the pyritic ore deposits typical for the southern provinces of Spain and Portugal.

Samples of the natural Mediterranean seawater used in the present study were obtained from the area near Tarragona (Spain). Natural seawater was boiled and then filtered for removal of organic matter before its use in the experiments. The composition (macrocomponents) of seawater was as follows: ionic species/C(ppm): Ca^{2+}/450; Mg^{2+}/1,370; Na^{+}/11,135 and pH=8.1. The ion exchanger, a macroporous polyacrylic resin bearing carboxylic groups, Lewatit R 250-K, was kindly supplied by Bayer Hispania Industrial, S.A., NaOH and H_2SO_4 of A.G. were purchased from Probus (Spain) and used as received. The concentration of metal ions were determined by atomic emission spectroscopy (ICP-AES technique) using ARL Model 3410 spectrometer (Fisons, USA) provided with minitorch. The uncertainty of metal ions determination was less than 1.5%. Determination of H^{+} and OH^{-} ions was carried out by potentiometric titration using a Crison pH-meter 507 (Spain) provided with a combined glass electrode. Thermostatic glass columns (of 1.4 cm i. d.) connected with a thermostat (Haake D1, Germany) were used to study the ion-exchange equilibrium at different temperatures. The construction of these columns provides simultaneously the heating (or cooling) of both resin and entering solution phases.

The conditioning of Rio Tinto water samples (RTW) was carried out by adjusting pH to 3.4-3.5 with concentrated NaOH solution and the bubbling of air through the solution during several days to oxidize Fe(II) to Fe(III). The final removal of the $Fe(OH)_3$

precipitate was carried out by filtration using a sintered glass filter and a water-pump. The composition of RTW samples, before and after this treatment, are shown in Table 1, where the compositions of artificially prepared RTW concentrates are also given.

Table 1.

Methods

Thermostripping and Thermosorption

All the experiments were carried out under dynamic conditions in the thermostatic columns previously described *(11)*. The columns were loaded with a certain portion of the ion exchanger which remained constant during all the series of experiments. The total capacity of the resin bed was determined prior to the equilibrium studies by applying a standard technique *(11)*. Then, the resin was converted into either RTW or seawater ions form and equilibrated at a selected temperature.

Thermostripping and thermosorption experiments were carried out as follows: after equilibration of the resin with RTW sample at 80°C and 20°C respectively, the excess of the solution over the resin bed was removed so that its level coincided with that of the resin bed. Then, the temperature was decreased or increased (for thermosorption or thermostripping). After equilibration of the system at a given temperature, RTW of the same composition was passed through the column at a constant flow rate and collected in portions where concentrations of metal ions were determined. RTW solution was passed until the ion-exchange equilibrium at each temperature was achieved. In the series of consecutive thermostripping-thermosorption experiments with RTW concentrates, the composition of the initial solutions used corresponded to that of the sample of thermostripping solution obtained during the previous thermostripping-thermosorption cycle which contained the highest

concentration of Cu^{2+} (see Table 1). Thermosorption from RTW samples on the resin in the seawater ions form was carried out by passing the solution through the column in a fluidized mode (from bottom to top) at constant flow rate of 40 cm^3/min to prevent clogging of the resin bed with $Al(OH)_3$ precipitate which appeared in the first portions of solution passing through the column. The regeneration of the resin with seawater was carried out at 80°C after equilibration of the resin bed with RTW at the same temperature.

RESULTS AND DISCUSSION

The typical concentration-volume histories obtained in two sequential thermostripping-thermosorption cycles are shown in Fig. 1. The first cycle was carried out after the loading of Lewatit R 250-K resin in the initial sea water ions form with natural RTW at 20° C by thermostripping with the same RTW sample at 80° C (see curve 1 in Fig. 1). Then the resin was cooled and equilibrated with cold RTW at 20° C (thermosorption), followed by the second thermostripping at 80° C. The total capacity of the resin bed used in this series of experiments was 8.4 mequiv/g. RTW was passed at 1.6 cm^3/min of flow rate. As seen in Fig. 1, the first thermostripping leads to intensive desorption of copper from the resin while Al^{3+} is sorbed. This results in a decrease of Al^{3+} concentration in the first portions of the eluate and to an increase of Cu^{2+} ions concentration. The concentration degrees of the rest RTW metal ions have been shown to be much less than those of Cu^{2+} and Al^{3+} (depletion degree in this case) and are not shown in Fig. 1 *(15)*.

The thermostripping process leads to a partial desorption of RTW metal ions such as Cu^{2+} and some others (except Al^{3+}) from the resin. The unloaded resin phase

is able to take them up again without any additional treatment after decreasing the temperature (in our case 20°C) in the system and carrying out the repetitive thermosorption *(11)*. However this latter process has been observed to be of far less efficient than the first loading of the resin in the sea water ions form. This can be attributed to unfavorable conditions of the second thermosorption process which in fact proceeds "against" the selectivity of the resin that follows from the respective values of equilibrium separation factors for RTW ion couples reported elsewhere *(15)*. Nevertheless, the repetition of the thermosorption-thermostripping cycles with RTW concentrates (see Table 1) on the resin in the RTW ions form allows to carry out reagentless dual-temperature concentration of copper as has been reported elsewhere *(13)*. As follows from the results shown in Fig. 2, the degrees of copper concentration and aluminium depletion in each sequential cycle are of the same order of magnitude as in the second one shown in Fig. 1 (see curve 2). On the other hand, the situation can be significantly improved after treating (regeneration) the resin with seawater (see curve 1 in Fig. 1). Since the regeneration of the resin bed must be fulfilled right after the thermostripping, it seems reasonable to carry out this stage of the process without alteration of the temperature, i.e. at 80°C.

The concentration-volume histories of the regeneration of the resin with hot seawater at 80°C are shown in Fig. 3. Desorption of Zn^{2+} and Mn^{2+} from the resin proceeds much faster than Cu^{2+} and Al^{3+} (see Fig. 3a). The formers are completely removed from the resin phase with 5 bed volumes of seawater while for the elution of Cu^{2+} 15 bed volumes of the regenerant are needed. Al^{3+} appears the most difficult to remove admixture and the complete regeneration of the resin bed can be achieved after passing approximately 30 bed volumes of hot seawater. As seen in Fig. 3b Mg^{2+}

and Na^+ fulfil in fact the functions of displacers and are sorbed during the regeneration. After treatment with seawater and a proper cooling, the resin is prepared for the next thermosorption-thermostripping cycle.

Results of the repetitive experiments on sequential thermostripping-thermosorption cycles with RTW concentrates (see Fig. 2) on the resin in the seawater ions form (in regeneration of the resin with seawater after each thermostripping) testifies to the significant enhancement of copper concentration process, that is seen in Fig. 4. Indeed, as follows from the comparison of the results shown in Fig. 2 with those presented in Fig. 4, concentration degrees of copper in each cycle are much higher when using the resin in the seawater ions form at the loading stage.

The effect observed can be attributed to the partial hydrolysis of the resin in the seawater ions form. The capacity of Lewatit R 250-K resin towards macrocomponents of seawater has been determined to equal (in equivalent fractions): 0.31 (Ca^{2+}); 0.50 (Mg^{2+}), and 0.19 (Na^+) *(11)*. A carboxylic resin in the Na-form readily undergoes the hydrolysis (as a salt formed by a weak polyacid and a strong base) according to the following reaction:

$$R\text{-}COONa + H_2O \leftrightharpoons R\text{-}COOH + NaOH \qquad \textbf{(1)}$$

Loading of the partially hydrolized resin with RTW is accompanied by precipitation of RTW metal ion hydroxides (due to presence of alkali in the resin phase) in accordance with their solubility. The solubility sequence for cations of conditioned (iron free) RTW can be written in terms of the respective solubility products *(19)*, K_{SP}, as follows:

$$Al(OH)_3(pK_{SP}=32.9)<<Cu(OH)_2(19.7)<Zn(OH)_2(16.7)<Mn(OH)_2(12.7)<Mg(OH)_2(10.7)<Ca(OH)_2(5.3) \quad (2)$$

where $pK_{SP} = -\log K_{SP}$. In accordance with sequence (2) one can expect mainly the formation of $Al(OH)_3$ precipitate, that is confirmed by the analysis of the precipitate collected from the first portions of the eluate passed through the column during the thermosorption stage. Removal of aluminium from RTW during the loading of the resin proceeds in the interbed space of the column and leads to the increase of the resin capacity towards the rest RTW metal ions following the sequence of the resin selectivity. The selectivity sequence of Lewatit R 250-K towards RTW cations is easily evaluated from the respective separation factor values reported elsewhere *(15)*, and can be written as follows:

$$Al^{3+} > Cu^{2+} > Zn^{2+} > Mn^{2+} > Ca^{2+} > Mg^{2+} > Na^{+} \quad (3)$$

Hence, removal (at least partial) of aluminium from RTW must result in additional accumulation of copper (and some other metal ions as well) in the resin. Hence, a significant enhancing of copper concentration is observed.

The results of thermostripping shown in Figs. 1 (curve1) and 4 have been obtained on the resin bed of 5 cm height. Increase of the bed height must result in the increase of the concentration degrees of metal ions stripped *(15)*. This is clearly seen in Fig. 5, where the concentration-volume histories for Cu^{2+} obtained by thermostripping from resin beds of different heights (5 and 18.5 cm) are shown.

Finally, we consider the results obtained in the present study from a practical viewpoint to propose a flowsheet of the ion-exchange process for the treatment of

acidic mine waters. The block-scheme of the process is presented in Fig. 6. The unit comprises three counter-current columns operating at different temperatures T_1=20°C and T_2=80°C. Cold RTW (after removal of Fe(III) hydroxide) is treated in the first column with fluidized resin that has been treated with seawater. After loading with RTW metal ions, the resin is directed into the second (thermostripping) column which is fed with hot RTW and produces RTW concentrate enriched with Cu^{2+}, Zn^{2+}, etc., and depleted with Al^{3+} *(20, 21)*. The construction of the thermostripping column may be similar to that of counter-current ion-exchange contactors with moving packed bed *(22, 23)*. The third column, where the resin is underwent the final regeneration, must be of the same type as column 2 and must provide the conditions for the treatment of the resin bed with seawater at high flow rate (see Fig. 3), i.e. the column must be highly productive *(23-26)*. The regenerated resin is returned back into the column 1 and the treatment cycle repeats. The wastes produced from column 1 represent in fact the mixture of Mg^{2+}, Na^{+} and Ca^{2+} sulfates at pH~6. They can be mixed with those produced by column 3 (at pH=8.1) and discharged after elimination of sulfates content to seawater level (~ 3,500 ppm) with, e.g. lime milk.

The results shown in Fig. 2 can serve as a base for designing a flowsheet of the reagentless dual-temperature copper concentration process. The scheme of this process for the counter-current mode of operation has been proposed elsewhere *(13)*. The same process can be realized in a fixed bed mode of operation as shown schematically in Fig. 7. The columns with fixed bed of Lewatit R 250-K resin are periodically treated with cold (thermosorption) and hot (thermostripping) RTW. Stripping solution (copper concentrate) obtained is collected separately and is underwent to the futher treatment in the next column. Sequential repetition of the

thermostripping-thermosorption cycles leads to the accumulation of copper in the stripping solution (see Fig. 2 and Table 1). Comparison of the results shown in Fig. 2 with those presented in Fig. 4, testify to the possibility of combining processes shown schematically in Figs. 6 and 7 within one technological flowsheet. This can be done by applying the former process (Fig. 6) for the final concentrating of RTW concentrates obtained at any stage of the latter process (Fig. 7). As follows from Figs. 4 and 5, such a combination will lead to an increase of copper concentration in the final eluate at least by factor 3.

In conclusion, the results of this study are the first successful demonstration of the practical possibility for designing ion-exchange treatment technology based upon the use of sea water as the auxiliary regenerating agent.

ACKNOWLEDGMENTS

This work has been carried out with the financial support of CICYT, the Spanish Commission for Research and Development, project PTR930009. Dr. D. Muraviev thanks to the Spanish Ministry for Education and Science to support his sabbatical stay at Universitat Autónoma de Barcelona (SAB95-0073). Bayer Hispania Industrial, S.A. is gratefully acknowledged for supplying with samples of Lewatit resins. Rio Tinto Minera S.A. is also gratefully acknowledged for supplying with samples of acidic mine waters.

REFERENCES

1) Tiravanti, G.; Di Pinto, A.C.; Macchi, G.; Marani, D.; Santori, M.; Wang, Y. in *Metals Speciation, Separation and Recovery*; Patterson, J.W.; Passino, R., Eds.; Lewis Publ.: Chelsea, 1987; p. 665.

2) Ritcey, G.M.; Asbrook, A.W. *Solvent extraction, principles and applications to process metallurgy*, Part II, Elsevier: Amsterdam, 1979, p. 605.

3) Högfelt, E. In *Ion Exchangers*; Dorfner, K., Ed.; Walter de Gruyter: Berlin, 1990, p. 573.

4) Patterson, J.W. In *Metals Speciation, Separation and Recovery*; Patterson, J.W.; Passino, R., Eds.; Lewis Publ.: Chelsea, 1987; p. 63.

5) Streat, M. In *Ion Exchangers*; Dorfner, K., Ed.; Walter de Gruyter: Berlin, 1990, p. 1061.

6) Khamizov, R. ; Muraviev, D.; Warshawsky, A. In *Ion Exchange and solvent Extraction*; Marinsky, J.A.; Marcus, Y. Eds.; Marcel Dekker: New York, 1995; Vol.12, Chapter 3.

7) Ritcey, G.M. *Tailing Management, problems and solutions in the mining industry*, Elsevier: Amsterdam, 1989; p. 446.

8) Andreev, B.M.; Boreskov, G.K.; Katalnikov, S.G. *Khim. Prom-st*, **1961**, *6,* 389 (Russ).

9) Gorshkov, V.I.; Kurbanov, A.M.; Apolonnik, N.V. *Zhur. Fiz. Khim.*, **1971**, *45*, 2969 (Russ.)

10) Gorshkov, V.I.; Ivanova, M.V.; Kurbanov, A.M.; Ivanov, V.A. *Vestnik Moskov. Univ., Ser. Khim.*, **1977**, *5*, 535 (Russ.). English translation in: *Moscow Univ. Bull.*, 1977, *32*, 23.

11) Muraviev, D.; Noguerol, J.; Valiente, M. *Reactive Polymers*, **1996**, *28*, 111.

12) Muraviev, D.; Gonzalo, A.; Valiente, M. *Anal. Chem.*, **1995**, *67*, 3028.

13) Muraviev, D.; Noguerol, J.; Valiente, M. *Hydrometallurgy*, **1996**, in press.

14) Muraviev, D.; Gonzalo, A.; Gonzalez, M-J.; Valiente, M. *In Proc. IEX'96*; SCI; Greig, J. A., Ed.; Cambridge; 1996; 516.

15) Muraviev, D.; Noguerol, J.; Valiente, M. *Wat. Res.*, **1996**, submited.

16) Grevillot, G. In *Handbook for Heat and Mass Transfer*; Cheremisinoff, N.P., Ed.; Gulf Publ.: West Orange, NY USA, 1985; Chapter 36.

17) Bailly, M.; Tondeur, D. *J. Chromatogr.*, **1980**, *201*, 343.

18) Bailly, M.; Tondeur, D. *J. Chem. Eng. Symp. Ser.*, **1978**, *54*, 111.

19) *Lange's Handbook of Chemistry*, 11th edn.; Dean, J.A., Ed.; McGraw-Hill: New York, 1973; p.5-7.

20) The composition of this product has been shown to suit for the further processing in applying ion-exchange technique which allows to produce sufficiently pure copper and zinc sulfates *(21)*.

21) Muraviev, D.; Noguerol, J.; Valiente, M. *In Proc. ION-EX'95*; SCI: Oxford; 1996; in print.

22) Streat, M.; Naden, D. In *Ion Exchange and Sorption Processes in Hydrometallurgy*; Streat, M.; Naden, D., Eds.; John Willey & Sons: Chichester, 1987; p.20.

23) Gorshkov, V.I. In *Ion Exchange and solvent Extraction*; Marinsky, J.A.; Marcus, Y. Eds.; Marcel Dekker: New York, 1995; Vol.12, Chapter 2.

24) Gorshkov, V.I.; Medvedev, G.A.; Muraviev, D.N. *Tsvet. Met.*, **1974**, *1*, 53 (Russian).

25) Gorshkov, V.I.; Muraviev, D.N.; Medvedev, G.A.; Ferapontov, N.B. *Zh. Fiz. Khim.*, **1977**, *55*, 980 (Russian)

26) Gorshkov, V.I.; Medvedev, G.A.; Muraviev, D.N.; Ferapontov, N.B. In *Theory and Practice of Sorption Processes*; Izd. VGU: Voronezh; 1978; Vol. 12, p. 83 (Russian).

LEGENDS TO FIGURES

Fig. 1 Thermostripping breakthrough curves for Cu^{2+} and Al^{3+} from Lewatit R 250-K resin: 1st thermostripping (1) and 2nd thermostripping (2). T=80°C, solution flow rate = 1.6 cm^3/min.

Fig. 2 Concentration-volume histories for 2nd thermostripping in different sequential cycles: 1st cycle (solid line), 2nd cycle (dashed line) and 3er cycle (dotted line).

Fig. 3 Concentration-volume histories of the regeneration of the resin with hot seawater at 80°C, a) Zn^{2+} (1), Mn^{2+} (2), Cu^{2+} (3), Al^{3+} (4) and b) Ca^{2+} (1), Mg^{2+} (2), Na^{+} (3). C_o for Ca^{2+}, Mg^{2+} and Na^{+} is concentration of these ions in seawater. Solution flow rate = 1.6 cm^3/min.

Fig. 4 Concentration-volume histories for 1st thermostripping in different sequential cycles: 1st cycle (solid line), 2nd cycle (dashed line) and 3er cycle (dotted line).

Fig. 5 Concentration-volume histories for Cu^{2+} obtained by thermostripping from resin beds of different heights: h=18.5 cm (1) and h=5 cm (2). T=80°C, solution flow rate = 1.6 cm^3/min.

Fig. 6 Flowsheet of the process for ion-exchange treatment of acidic mine waters in applying seawater as regenerant.

Fig. 7 Flowsheet of the process for reagentless dual-temperature ion-exchange treatment of acidic mine waters.

Table 1. Composition of natural (before and after treatment) and artificial (used in different thermo-stripping-sorption cycles) Rio Tinto water samples.

C (ppm)	pH	SO_4^{2-}	Fe^{3+}	Cu^{2+}	Zn^{2+}	Al^{3+}	Mn^{2+}	Mg^{2+}	Ca^{2+}	Na^{+}
Initial	1.8	17,430	4,527	117	1,217	560	87	940	480	22
Treated	3.5	17,350	3	115	1,275	530	90	950	475	3,550
Artificial	3.5	17,884	0	120	4,700	530	0	0	0	3,500
1st Conc.	3.5	17,365	0	171	4,731	318	0	0	0	3,565
2nd Conc.	3,5	17,557	0	200	4,706	186	0	0	0	3,565
3rd Conc.	3.5	17,212	0	255	4,668	106	0	0	0	3,588
4th Conc.	3.5	17,106	0	326	4,519	49	0	0	0	3,687

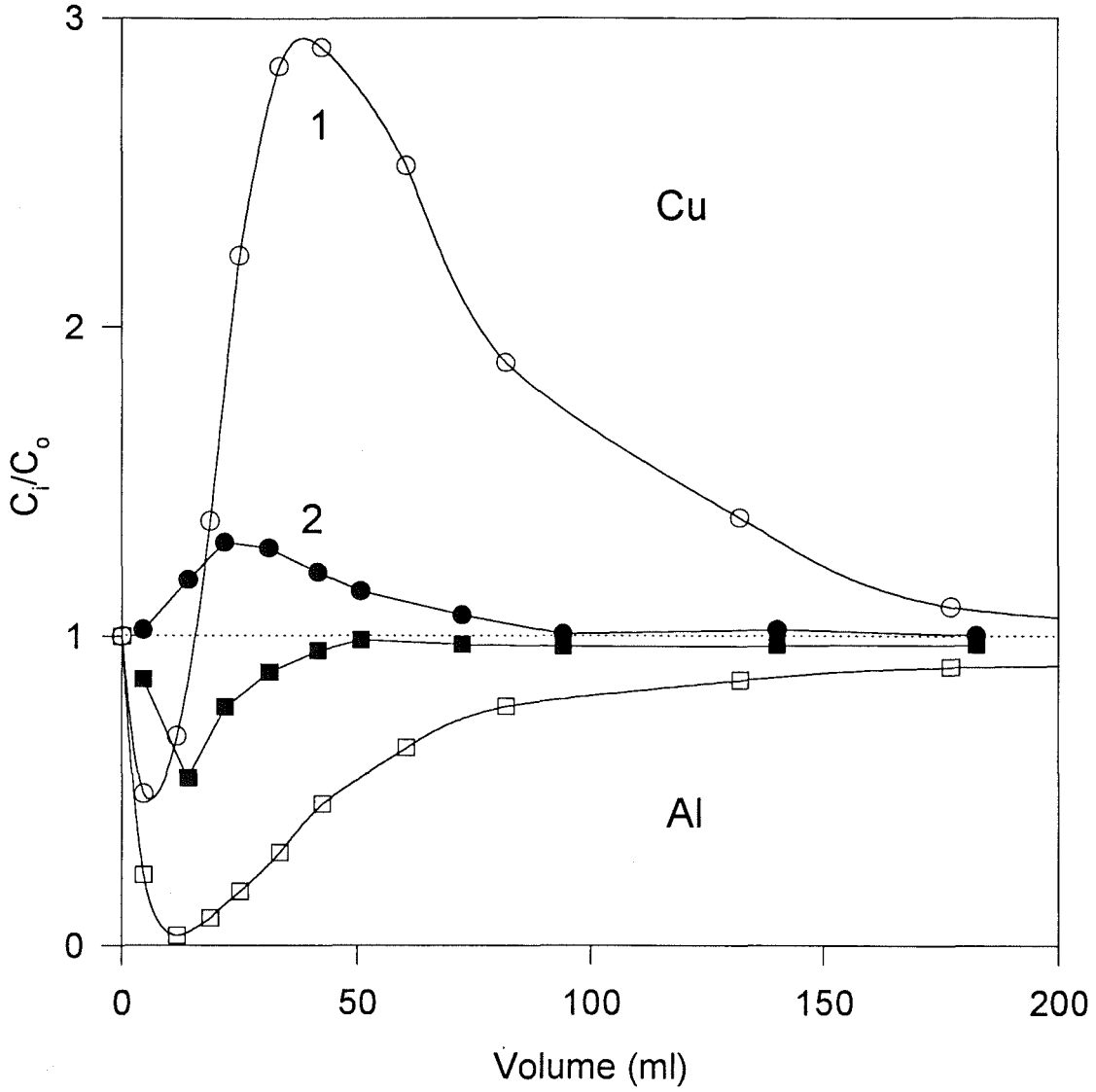
3
2
1
0
C_i/C_o
1
2
Cu
Al
0
50
100
150
200
Volume (ml)

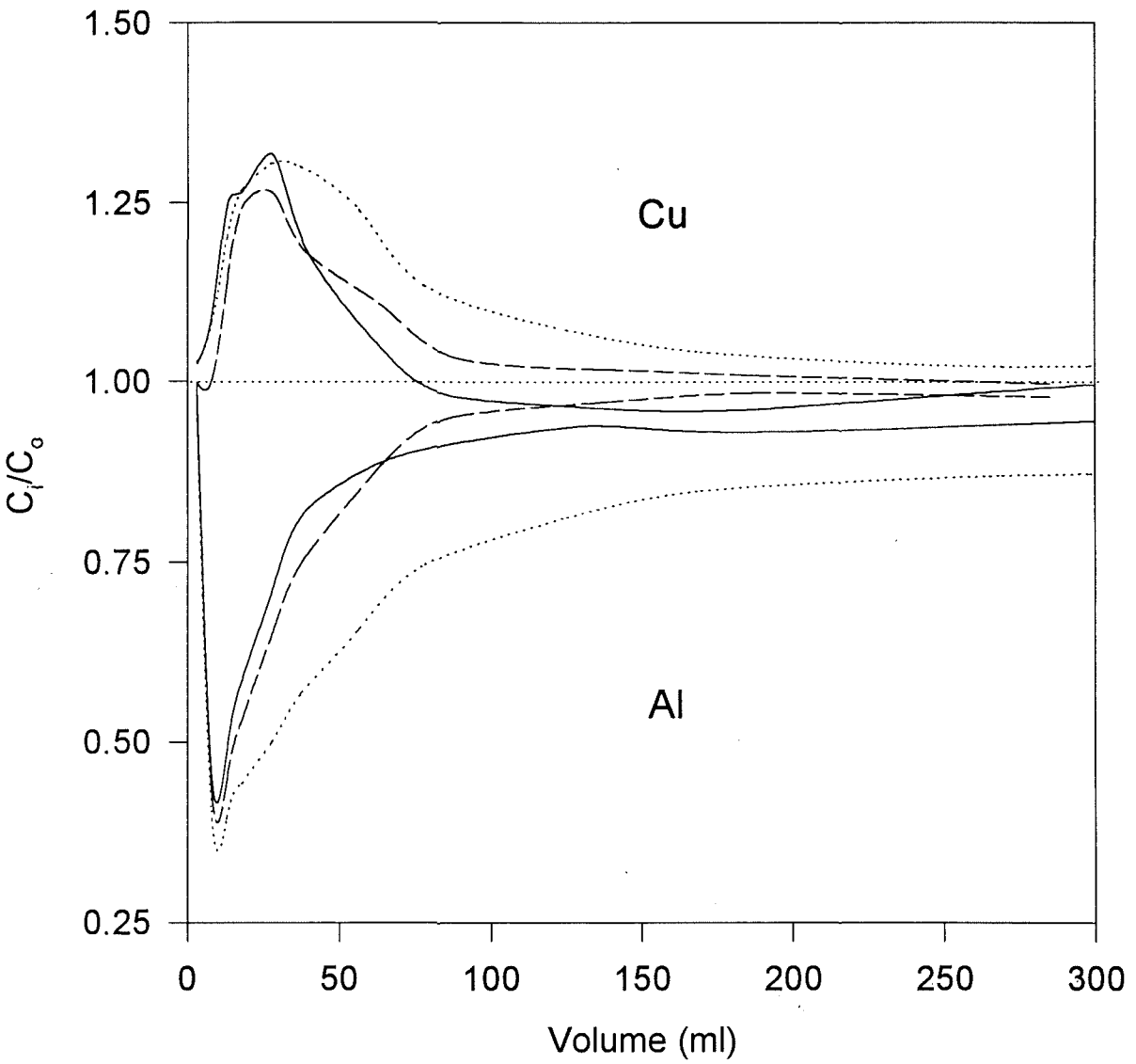
1.50
1.25
1.00
0.75
0.50
0.25
C_i/C_o
Cu
Al
0
50
100
150
200
250
300
Volume (ml)

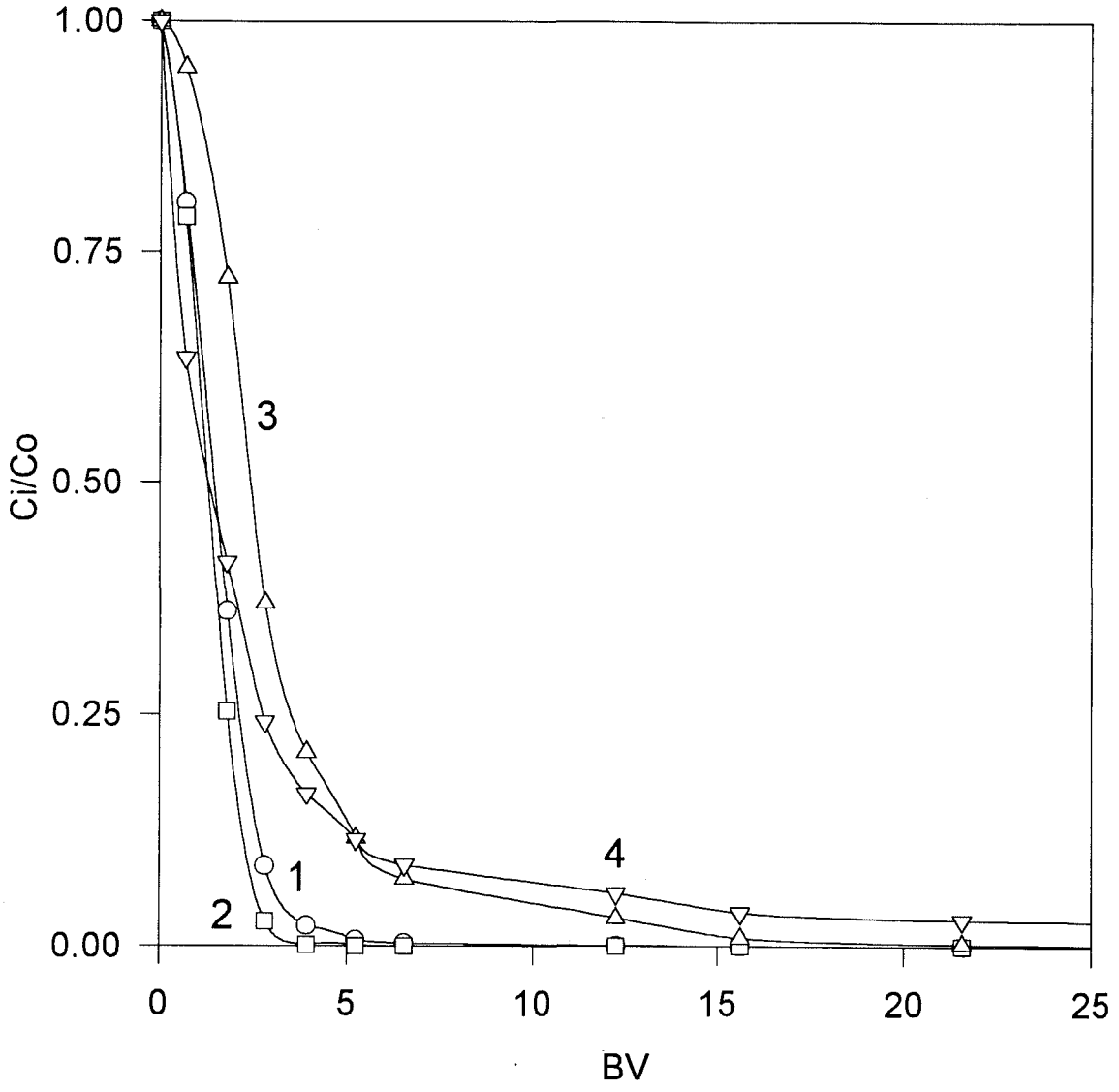
1.00
0.75
0.50
0.25
0.00
Ci/Co
0
5
10
15
20
25
BV
1
2
3
4

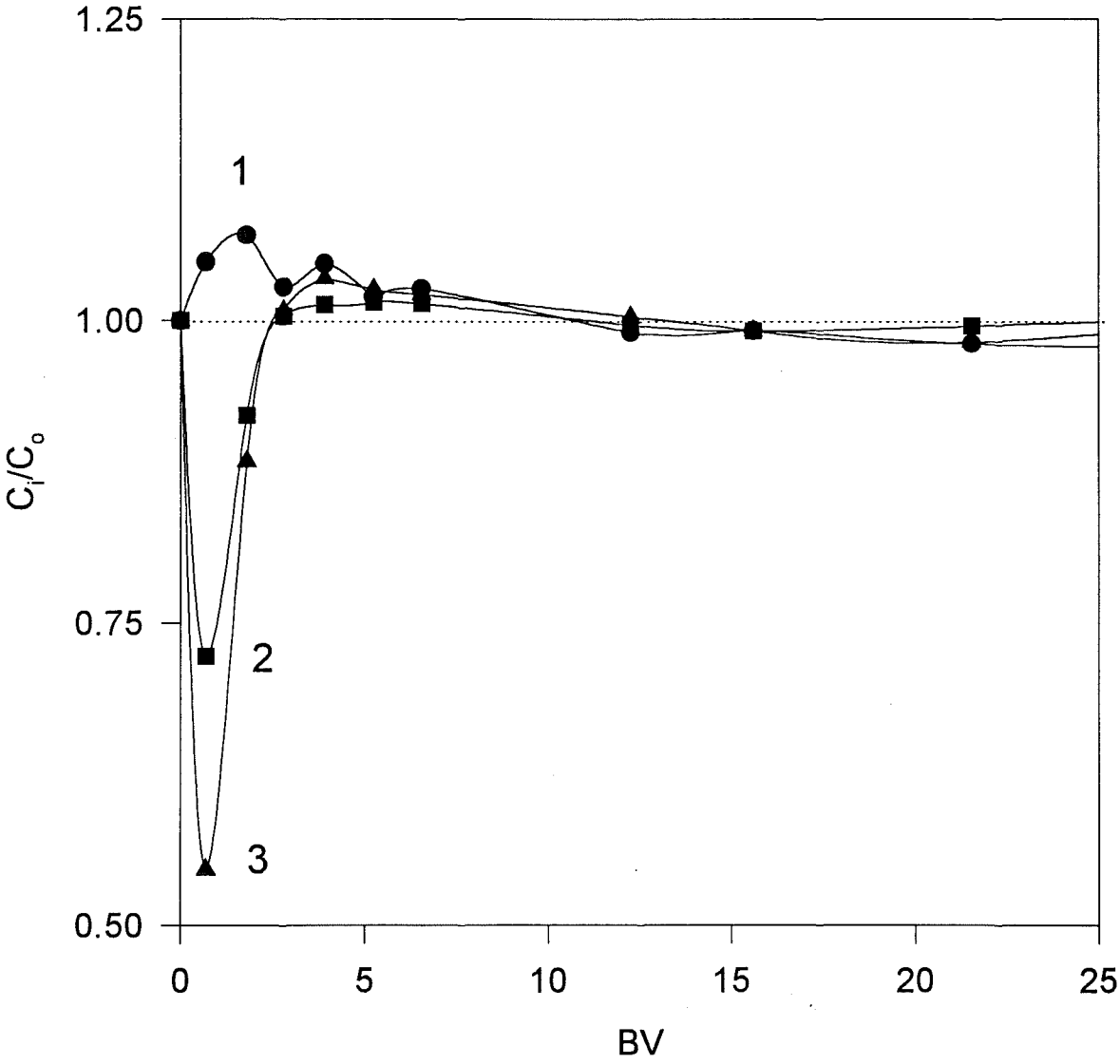
1.25
1.00
0.75
0.50
C_i/C_o
1
2
3
0
5
10
15
20
25
BV

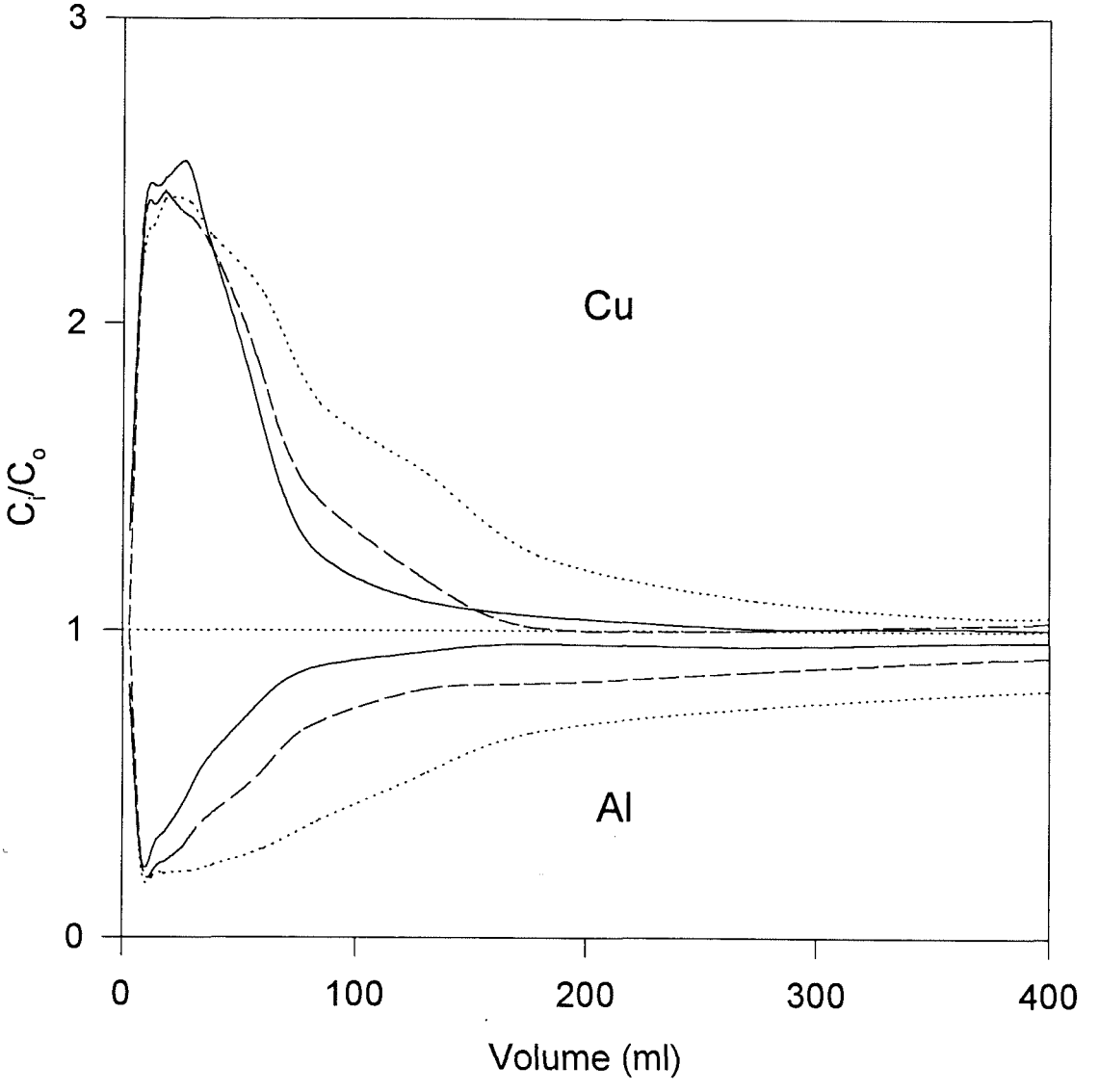
3
2
1
0
C_i/C_o
Cu
Al
0
100
200
300
400
Volume (ml)

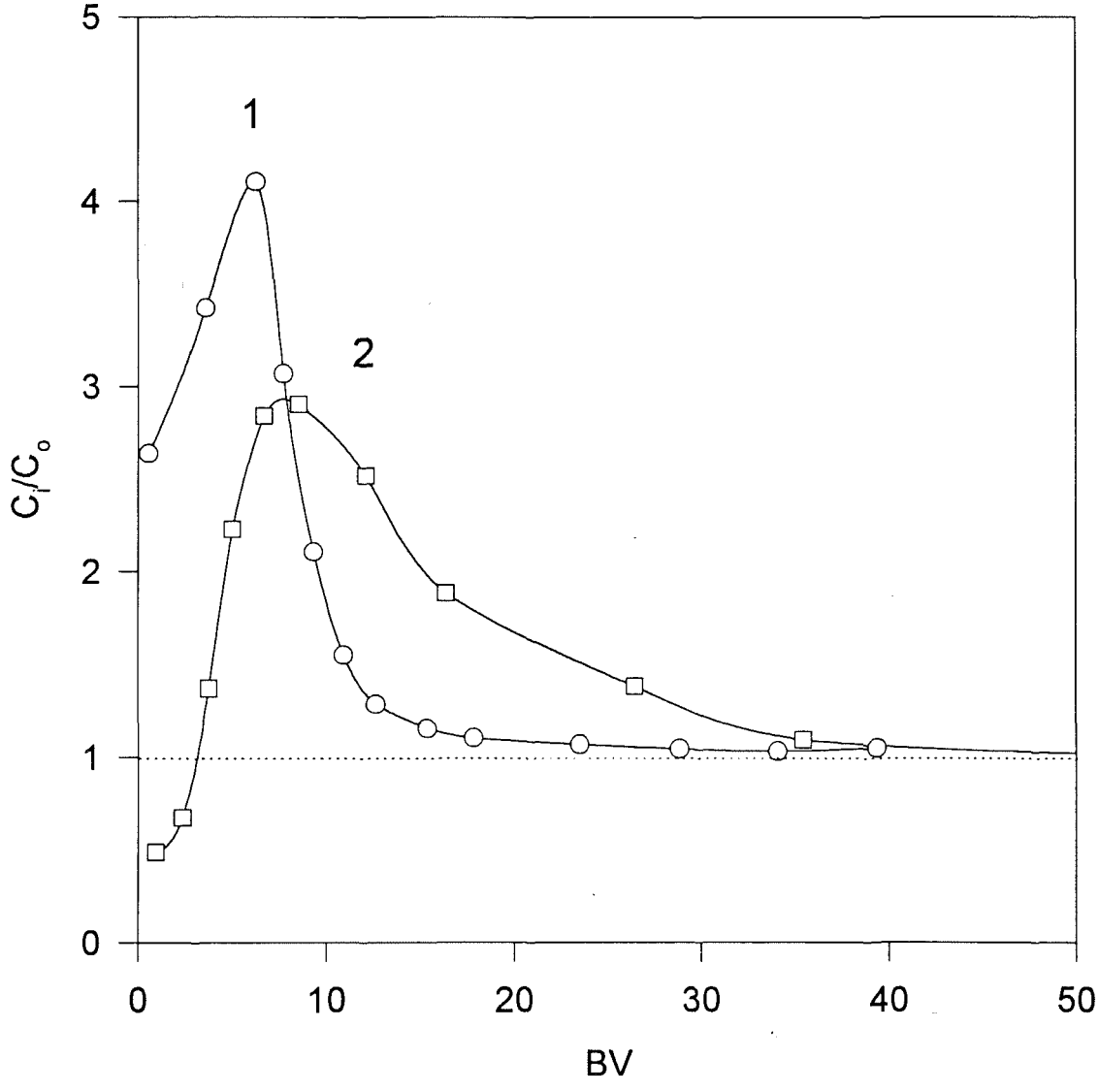
5
4
3
2
1
0
1
2
C_i/C_o
0
10
20
30
40
50
BV

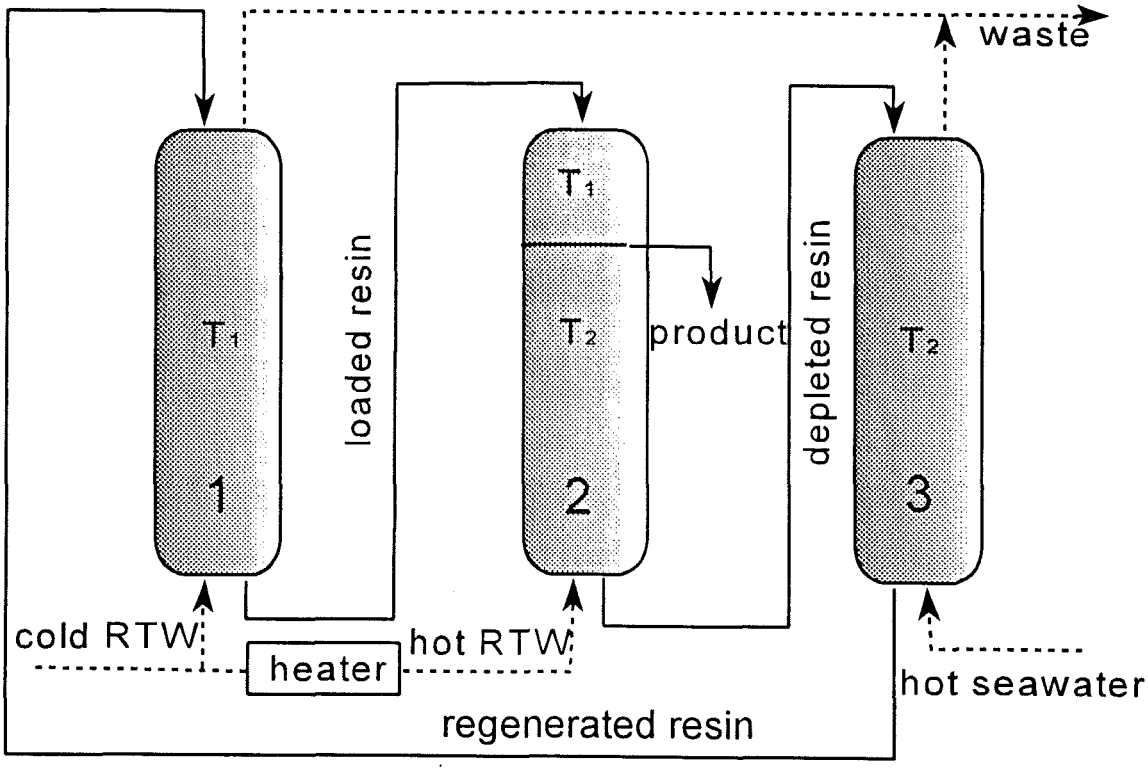
waste
T1
1
loaded resin
T1
T2
2
product
depleted resin
T2
3
cold RTW
heater
hot RTW
hot seawater
regenerated resin

Fig. 6.

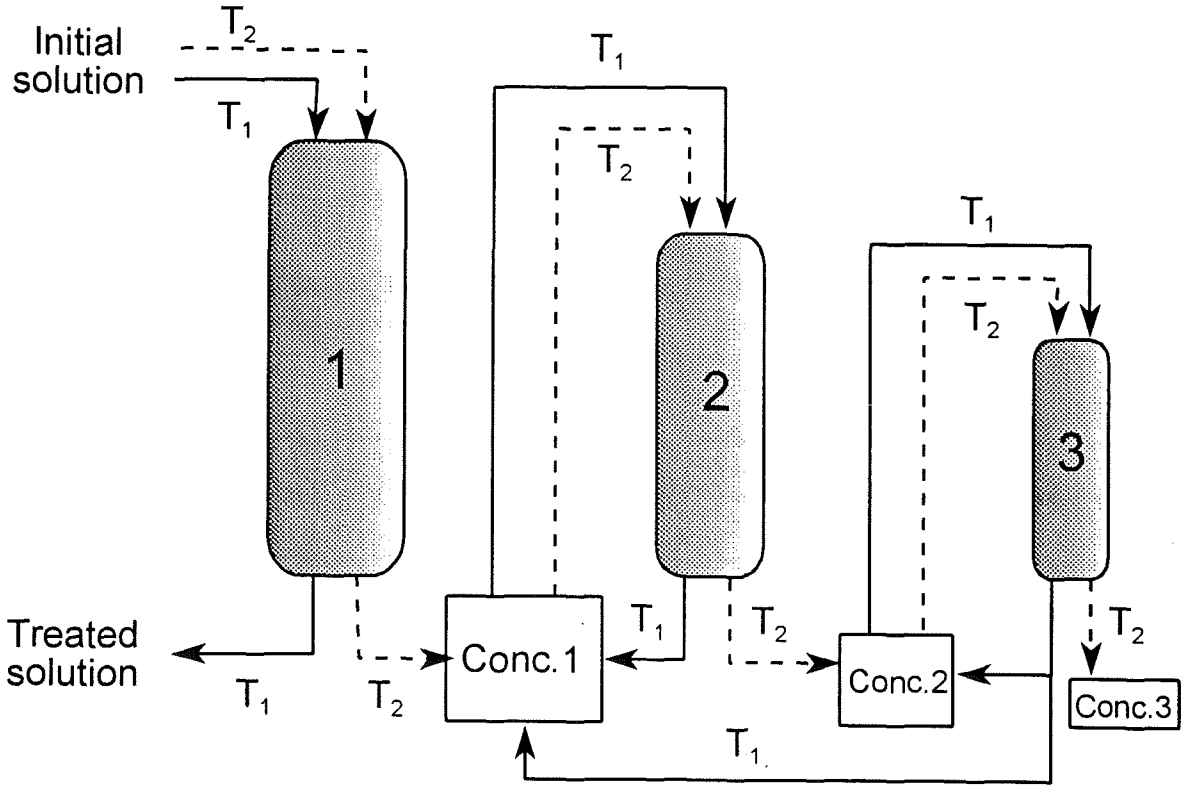
Initial solution
T2
T1
1
T1
T2
2
T1
T2
3
Treated solution
T1
T2
Conc.1
T1
T2
Conc.2
T2
Conc.3
T1

Fig. 7

ANEXO V

Tandem Ion-Exchange Fractionation: New Preparative Mode for Separation of Multicomponent Ionic Mixtures

Dmitri Muraviev[1], Joan Noguerol and Manuel Valiente*
Departament de Química Analítica, Universitat Autònoma de Barcelona
E-08193 Bellaterra (Barcelona), Spain.

* Author for correspondence. [1] On sabbatical leave from Lomonosov Moscow State University, Department of Physical Chemistry, 119899 Moscow, Russia.

ABSTRACT

The paper reports the results on the development of the Tandem-Ion-Exchange-Fractionation (TIEF) concept for separation of n-component (n > 2) ionic mixtures on (n-1) ion-exchange columns. TIEF technique is based on a sequential combination of Frontal Separation (FS) and Reverse Frontal Separation (RFS) of the mixture components. The appropriate sequence of the FS leads to a stepwise elimination of the number of components and it allows to recover all ions under separation in a sufficiently pure state. A practical demonstration of this concept has been carried out by its application to a typical mixture of metal ions present in nonferrous metal alloys, i.e. Cu^{2+}, Al^{3+}, Zn^{2+} and Mg^{2+}. The values of equilibrium separation coefficient, α, for quadri-, tri- and bi-component mixtures involving the mentioned metal ions on polyacrylic and iminodiacetic resins have been determined. The increase of α values for, e.g. Zn^{2+}-Mg^{2+} exchange from 3.3 to 15.8 in reducing of the number of mixture components from 4 to 2 has been observed to illustrate the validity of the TIEF concept. The preparative separation of Cu^{2+}, Al^{3+}, Zn^{2+} and Mg^{2+} mixture with equivalent ratio of Cu : Al : Zn : Mg = 1:1:1:1 carried out by applying TIEF technique has shown to yield Mg^{2+} of around 100 % purity and Cu^{2+}, Al^{3+} and Zn^{2+} of 96.1%, 98.8% and 95.1% average purity, respectively, at a reasonably high yield. The differential stripping during the RFS stage improves significantly the purity of the products obtained.

INTRODUCTION

The application of ion-exchange resins in scientific research and industry is permanently growing within the last years. Two main groups of problems can be successfully solved by applying ion-exchange separation techniques. The former comprises separation and purification of non- or weak electrolytes from electrolyte impurities and involves, for example, water demineralization[1-3], purification of amino acids from mineral salt admixtures[4-6], manufacture of high purity silica[7] and some others[8]. The later group refers to the purification of electrolytes from electrolyte impurities and to the separation of electrolyte mixtures. The last task is a far more complex in comparison with the first one. This is particularly true when concerns separation of the multicomponent ionic mixtures such as, for example, seawater[9], acidic mine waters[10-12] etc., aiming to recover valuable and/or toxic constituents from complex natural and industrial hydromineral and other sources[13,14]. In this context, further development of simple and highly effective ion-exchange separation methods plays a particularly essential role.

Several ion-exchange fractionation techniques are known to be applied for this purpose such as, a frontal separation (FS), known also as a frontal ion-exchange chromatography[15], reverse frontal separation[16] (RFS) and displacement chromatography[17] (DC). The FS is applicable for the separation of the component of the weakest sorbability from the mixture components, which are sorbed stronger. The RFS allows to separate an ionic species, which is sorbed better than the rest mixture ions. The DC technique can be considered, in fact, as a "parallel combination" of FS and RFS, since both of these separation processes proceed simultaneously. Therefore, such a combination within one fractionation method (DC) makes it possible to separate any number of components of either sorbability from each other. One of the first and most impressive applications of DC was the early works of Spedding with co-workers on isolation of transuranium elements[18,19] and separation of rare earths[20-22]. Since then, *DC remains the only fractionation technique*, which is widely applied for preparative separation of complex multicomponent mixtures, such as proteins[23], protein hydrolyzates[24], rare earth elements[25-27] and others[28,29]. Although DC represents one of the most powerful tools in ion-exchange separation and still is under intensive

development[30-34], it is characterized by a number of drawbacks such as, for example, a long time and high resin bed needed for the complete preparative separation of mixture components, low productivity of the separation process and some others, which limit a wider practical application of this ion-exchange fractionation technique. The above drawbacks can be overcome by applying a new FS-RFS combination, which can be characterized as their "sequential combination". Such a combination will be identified by the term "Tandem-Ion-Exchange-Fractionation" (TIEF), to emphasize that this FS-RFS coupling leads to the enhancing of the separation efficiency of each single fractionation method.

The present study has been undertaken (1) to develop the TIEF concept for the preparative separation of multicomponent ionic mixtures; (2) to obtain information on the ion-exchange equilibrium in the bi-, tri- and quadri-component mixtures containing Cu^{2+}, Al^{3+}, Zn^{2+} and Mg^{2+} on polyacrylic and iminodiacetic resins and (3) to demonstrate a preparative separation of four components by applying the TIEF concept. This is the first time that such an approach has been applied successfully to the separation of metal ions from a quadri-component mixture.

EXPERIMENTAL SECTION

Reagents, Ion Exchangers, and Apparatus. Magnesium, zinc, aluminum and copper sulfates, sodium chloride, sodium hydroxide and sulfuric acid (all of p.a. quality) were purchased from Panreac (Barcelona, Spain) and used as received. Iminodiacetic ion-exchanger, Lewatit TP-207 and polyacrylic resin, Lewatit R 250-K, were kindly supplied by Bayer Hispania Industrial, S.A. Doubly distilled water was used in all experiments. The total concentration of metal ions in the stock solution in all cases was keep constant at a 0.04 equiv/dm^3. The ratio of metal ion concentrations in the respective feed solutions was always equaled to 1. pH of the initial solution was adjusted to 3.5 using 0.1 M H_2SO_4. Standard precautions recommended for handling sulfuric acid solutions[35] were followed when adjusting pH and preparing the 0.1 M H_2SO_4 solution from concentrated acid. The concentration of metal ions was determined by atomic emission spectroscopy (ICP-AES technique) using ARL Model 3410 spectrometer (Fisons, USA) provided with minitorch. The emission lines used for the spectrochemical

analysis were 324.754 nm for Cu^{2+}; 213.856 nm for Zn^{2+}; 279.806 nm for Mg^{2+} and 394.401 nm for Al^{3+}. The uncertainty of metal ions determination was in all cases < 1.5%. pH was controlled using a Crison pH meter 507 (Barcelona, Spain) supplied with a combined glass electrode. Glass columns of 0.5x5 cm and 1.0x10 cm from Bio-Rad (Richmond, USA) were used for studying ion-exchange equilibrium and to carry out the TIEF experiments. Prior to the column experiments the resins were air-dried, then grinded and sieved, so that only a granulometric fraction between 0.100 and 0.250 mm was collected and used for loading the columns.

Procedures. Ion-exchange equilibrium was studied under dynamic conditions by using fixed bed columns. Experiments were carried out in an air conditioned room at 22 ± 0.5° C. The initial solution was passed through the columns containing the respective resins (300 and 200 mg of Lewatit TP-207 and Lewatit R 250-K, respectively) in the Na^+-form at constant flow rate of 0.33 ml/min up to achieving the equilibrium. The eluate was collected in portions of known volume where the concentrations of metal ions were determined. The achievement of ion-exchange equilibrium in the systems under study was followed by the comparison of the metals concentration in the column outlet with that of the initial feed solution. After collecting the sample with concentrations of metal ions close to the initials, the flow of solution was stopped and then resumed after a certain period of time. The coincidence of the initial concentration with that of the sample collected after the break was considered as the criterion indicating the equilibrium in the system. After equilibration, the resin was rinsed with twice distilled water, then, the stripping was carried out with 0.05 M H_2SO_4, followed by the analysis of the desorbed metal ions in the resulting eluate. Data of the stripping solution analysis were used to determine both the capacity of the resin towards the mixture components and the equilibrium separation coefficient α, expressed as follows:

$$\alpha_{M_2}^{M_1} = \frac{Y_{M_1} X_{M_2}}{Y_{M_2} X_{M_1}} \qquad (1)$$

where Y and X are the equivalent fractions of metal ions (M_1 and M_2) under separation

in resin and solution phases, respectively. Indices 1 and 2 are chosen so that $\alpha > 1$. The relative uncertainty on α determination in all cases did not exceed 7 %.

The final experiment on TIEF of the Cu^{2+}-Al^{3+}-Zn^{2+}-Mg^{2+} mixture, was carried out by passing the initial solution through the system of three columns connected in the sequential series as shown in Fig.1. The first column (1.0x10 cm) was loaded with 2.00 g of Lewatit TP-207 resin. The second and the third columns (of 0.5x5 cm each) were loaded with 200 mg of Lewatit R 250-K and 75 mg of Lewatit TP-207 resins, respectively. After appearance of Al^{3+} in the second column outlet, the third column was disconnected. When Cu^{2+} appeared in the outlet of the first column, the second one was also disconnected, and the solution was continued to pass through the first one until the equilibrium was achieved. Then the resins were rinsed separately with twice distilled water, and the stripping of each column with 0.05 M H_2SO_4 was carried out, followed by the analysis of metals ions in the eluate obtained. The results of the stripping solution analysis were used to determine (1) the capacity of each resin towards mixture components, (2) the values of equilibrium separation factors α (see eq. 1), (3) the purity of the product in each solution portion collected according to:

$$P_{A,\,i}\ (mass\ \%) = \frac{C_{A,\,i}\ 100}{C_{A,\,i} + C_{B,\,i} + C_{C,\,i} + C_{D,\,i}} \qquad (2)$$

and (4) an average purity of the products obtained, which can be expressed as follows:

$$P_{A,\,av}\ (mass\ \%) = \frac{(\sum_i V_i\ C_{A,\,i})\ 100}{\sum_i V_i\ (C_{A,\,i} + C_{B,\,i} + C_{C,\,i} + C_{D,\,i})} \qquad (3)$$

in equation number (2) and (3) V_i is the volume of the "i" solution sample, dm^3, and C_i is the concentration of the respective ionic species in this sample, g/dm^3.

TIEF Concept

A conceptual scheme of the TIEF for the separation of a quadri-component mixture of **A; B, C** and **D** cations with the equivalent ratio **A : B : C : D** = 1:1:1:1 is shown in Fig.2. The initial mixture of **AX; BX; CX** and **DX** (**X** denotes the mutual anion) is passed through three columns, which are sequentially connected with each other. Each column contains a specific cation exchanger (or exchangers), which preferentially sorb one of the mixture components, but *all of them manifest the weakest affinity towards the same cation,* for example **A**. The last condition is a necessary requirement in the TIEF technique. We will suppose the sorbability of the mixture components in all columns to follow the sequence: **D > C > B > A.**

As seen in Fig.2, the loading of each column is accompanied by the FS process (see Fig.2b). The loading of the first column is carried out until the breakthrough of ion **D** is observed[36]. Hence, the number of ionic species entering the second column is diminished to three (**A, B** and **C**). Note that, at a determined loading of the resin bed, the equivalent ratio of components in the solution leaving column 1 becomes the same, i.e. 1:1:1. The above condition must be fulfilled in the loading of columns 2 and 3. In this case, the equivalent ratio of ion concentrations in the mixture entering column 3 also equals 1:1. The FS of **A, B** and **C** mixture in column 2 leads to the additional accumulation of **A** in the head part of the solution leaving the column, while component **C** is retarded by the resin phase. The final separation of the residual mixture of **A** and **B** is accomplished in column 3. The distribution of components in the solution leaving each column is shown in Fig.2b. As seen in Fig.2b , **A** is the only component which can be recovered in a pure state from the solution collected after the last column. On the other hand, components **D; C** and **B** accumulated in the resin phases of columns 1, 2 and 3, respectively, (as shown in Fig.2a by dotted lines) can be recovered in a pure state during the stripping stage by using RFS technique. The distribution of components in the stripping solution is shown in Fig.2c.

We will consider now the ion-exchange equilibria in each column to characterize them in terms of the respective α values. As follows from equation 1, for a mixture of ions of equal concentration, for example **A** and **B**, α_A^B can be expressed as follows:

$$Column\ 1: \quad \alpha_A^B\,[4] = \frac{Y_B}{Y_A} = \frac{1 - Y_A - Y_C - Y_D}{Y_A} \tag{4}$$

$$Column\ 2: \quad \alpha_A^B\,[3] = \frac{Y_B}{Y_A} = \frac{1 - Y_A - Y_C}{Y_A} \tag{5}$$

$$Column\ 3: \quad \alpha_A^B\,[2] = \frac{Y_B}{Y_A} = \frac{1 - Y_A}{Y_A} \tag{6}$$

the number in brackets denotes the number of components in the respective feed solution.

Equations 4-6 can be rewritten in the form:

$$\alpha_A^B\,[4] = \frac{1 - Y_A}{Y_A} - (\alpha_A^C + \alpha_A^D) \tag{7}$$

$$\alpha_A^B\,[3] = \frac{1 - Y_A}{Y_A} - \alpha_A^C \tag{8}$$

$$\alpha_A^B\,[2] = \frac{1 - Y_A}{Y_A} \tag{9}$$

By assuming $(1 - Y_A)/Y_A$ in equations 7-9 to be of the same order of magnitude (this approximation is rather rough, but for the discussion given below, better accuracy is not important) and taking into account that $\alpha_A^D > \alpha_A^C$, it follows $\alpha_A^B[2] > \alpha_A^B[3] > \alpha_A^B[4]$, i.e. the separation conditions of **B-A** ion couple are far better in column 3 than in column

1. This conclusion can be formulated in a more general form as follows: *sequential elimination of the number of mixture components results in improving the separation conditions for the rest of ions.* The general conditions for the separation of **A; B; C;** and **D** mixture are summarized in Table 1, where the products to be obtained from each column in a pure state are also indicated.

RESULTS

Fig. 3 shows a typical concentration-volume history obtained with column 1 when loading with a quadri-component mixture of Mg^{2+}; Zn^{2+}; Al^{3+} and Cu^{2+} (Fig. 3a) and stripping of metal ions with 0.05 M H_2SO_4 (Fig.3b). As seen, the FS of the mixture components leads to the formation of a pure Mg^{2+} zone in the head part of the loading curve shown in Fig.3a. The RFS of metal ions proceeds within the stripping stage and results in the formation of the pure Cu^{2+} zone in the last portions of the solution collected (see Fig.3b).

FS and RFS fractionation of Al-Zn-Mg and Zn-Mg mixtures, shown in Figs. 4 and 5, follow the same pattern on columns 2 and 3, respectively. Indeed, formation of a pure Mg^{2+} zone during the loading stage is observed in both systems studied (see Figs.4a and 5a), whereas pure Al^{3+} and Zn^{2+} are yielded within the stripping step as demonstrated in Figs.4b and 5b, respectively.

The results on α determination for binary exchange of metal ion couples from the bi-, tri- and quadri-component mixtures on Lewatit TP-207 and Lewatit R 250-K resins are collected in Table 2.

Fig.6 presents the concentration-volume history, obtained in the TIEF experiment (see Experimental). As seen in Fig.6a, the head part of the breakthrough curve contains a practically pure Mg^{2+}. The width of the pure product zone is far wider, than that obtained in a single FS procedure (see Figs.3a, 4a and 5a). As follows from the results on the stripping of metal ions, shown in Figs. 6b, 6c and 6d, Cu^{2+} and Al^{3+} of sufficiently high purity are obtained as a result of the RFS process. Although Zn^{2+} is yielded in a less pure state due to contamination with Al^{3+} and Mg^{2+}, the eventual zinc purity appears to be quite high (see below).

DISCUSSION

A comparison of the results presented in Figs.3 and 4 with those shown in Fig.6 will provide the main conclusion on the present work. As follows from Figs. 3a and 3b, a combination of the FS and RFS within one separation step (loading-stripping procedure) allows to recover only two ionic species of the weakest (Mg^{2+}) and strongest (Cu^{2+}) sorbabilities in a pure state. The intermediate tri-component mixture of Zn^{2+}, Al^{3+} and Mg^{2+} remains nonseparated and is usually wasted. The same conclusion follows from the results shown in Fig.4. Here Mg^{2+} and Al^{3+} can be yielded as pure products, while the component of the intermediate sorbability, Zn^{2+}, remains contaminated with both of these metal ions. This limitation of a single FS-RFS procedure can be overcome by applying the TIEF technique. This is illustrated by the results presented in Fig.6. Indeed, a sequential one-by-one elimination of the mixture components proceeding in columns 1 (Cu^{2+}); 2 (Al^{3+}) and 3 (Zn^{2+}) leads 1) to the concentration of Mg^{2+} in the solution phase up to the maximum level, which corresponds to the total concentration of the initial mixture (cf., $C_i/C_0 = 4$ in Fig.6a with $C_i/C_0 \approx 3$ in Fig. 3a) and (2) to the widening of the pure product (magnesium) zone (cf., Figs.4a and 6a). As a result, the purity of the recovered magnesium from the first eluate portions appears to be > 99.9%, as seen in Fig.7a.

The purity of Cu^{2+}, Al^{3+} and Zn^{2+} vs volume of the eluate plots shown in Figs.7b, 7c and 7d, respectively, testify to the high effectivity of the TIEF technique. Indeed, the purity of Cu^{2+} and Al^{3+} in the last portions of the stripping solution exceeds 99.9%. Values of the initial, maximum and average purity of the components under separation are collected in Table 3, where the yields of the products obtained by RFS with purity $\geq$ 95% are also shown. As seen in Table 3, despite the initial purity of all mixture components is quite low, an average purity of metals obtained with good yields appears to be sufficiently high and can be increased up to ~ 100% (for Cu^{2+} and Al^{3+}) by using the differential stripping. Lower purity of Zn^{2+} is attributed to the breakthrough of Al^{3+} from column 2 into column 3 during the loading stage, that results to the contamination of the product with this ionic species. This situation can be easily improved by applying two-column set-up[36] or by carrying out FS and RFS processes in counter-current columns[34].

The results on α determination shown in Table 2 confirm the above mentioned conclusion about improving the separation conditions of metal ions after elimination the number of mixture components. This is clearly seen from α values of Zn^{2+}-Mg^{2+} exchange determined in bi-, tri- and quadri-phase systems. Note that α values under consideration refer to a Lewatit TP-207 (quadri- and bi-component systems) and a Lewatit R 250-K (tri-component system).

In conclusion, the results of this study is the first successful application of the Tandem-Ion-Exchange-Fractionation technique for the preparative separation of four metal ions.

ACKNOWLEDGMENTS.

This work was supported by Research Grant No. EV5V-CT94-556 from the Commission of the European Communities, Programme Environment 1990-1994. DM was a holder of the Visiting Professorship from the Ministry of Science and Education of Spain, which financial support is gratefully acknowledged (SAB95-0073).

REFERENCES AND NOTES.

1. Calmon,C. *React. Polym.*,**1986**, *4*, 131.
2. Smith, Ch.W. *Ultrapure Water*, **1989**, *6(9)*, 16.
3. Arden, T.V. In *Ion Exchangers*, Dorfner, K., Ed.; Walter de Gruyter: Berlin, 1991, p.717.
4. Muraviev, D.; Gorshkov, V.I.; Medvedev, G.A.; Ferapontov, N.B.; Sholin, A.F.; Demina, N.G.; Gribanovskaja, M.G. Method of Amino Acids Purification, Pat.USSR 535291, 1975.
5. Muraviev, D.; Gorshkov, V.I.; Medvedev, G.A.; Ferapontov, N.B.; Kovalenko, Yu.A. *Zh. Prikl. Khim.*, **1979**, *52(5)*, 1183 (Russian).
6. Gorshkov, V.I.; Medvedev, G.A.; Muraviev, D.; Ferapontov, N.B. In *Theory and Practice of Sorption Processes*, v.12, VGU: Voronezh, 1978, p.83 (Russian).
7. Tipnis, U.K.; Maudalia, B.T. *Res. Ind.*, **1987**, *32(4)*, 266.
8. Watanabe, S.; Ohura, O. Manufacture of High Purity Hydrogen Peroxide, Pat. BRD 3826720, 1989.
9. Khamizov, R.Kh.; Muraviev, D.; Warshawsky, A. In *Ion Exchange and Solvent Extraction*, Marinsky, J.A.; Marcus, Y., Eds.; Marcel Dekker: New York, 1995, p.93.
10. Muraviev, D.; Noguerol, J.; Valiente, M. In Proc. Ion' EX-95, Oxford Univ. Press, 1996, in press.
11. Muraviev, D.; Noguerol, J.; Valiente, M. React. Polym., **1996**, *28*, 111.
12. Muraviev, D.; Noguerol, J.; Valiente, M. Envir. Sci. Technol., in press.
13. Metals Handbook, desk ed., Boyer, H.E.; Gall, T.L., Eds.; Am. Soc. Met.: Metals Park, Ohio (1992), p.7-1.
14. An acute problem in the secondary processing of nonferrous metal alloys also includes a separation of alloy components stage, which remains practically unsolved up to now. Separation and recovery of brasses and bronzes constituents such as, copper, zinc, aluminum, magnesium and some others as secondary metals is of particular importance since allows to safe vast amounts of energy in comparison with their recovery from the respective ores (primary metals). The difference of energy consumption in the production of primary and secondary metals (energy saving) is of 362 GJ/ ton for magnesium; 340 GJ/ ton for aluminum;